USE OF EXTRUSION FOR SYNTHESIS OF STARCH-CLAY NANOCOMPOSITES FOR BIODEGRADABLE PACKAGING FILMS

by

XIAOZHI TANG

B.S., HARBIN UNIVERSITY OF COMMERCE, CHINA, 1998
M.S., JIANGNAN UNIVERSITY, CHINA, 2001

AN ABSTRACT OF A DISSERTATION

submitted in partial fulfillment of the requirements for the degree

DOCTOR OF PHILOSOPHY

Food Science Institute
College of Agriculture

KANSAS STATE UNIVERSITY
Manhattan, Kansas

2008

Abstract

One of the worst pollution menaces of modern times is plastic packaging, because of its poor degradability. Packaging materials based on starch utilize the benefits of natural polymerization, abundant availability of raw material, and fast biodegradability. However, the highly hydrophilic nature and poor mechanical properties of starch based films limit their application. This problem was sought to be overcome by forming a nanocomposite of starch and layered silicate clay. This study utilizes melt extrusion processing to synthesize starch-clay nanocomposites for biodegradable packaging films and investigate the effects of chemical compatibility of starch, plasticizer and nanoclay and melt extrusion conditions on the structure and properties of composite films. In the first part of the study, the influence of clay type, clay content, starch source and amylose content was investigated. Starch-montmorillonite (MMT) hybrids showed an intercalated nanostructure due to the compatibility of the two components and led to cast film with higher tensile strength and better water vapor barrier properties as compared to starch-organically modified montmorillonite (I30E) hybrids, as well as native starch only. With increase in clay content (0-21 wt%), significantly higher (15-92%) tensile strength (TS) and lower (22-67%) water vapor permeability (WVP) were obtained. The results indicated that nanocomposite technology could be applied to improve the properties of starch-based packaging films. The barrier and mechanical properties of nanocomposite films did not vary significantly with different starch sources (corn, wheat and potato starch), whereas films from regular corn starch showed better properties than either high amylopectin or high amylose-based nanocomposite films. The second part of the study investigated the effects of glycerol content (0-20 wt%) and three plasticizers (glycerol, urea, formamide) on the structure and properties of the starch-clay nanocomposite films. With decreasing glycerol content, the extent of clay exfoliation increased. Films with 5% glycerol exhibited the lowest WVP, and the highest TS and glass transition temperature (T_g). The use of urea and formamide improved the dispersion of clay platelets. Compared to glycerol and urea, formamide has an intermediate hydrogen bond forming ability with starch. However, at the same level of plasticizer (15 wt%), formamide plasticized nanocomposite films exhibited the lowest WVP, highest TS and T_g. Results indicated that a

balance of interactions between starch, clay surface modifications and plasticizers might control the formation of nanocomposite structure, and in turn affect the performance of the nanocomposite films. The last part of the study investigated the effects of extrusion conditions (screw configuration, barrel temperature profile, screw speed and barrel moisture content) on the structure and properties of the starch-clay nanocomposite films. Increasing the shear intensity significantly improved the exfoliation and dispersion of clay platelets. The combination of lowest barrel moisture content (20%) and high shear screw configuration exhibited almost complete clay exfoliation and the lowest WVP and highest TS of all treatments. Increasing the barrel temperature also improved clay exfoliation and performance of films. The results suggested that, when polymer and clay are chemically compatible, optimization of process conditions (shear intensity, temperature etc.) can enable significant improvement in clay exfoliation and dispersion and the performance of nanocomposite films.

USE OF EXTRUSION FOR SYNTHESIS OF STARCH-CLAY NANOCOMPOSITES FOR BIODEGRADABLE PACKAGING FILMS

by

XIAOZHI TANG

B.S., HARBIN UNIVERSITY OF COMMERCE, CHINA, 1998
M.S., JIANGNAN UNIVERSITY, CHINA, 2001

A DISSERTATION

submitted in partial fulfillment of the requirements for the degree

DOCTOR OF PHILOSOPHY

Food Science Institute
College of Agriculture

KANSAS STATE UNIVERSITY
Manhattan, Kansas

2008

Approved by:

Major Professor
Dr. Sajid Alavi

Copyright

Abstract

One of the worst pollution menaces of modern times is plastic packaging, because of its poor degradability. Packaging materials based on starch utilize the benefits of natural polymerization, abundant availability of raw material, and fast biodegradability. However, the highly hydrophilic nature and poor mechanical properties of starch based films limit their application. This problem was sought to be overcome by forming a nanocomposite of starch and layered silicate clay. This study utilizes melt extrusion processing to synthesize starch-clay nanocomposites for biodegradable packaging films and investigate the effects of chemical compatibility of starch, plasticizer and nanoclay and melt extrusion conditions on the structure and properties of composite films. In the first part of the study, the influence of clay type, clay content, starch source and amylose content was investigated. Starch-montmorillonite (MMT) hybrids showed an intercalated nanostructure due to the compatibility of the two components and led to cast film with higher tensile strength and better water vapor barrier properties as compared to starch-organically modified montmorillonite (I30E) hybrids, as well as native starch only. With increase in clay content (0-21 wt%), significantly higher (15-92%) tensile strength (TS) and lower (22-67%) water vapor permeability (WVP) were obtained. The results indicated that nanocomposite technology could be applied to improve the properties of starch-based packaging films. The barrier and mechanical properties of nanocomposite films did not vary significantly with different starch sources (corn, wheat and potato starch), whereas films from regular corn starch showed better properties than either high amylopectin or high amylose-based nanocomposite films. The second part of the study investigated the effects of glycerol content (0-20 wt%) and three plasticizers (glycerol, urea, formamide) on the structure and properties of the starch-clay nanocomposite films. With decreasing glycerol content, the extent of clay exfoliation increased. Films with 5% glycerol exhibited the lowest WVP, and the highest TS and glass transition temperature (T_g). The use of urea and formamide improved the dispersion of clay platelets. Compared to glycerol and urea, formamide has an intermediate hydrogen bond forming ability with starch. However, at the same level of plasticizer (15 wt%), formamide plasticized nanocomposite films exhibited the lowest WVP, highest TS and T_g . Results indicated that a

balance of interactions between starch, clay surface modifications and plasticizers might control the formation of nanocomposite structure, and in turn affect the performance of the nanocomposite films. The last part of the study investigated the effects of extrusion conditions (screw configuration, barrel temperature profile, screw speed and barrel moisture content) on the structure and properties of the starch-clay nanocomposite films. Increasing the shear intensity significantly improved the exfoliation and dispersion of clay platelets. The combination of lowest barrel moisture content (20%) and high shear screw configuration exhibited almost complete clay exfoliation and the lowest WVP and highest TS of all treatments. Increasing the barrel temperature also improved clay exfoliation and performance of films. The results suggested that, when polymer and clay are chemically compatible, optimization of process conditions (shear intensity, temperature etc.) can enable significant improvement in clay exfoliation and dispersion and the performance of nanocomposite films.

Table of Contents

List of Figures

List of Tables

Acknowledgements

I express my sincere gratitude to my major advisor Dr. Sajid Alavi, for his guidance, understanding, patience, and most importantly, his friendship during my graduate studies at K-State. His mentorship was paramount in providing a well rounded experience consistent with my long-term career goals.

I would like to thank my committee members, Dr. Paul Seib, Dr. Finlay MacRitchie, Dr.Thomas Herald, and Dr. Dale Schinstock, for their constant support and critical suggestions and advice that set the direction and focus of my research.

I would also like to thank Mr. Eric Maichael, Ron Stevenson, Zhiqiang Yang for their generous help in the experimental phase of this research. I would like to express my deep gratitude to my coworkers in our group: Dr. Enzhi Cheng, Dr. Shaowei Liu, Dr. Roderick Agbisit, Hyma Gajula for their friendship and companionship.

Most importantly, I would like to thank my wife Jianmin Zhou. She had taken most of the responsibilities for taking care of our baby and family during the past three and a half years. I thank her support, encouragement, understanding and love in dealing with all the challenges I have faced. Finally, I'd like to thank my parents for their incessant help and support; none of this would be possible without them.

CHAPTER 1 - Introduction

1.1 Food packaging

Foods are packaged to protect them from their environment and keep them in good condition while they are delivered to shops, stacked on market shelves or stored at home. Quality and shelf life are reduced when foods, through interaction with their environment, gain or lose moisture or aroma, take up oxygen (leading to oxidative rancidity), or become contaminated with microorganisms. Food packaging also provides important information to the consumer and enables convenient dispensing of food. Food packaging, however, has become a central focus of waste reduction efforts. Packaging represents approximately 30% of the weight of municipal solid waste but appears more significant because it constitutes close to two-thirds of trash volume due to its bulk (Krochta and De Mulder-Johnston 1997).

Plastics are widely used packaging materials for food and non-food products due to their desirable material properties and low cost. However, the merits of plastic packaging have been overshadowed by its non-degradable nature, thereby leading to waste disposal problems. The public is also gradually coming around to perceive plastic packaging as something that uses up valuable and scarce non-renewable natural resources like petroleum. Moreover, the production of plastics is relatively energy intensive and results in the release of large quantities of carbon dioxide as a byproduct, which is often believed to cause, or at least contribute to, global warming. Some recent research findings have also linked plastic packaging to some forms of cancer (Kirsch 2005; ElAmin 2005).

1.2 Bio-based packaging

Packaging materials based on polymers that are derived from renewable sources may be a solution to the above problems. Such polymers include naturally existing ones such as proteins, cellulose, starches and other polysaccharides, with or without modifications, and those synthesized chemically from naturally derived monomers such as lactic acid. These renewable polymers (or biopolymers) are not only important in the context of petroleum scarcity, but are

also generally biodegradable under normal environmental conditions.

Interest and research activity in the area of biopolymer packaging films have been especially intensive over the past ten years (Krochta and De Mulder-Johnston 1997; Tharanathan 2003). Table 1.1 contains examples of biopolymer films prepared using different techniques (Krochta and De Mulder-Johnston 1997). For food packaging, important film characteristics include mechanical properties such as tensile strength and elongation at break, and barrier properties such as moisture and oxygen permeabilities. For biopolymer materials to compete with synthetic plastics, they should be cost effective, and also the critical mechanical and/or barrier properties for the intended application must be matched. The latter is especially difficult in the case of moisture barrier properties, as can be seen from Table 1.1, because of the hydrophilic nature of most biopolymers, in comparison with hydrophobic synthetic polymers such as low density polyethylene (LDPE). Mechanical and oxygen barrier properties of most biodegradable packaging materials are moderate to good at low relative humidity (RH), but deteriorate exponentially with increase RH.

Among all biopolymers, starch is one of the leading candidates as it is abundant and cheap. The cost of regular and specialty starches ($ 0.20-0.70/lb) compares well with that of synthetic polymers such as LDPE, polystyrene (PS) and polyethylene terephthalate (PET) ($0.50-0.75/lb) (Krochta and De Mulder-Johnston 1997). Moreover, starch is completely and quickly biodegradable and easy to process because of its thermoplastic nature (Doane 1994). However, the earlier mentioned drawbacks of biopolymer packaging materials also need to be addressed for starch.

Many strategies have been developed to improve the barrier and mechanical properties of starch-based biodegradable packaging films. These include – 1) addition of plasticizers such as glycerol, urea and formamide, which aid in the thermoplastic process and also increase flexibility of the final product by forming hydrogen bonds with starch that replace the strong interactions between its hydroxyl groups (Ma et al 2004); 2) addition of other polymers or biodegradable polymers, like poly (vinyl alcohol) (PVOH), and polylactic acid (PLA), to produce materials with properties intermediate between the two components (Chen et al 1996; Ke and Sun 2000). The resultant blends can be better processed via extrusion or film blowing, and have mechanical and/ or barrier properties superior to starch alone; and 3) addition of compatilizers to lower the interfacial energy and increase miscibility of two incompatible phases (e.g., starch and synthetic

biodegradable polymers), leading to a stable blend with improved characteristics (Mani et al 1998).

However, none of the above mentioned methods can adequately meet the requirements of a cost effective biopolymer-based film that has properties close to those of synthetic plastic packaging. High costs of compatilizers and synthetic biodegradable polymers, such as PLA and PVOH, limit the level of their incorporation in starch. The resultant improvement in barrier and mechanical properties is also not very satisfactory. Therefore, there is a significant need for exploring new techniques to meet the challenges of developing high quality starch-based packaging films.

1.3 Nanotechnology and nanocomposites

Nanotechnology involves the study and use of materials at an extremely small scale – a few nanometers– and exploits the fact that the same material might have very different properties at this ultra-small scale than at the micro or macro level. The unique properties of nanostructured substances have opened windows of opportunity for the creation of high performance materials with a critical impact on food manufacturing, packaging, and storage (Moraru et al. 2003). An example is polymer-layered silicate (PLS) nanocomposites, a promising class of new materials that represent polymers filled with small inorganic layered silicate clays with a high aspect ratio. These PLS nanocomposites have been the focus of academic and industrial attention in recent years because they often exhibit substantially enhanced physical and/or chemical properties relative to the original polymer matrix (Sinha Ray and Okamoto 2003). The clays used in PLS nanocomposites include montmorillonite (MMT), hectorite and saponite, and their various modifications. Most importantly, these silicate clays are environmentally friendly, naturally abundant and economical.

The nanocomposites can be obtained by several methods, including in-situ polymerization, intercalation from solution or melt intercalation (Sinha Ray and Okamoto 2003). For real nanocomposites, other than micro- or macrocomposites, the clay layers must be uniformly dispersed in the polymer matrix, forming intercalated or exfoliated structure. Once clay intercalation or exfoliation has been achieved, improvement in properties can manifest as increase in tensile properties, as well as enhanced barrier properties, decreased solvent uptake, increased thermal stability and flame retardance. A diverse array of polymers have been used in

PLS nanocomposite formation to improve the properties of original polymers, ranging from synthetic non-degradable polymers, such as nylon (Kojima et al 1993a, 1993b), polystyrene (Vaia et al 1995; Vaia and Giannelis 1997), and polypropylene (Kurokawa et al 1996; Usuki et al 1997), to biopolymers, such as polylactic acid (Sinha Ray et al 2002a, 2002b).

Recently, there have been several attempts to enhance the end-use properties of starch in biodegradable packaging by fabricating starch-clay nanocomposites. De Carvalho et al (2001) provided an initial insight into the preparation and characterization of thermoplasticized starch-kaolin composites by melt intercalation techniques. Park et al (2002 and 2003) reported an increase in elongation at break and tensile strength by more than 20 and 25%, respectively, and a decrease in water vapor transmission rate by 35% for potato starch/MMT nanocomposites on addition of 5% clay. Wilhelm et al (2003) observed a 70% increase in tensile strength of Cará root starch/hectorite nanocomposite films at 30% clay level. However, the percentage of elongation decreased by 50%. Very recently, Avella et al (2005) reported the preparation of potato starch/MMT nanocomposite films for food packaging applications. Results showed an increase in mechanical properties. Furthermore, the conformity of the resulting material samples with actual packaging regulations and European directives on biodegradable materials was verified by migration tests and by putting the films into contact with vegetables and stimulants. Success of the above studies indicates that nanoclays show much promise in improving the mechanical and barrier properties of starch-based packaging materials.

1.4 Scope of this study

The research presented in this work will focus on the use of melt extrusion processing for synthesis of starch-clay nanocomposites to improve the barrier and mechanical properties of starch-based packaging films. The effects of chemical compatibility of starch, plasticizer and nanoclay, and melt extrusion conditions on the formation of nanostructure and properties of the resulted composite films will be investigated.

Chapter 2 presents a review of recent developments in biodegradable polymer-based nanocomposites, including a brief outline of layered silicate structures, nanocomposite synthesis, characterization, various biodegradable polymer-clay nanocomposites reported in literature and future trends in this area.

Chapter 3 investigates the influence of clay type (unmodified and organically modified

montmorillonite), clay content (0-21 wt%), starch source (corn, wheat and potato starch) and amylose content on the formation of nanostructure and properties of the starch-clay composite films. X-ray diffraction (XRD) and transmission electron microscopy (TEM) were utilized to characterize the structure and morphology of the starch-clay composites. Water vapor permeability (WVP) and tensile properties of the composite films were measured to analyze the improvement of material properties.

Chapter 4 deals with the effects of glycerol content (0–20 wt%) and three plasticizers (glycerol, urea, formamide) on the formation of nanostructure and properties of the starch-clay nanocomposite films. The chemical compatibility of starch, plasticizer, and clay and its effect on the structure and properties of nanocomposites are discussed.

Chapter 5 studies the effects of extrusion conditions (screw configuration, barrel temperature profile, screw speed and moisture content) on the formation of nanostructure and properties of the starch-clay nanocomposite films. In addition, the mechanisms of clay exfoliation and dispersion in the polymer matrix are elucidated.

Chapter 6 briefly summarizes the results and future research needs.

1.5 Reference

Avella, M., De Vlieger, J. J., Errico, M. E., Fischer, S., Vacca, P., and Volpe, M. G. 2005. Biodegradable starch/clay nanocomposite films for food packaging applications. Food Chemistry. 93: 467-474.

Chen, L., Iman, S. H., Stein, T. M., Gordon, S. H., Hou, C. T., and Greene, R. V. 1996. Starch-polyvinyl alcohol cast film-performance and biodegradation. Polym. Prepr. 37: 461-462.

De Carvalho, A. J. F., Curvelo, A. A. S., and Agnelli, J. A. M. 2001. A first insight on composites of thermoplastic starch and Kaolin. Carbohydrate Polymers. 45: 189-194.

Doane, W. M. 1994. Opportunities and challenges for new industrial uses of starch. Cereal Foods Worlds. 39(8): 556-563.

ElAmin, A. 2005. Common plastics packaging chemical linked to cancer. FoodProductionDaily e-newsletter (May 31, 2005). Retrieved from http://www.foodproductiondaily.com/news/ng.asp?id=60333-common-plastics packaging.

Ke, T., and Sun, X., 2000. Physical properties of poly(lactic acid) and starch composites with various blending Ratios. Cereal Chem. 77(6): 761-768.

Kirsch, C. 2005. Compounds in plastic packaging act as environmental estrogens altering breast genes. EurekAlert e-newsletter (April 18, 2005). Retrieved from http://www.eurekalert.org/pub_releases/2005-04/fccc-cip041405.php.

Kojima, Y., Usuki, A., Kawasumi, M., Okada, A., Fukushima, Y., Kurauchi, T., and Kamigaito, O. 1993a. Mechanical properties of nylon 6-clay hybrid. J. Mater. Res. 8: 1185-1189.

Kojima, Y., Usuki, A., Kawasumi, M., Okada, A., Kurauchi, T., and Kamigaito, O. 1993b. Sorption of water in nylon 6-clay hybrid. J. Appl. Polym. Sci. 49 : 1259-1264.

Krochta, J.M., and De Mulder-Johnston, C., 1997. Edible and biodegradable polymer films: challenges and opportunities. Food Technology. 51(2): 61-74.

Kurokawa, Y., Yasuda, H., and Oya, A., 1996. Preparation of a nanocomposite of polypropylene and smectite. J. Mater. Sci. Lett. 15: 1481-1483.

Ma, X., Yu, J., and Feng, J., 2004. Urea and formamide as a mixed plasticizer for thermoplastic starch. Polymer International. 53: 1780-1785.

Mani, R., Tang, J., and Bhattacharya, M. 1998. Synthesis and characterization of starch-graft-polycaprolactone as compatibilizer for starch/polycaprolactone blends. Macromolecular

Rapid Communications. 19(6): 283-286.

Moraru, C. I., Panchapakesan, C. P., Huang, Q., Takhistov, P., Liu, S., and Kokini, J. L. 2003, Nanotechnology: A new fronitier in food science. Food Technology. 57(12): 24-29.

Park, H., Li, X., Jin, C., Park, C., Cho, W., and Ha, C. 2002. Preparation and properties of biodegradable thermoplastic starch/clay hybrids, Macromol. Mater. Eng. 287: 553-558.

Park, H., Lee, W., Park, C., Cho, W., and Ha, C. 2003. Enviromentally friendly polymer hybrids part 1 Mechanical, thermal and barrier properties of thermoplastic starch/clay nanocomposites, Journal of Materials Science. 38: 909-915.

Sinha Ray, S., Yamada, K., Okamoto, M., and Ueda, K. 2002a. New polylactide/layered silicate nanocomposite: a novel biodegradable material. Nano Lett. 2: 1093–1096.

Sinha Ray, S., Maiti, P., Okamoto, M., Yamada, K., and Ueda, K. 2002b. New polylactide/layered silicate nanocomposites. 1. Preparation, characterization and properties. Macromolecule. 35: 3104–3110.

Sinha Ray, S., and Okamoto, M. 2003. Polymer/layered silicate nanocomposites: a review from preparation to processing. Prog. Polym. Sci. 28: 1539-1641.

Tharanathan, R. N. 2003. Biodegradable films and composite coatings: past, present and future. Trends in Food Science & Technology. 14: 71-78.

Usuki, A., Kato, M., Okada, A., and Kurauchi, T., 1997. Synthesis of polypropylene-clay hybrid. J. Appl. Polym. Sci. 63 : 137-139.

Vaia, R. A., Jandt, K. D., Kramer, E. J., and Giannelis, E. P. 1995. Kinetics of polymer melt intercalation. Macromolecules. 28: 8080-8085.

Vaia, R. A., and Giannelis, E. P., 1997. Polymer melt intercalation in organically-modified layered silicates: model predictions and experiment. Macromolecules. 30: 8000-8009.

Wilhelm, H. M., Sierakowski, M. R., Souza, G. P., and Wypych, F. 2003. Starch films reinforced with mineral clay. Carbohydrate Polymers. 52: 101-110.

Tables

Table 1.1 Examples of researched biopolymer films and their properties (Krochta and De Mulder-Johnston 1997).

Material	Film preparation	Moisture barrier[a]	Oxygen barrier[b]	Mechanical properties[c]	Cost, $/lb
Cellophane	Aqueous	Moderate	Good	Good	2.20
NC-W/Cellophane	NC-W coating	Good	Good	Good	2.40
Cellulose Acetate	Extrusion	Moderate	Poor	Moderate	1.60-2.10
Starch/PVOH	Extrusion	Poor	Good	Good	1.50-3.00
PHB/V	Extrusion	Good	Good	Moderate	3.00-6.00
PLA	Extrusion	Moderate	Poor	Good	1.00-5.00
MC	Aqueous-EtOH	Moderate	Moderate	Moderate	4.50-7.00
HPMC	Aqueous-EtOH	Moderate	Moderate	Moderate	4.75-7.00
HPMC:SA-PA/Wax	Aqueous-EtOH	Good	Moderate	NA	NA
High Amylose Starch	Aqueous	Poor	Moderate	Moderate	0.60-0.70
Gelatin	Aqueous	Poor	Good	NA	2.40-2.60
Zein	95%EtOH	Moderate	Moderate	Moderate	10.25-15.50
Gluten	Aqueous-EtOH	Moderate	Good	Moderate	0.80-0.90
SPI	Aqueous	Poor	Good	Moderate	1.30-1.70
Casein	Aqueous	Poor	Good	NA	2.75-3.25
WPI	Aqueous	Poor	Good	Moderate	6.00-12.00
Beeswax	Melt	Good	Poor	Poor	3.00-4.50

[a]Test conditions:38°C,90/0%RH
Poor=10-100 g*mm/m^2*d*kPa
Moderate=0.1-10 g*mm/m^2*d*kPa
Good=0.01-0.1 g*mm/m^2*d*kPa
(LDPE: 0.08 g*mm/m^2*d*kPa)

[b]Test conditions:25°C,0-50%RH
Poor=100-1000 cm^3*µm/m^2*d*kPa
Moderate=10-100 cm^3*µm/m^2*d*kPa
Good=1-10 cm^3*µm/m^2*d*kPa
(EVOH: 0.1 cm^3*µm/m^2*d*kPa)

[c]Test conditions:25°C,50%RH
Moderate TS=10-100MPa
Moderate E=10-50%
(LDPE: TS=13 MPa, E=500%)
(OPP: TS=165 MPa, E = 60%)

E=elongation, EVOH=ethylene vinyl alcohol polymer, HPMC=hydroxypropyl methyl cellulose, LDPE=low density polyethylene, MC=methyl cellulose, NC-W=nitrocellulose-wax, OPP=oriented polypropylene, PA=palmitic acid, PHB/V= poly(3-hydroxybutyrate)-co-(3-hydroxyvalerate), PLA=poly(lactic acid), PVOH=polyvinyl alcohol, SA=stearic acid, SPI=soy protein isolate, TS=tensile strength, WPI=whey protein isolate, NA=not applicable.

CHAPTER 2 - Recent Developments in Biodegradable Polymer Based Nanocomposites

Part of review manuscript

To be submitted to Critical Reviews in Food Science and Nutrition, Jan. 2008

2.1 Introduction

Recently, the utility of inorganic nanoparticles as additives to enhance polymer performance has been established. Various nanoreinforcements currently being developed are nanoclay (layered silicates) (Pinnavaia and Beall 2001), cellulose nanowhiskers (Neus Angles and Dufresne 2000, 2001), ultra fine layered titanate (Hiroi *et al*. 2004), and carbon nanotubes (Kumar 2004). Among these, up to now only the layered inorganic silicates like clays have attracted great attention by the packaging industry. This is not only due to their environmental friendliness, natural abundance and low cost but also due to their significant enhancements and relatively simple processability.

Polymer layered silicate (PLS) nanocomposite technology was first developed for automotive applications by Toyota researchers in the late 1980s (Fukushima and Inagaki 1987; Okada *et al*.1987) and Toyota was the first company to commercialize the nanocomposites (nylon 6-clay nanocomposites) (Ray 2006). In the following years, PLS nanocomposites have attracted increasing interest as a means for improving properties of synthetic polymers. These studies include nanocomposites of nylon 6-clay (Kojima *et al.* 1993 a, 1993 b), polyurethane-clay (Wang and Pinnavaia 1998), polypropylene-clay (Kurokawa *et al.* 1996; Usuki *et al.* 1997; Kawasumi *et al.* 1997), polyimide-clay (Yano *et al.* 1993, 1997), polystyrene-clay (Vaia *et al.* 1995; Vaia and Giannelis 1997) and polysiloxane-clay (Mark 1996) etc. With only a small percentage of silicate content (≤5%), the nanocomposites exhibit remarkable improvement in materials properties when compared with pristine polymer or conventional micro- and macro-composites. These improvements can include high modulus, increased strength and heat resistance, decreased moisture and gas permeability and flammability. Nanocomposites also offer extra benefits like low density, transparency, good flow, better surface properties and recyclability (Giannelis 1996).

Potential applications of these nanocomposites include automobiles (gasoline tanks, bumpers, interior and exterior panels etc.), construction (building sections, structural panels), aerospace (flame retardant panels, high performance components), electronics (printed circuit boards, electric components) and pigments (Ray 2006). In order to take advantage of their substantially enhanced properties, polymer nanocomposites have also been studied and commercialized for food packaging applications including injection molded bottles and orange

juice containers, coatings for paperboard juice cartons, and cast and blown films. Use of these nanocomposites for packaging with oxygen scavenging, reduced flavor scalping, increased heat resistance and high gas barrier properties has resulted in shelf-life of 3-5 years for packaged food (Sajilata *et al.* 2007).

In contrast to synthetic polymer based PLS nanocomposites, biodegradable polymer based PLS nanocomposites have received little attention in the open literature. However, several research groups did start the preparation and characterization of various kinds of biodegradable polymer nanocomposites showing properties suitable for a wide range of applications. In this part, the review will be restricted to biodegradable polymer based nanocomposites, including a brief outline of nanocomposite synthesis, characterization, recent developments in various biodegradable polymer nanocomposites reported and their future aspects.

2.2 Structure and properties of layered silicates

The most commonly used silicates in PLS nanocomposites include montmorillonite (MMT), hectorite and saponite, and their various modifications. Like talc and mica, which are better known minerals, these layered silicates belong to the general family of 2:1 layered silicates (or phyllosilicates) (Giannelis 1996). Their crystal lattice consists of a two-dimensional, 1nm thick layers which are made up of two tetrahedral sheets of silica fused to an edge-shaped octahedral sheet of either aluminum or magnesium hydroxide (Figure 2.1). The lateral dimensions of these layers vary from 30nm to several microns or larger, depending on the particular layered silicate. Stacking of the layers leads to a regular Van der Waals gap between the layers called the interlayer or gallery. Isomorphic substitution within the layers (for example, Al^{3+} replaced by Mg^{2+} or Fe^{2+}, or Mg^{2+} replaced Li^{+}) generates negative charges that are counterbalanced by alkali and alkaline earth cations situated inside the galleries.

In pristine layered silicates, the interlayer cations are usually hydrated Na^{+} or K^{+}, showing hydrophilic surface properties. Obviously, in this pristine state, layered silicates are only miscible with hydrophilic polymers. To render layered silicates miscible with hydrophobic polymers, one must convert the normally hydrophilic silicate surface to an organophilic one. Generally, this can be done by ion-exchange reactions with various organic cations (e.g.

alkylammonium cations, cationic surfactant etc.). The organic cations lower the surface energy of the silicate surface and result in a larger interlayer spacing. Additionally, the organic cations may contain various functional groups that react with the polymer to improve adhesion between the inorganic phase and the matrix.

Therefore, there are two particular characteristics of layered silicates exploited in PLS nanocomposites. The first is the ability of the silicate particles to disperse into individual layers. As a result, an aspect ratio as high as 1000 for fully dispersed individual layers can be obtained. The second characteristic is the ability to fine-tune their surface chemistry through ion exchange reactions with organic and inorganic cations.

2.3 Nanocomposite synthesis and characterization

For nanocomposite synthesis, polymer chains must diffuse into the galleries between silicate layers to produce structures ranging from intercalated to exfoliated (Figure 2.2). Intercalation occurs when a small amount of polymer penetrates into the galleries, resulting in finite expansion of the silicate layers. This leads to a well-ordered multilayered structure with a repeat distance of a few nanometers, and is observed in systems with limited miscibility. Extensive polymer penetration leads to exfoliation or delamination of silicate layers. An exfoliated nanocomposite consists of nanometer thick platelets distributed homogeneously throughout the polymer matrix. In contrast, when the polymer and silicate are immiscible, the layers do not separate and exist as agglomerates or tactoids.

The complete dispersion of clay platelets in a polymer optimizes the number of available reinforcing elements for carrying an applied load and deflecting cracks. The coupling between the tremendous surface area of the clay and the polymer matrix facilitates stress transfer to the reinforcement phase, allowing for such mechanical improvements. In addition, the impermeable clay layers mandate a tortuous pathway for a permeant to transverse the nanocomposites (Figure 2.3). The enhanced barrier characteristics, chemical resistance, reduced solvent uptake and flame retardance of polymer-clay nanocomposites all benefit from the hindered diffusion pathway through the nanocomposites.

Synthesis of PLS nanocomposites has initially involved either intercalation of a suitable

monomer followed by polymerization (in-situ polymerization) (Okada *et al*.1987; Messersmith and Giannelis 1993) or polymer intercalation from solution, (Ruiz-Hitzky,E. 1990; Wu and Lerner 1993) i.e., intercalation of dissolved polymer from a solution. Various mono and multifunctional monomers have already been used, yielding linear and cross-linked polymer matrices, respectively. Alternatively, a polymer solution can be used. However, for most important polymers, both in-situ polymerization and interaction from solution are limited because neither a suitable monomer nor a compatible polymer-silicate solvent system is always available. Vaia *et al*. (1993) discovered a more versatile and environmentally benign approach based on direct polymer melt intercalation. The process involves mixing the layered silicate with the polymer and heating the mixture above the softening point of the polymer. Accordingly some easy accessible processing techniques like hot-mixing, melt-extrusion can be directly used for nanocomposite synthesis. Recently, a new alternative method for the preparation of nanocomposites, which involves a solid-state mixing at room temperature (ball milling) (Sorrentino *et al*. 2005; Mangiacapra *et al*. 2006) was proposed. In this case, solid layered dispersion was promoted by the energy transfer between milling tools (generally balls) and polymer/inorganic particles mixture, which in turn results in grinding and intimate mixing.

Generally, the structure of nanocomposites can be characterized by two complementary analytical techniques, namely, X-ray diffraction (XRD) and transmission electron microscopy (TEM). XRD is used to identify intercalated structures by determination of the basal spacing (d-spacing). Intercalation of the polymer chains increases the interlayer spacing and according to Bragg's law, it should cause a shift of the diffraction peak towards lower angle. As more polymers enter the interlayer spacing, the clay platelets become disordered, thus causing broader peaks and a wider distribution of such peaks, which implies exfoliation of clay platelets in the polymer matrix (McGlashan and Halley 2003). In addition, TEM images provide further evidence for the occurrence of intercalation or exfoliation. TEM allows a qualitative understanding of the internal structure, spatial distribution and dispersion of the specific clay platelets within the polymer matrix through direct visualization.

Both TEM and XRD are essential tools for evaluating nanocomposite structure. However, there are still some other techniques used to gain greater insight about nanocomposite structure, such as DSC (Giannelis 1996), NMR (VanderHart *et al*. 2001), FTIR (Loo and Gleason 2003).

2.4 Biodegradable polymer based nanocomposites

The extraordinary success of the nanocomposite concept in the area of synthetic polymers has stimulated the new research on nanocomposites based on biodegradable polymers as matrix. So far, the most studied biodegradable polymer nanocomposites are starch, cellulose, pectin, chitosan, gluten, gelatin, plant oils, polylactide (PLA), polyhydroxy-butyrate (PHB), polycaprolactone (PCL), poly (butylenes succinate) (PBS), and poly (vinyl alcohol) (PVOH) etc.

2.4.1 Starch based nanocomposites

Owing to its complete biodegradability, wide availability and low cost, starch certainly attracted more attention than other natural biopolymers. De Carvalho *et al*. (2001) provided a first insight in the preparation and characterization of thermoplasticized starch-kaolin composites by melt intercalation techniques. After that, several researches have been performed on the preparation of starch/clay nanocomposites by melt intercalation in details (Park *et al*. 2002 and 2003; Wilhelm *et al.* 2003; Avella *et al.* 2005; Chen and Evans 2005; Huang *et al.* 2005). Park *et al*. (2002 and 2003) reported an increase in elongation at break and tensile strength by more than 20% and 25%, respectively, and a decrease in water vapor transmission rate by 35% for potato starch/MMT nanocomposites on addition of 5% clay. In addition, the decomposition temperature was increased, indicating a better thermal stability for starch/MMT nanocomposites. Wilhelm *et al*. (2003) observed a 70% increase in tensile strength of Cará root starch/hectorite nanocomposite films at 30% clay level. However, the percentage of elongation decreased by 50%. Very recently, Avella *et al.* (2005) reported the preparation of starch/MMT nanocomposite films for food packaging applications. Mechanical characterization results show an increase of modulus and tensile strength. Furthermore, the conformity of the resulting material samples with actual regulations and European directives on biodegradable materials was verified by migration tests and by putting the films into contact with vegetables and stimulants.

In some other reports, starch and biodegradable polyester blends were used for synthesis of starch/polyester/clay nanocomposites (McGlashan and Halley 2003; Kalambur and Rizvi 2004 and 2005). McGlashan and Halley (2003) used melt extrusion methods for the preparation of starch/polyester/organically modified clay (organoclay) nanocomposites. XRD data indicated that the best results were obtained for 30wt% starch blends, and the level of delamination

depends on the ratio of starch to polyester and amount of organoclay added. The results exhibited an increase in tensile strength of 40%, Young's modulus of 275% and strain at break of 40% on addition of 5% clay than without clay. Kalambur and Rizvi (2005) reported the preparation of starch/PCL/organoclay nanocomposites by reactive extrusion. The results showed that the elongation of these nanocomposites was comparable to that of 100% polyester.

2.4.2 Cellulose based nanocomposites

Cellulose from trees is attracting interest as a feedstock for making polymers that can substitute for petroleum-based polymers in the commercial market. Cellulosic derived plastics such as cellulose acetate (CA), cellulose acetate propionate (CAP), and celluose acetate butyrate (CAB) are thermoplastic materials produced through esterification of cellulose. CA is of particular interest because it is a biodegradable polymer and has excellent optical clarity and high toughness. Park *et al.* (2004a) first reported the preparation of biodegradable plasticized CA/clay hybrid nanocomposites. Melt processing through extrusion-injection molding is adopted in fabricating the nanocomposites from CA power, eco-friendly triethyl citrate (TEC) plasticizer and organoclay. The results showed that the addition of TEC plasticizer at 20 wt% exhibited the best intercalation and exfoliation of clays as well as the best physical and mechanical properties of the resulting nanocomposites. The tensile strength, modulus and heat deflection temperature was improved and the water vapor permeability was 2 times reduced, but the impact strength was decreased. In their later work (Park *et al.*, 2004b), they investigated the effect of compatilizer maleic anhydride grafted cellulose acetate butyrate (CAB-g-MA) on the nanostructure of the biodegradable CA/Organoclay nanocomposites. They reported that nanocomposites with 5 wt% compatilizer contents showed better exfoliated structure than the counterpart without compatilizer hybrid.

2.4.3 Pectin based nanocomposites

Pectin is a secondary product of fruit juice, sunflower oil, and sugar manufacture. As food processing industry wastes, pectin is therefore a very good candidate for eco-friendly biodegradable materials. Mangiacapra *et al.* (2006) reported the preparation of natural pectins and MMT nanocomposites to improve the mechanical and barrier properties of natural pectins. They used a new alternative method for the preparation of nanocomposites, which involves a solid-state mixing at room temperature (ball milling). It was found that the physical properties

were improved in the nanocomposites. The elastic modulus increased from 1630 to 2962 MPa, the oxidation was delayed by 30^{o}C and diffusion of water vapor and oxygen was found lower than the pure pectin.

2.4.4 Chitosan based nanocomposites

Chemically derived by deacetylation of chitin, an abundant polysaccharide found in shellfish, chitosan possesses a unique cationic nature relative to other neutral or negatively charged polysaccharides. In addition, chitosan is a nontoxic natural polysaccharide and is compatible with living tissue. These appealing features make chitosan widely applicable in wound healing, production of artificial skin, food preservation, cosmetics, and wastewater treatment (Weiss *et al.* 2006).

For chitosan based nanocomposite preparation, only one publication was found (Darder *et al.* 2003). In their work, the intercalation of chitosan in layered silicates giving biopolymer-clay nanocomposites appears as an improving way to develop robust and stable sensors useful for anionic detection in aqueous media.

2.4.5 Gluten based nanocomposites

Wheat gluten is an interesting alternative to synthetic plastics in food packaging applications due to its high gas barrier properties and relatively hydrophobic nature compared to other natural polymers. Currently only one publication was found dealing with wheat gluten based nancomposites (Olabarrieta *et al.* 2006). In their study, two types of nanoclay Cloisite Na^{+} (MMT) and Cloisite 10A (quaternary ammonium modified MMT) were used for the synthesis of nanocomposites. The films were cast from pH 4 or pH 11 ethanol/water solutions. It was shown that the film prepared from pH11 solution containing natural MMT was, as revealed by TEM and XRD, almost completely exfoliated. This film was consequently also the strongest, the stiffest, and the most brittle film. In addition, it also showed the greatest decrease in water vapor permeability.

2.4.6 Gelatin based nanocomposites

Gelatin is obtained by hydrolytic cleavage of collagen chains. Edible coatings with gelatin reduce oxygen, moisture, and oil migration or can carry an antioxidant or antimicrobial. However, its poor mechanical properties limit its application. Zheng *et al.* (2002) prepared

gelatin/MMT nanocomposites for the first time with the expectation that those material properties of gelatin will be improved after nanocomposite preparation. In their results, the tensile strength and Young's modulus of formed nanocomposites were improved notably, which varied with MMT content and the pH of the gelatin matrix.

2.4.7 Plant oil based nanocomposites

Natural oils are expected to be an ideal chemical feedstock because of their abundance and extensive applications such as coatings, ink, and agrochemicals. However, these oil-based polymeric materials do not show properties of rigidity and strength required for packaging applications. In this case, Uyama *et al.* (2003) synthesized new green nanocomposites consisting of plant oils and clay with much improved properties. They used epoxidized soybean oil (ESO) as an organic monomer. The nanocomposite was synthesized by the curing of ESO using thermally latent cationic catalyst in the presence of octadecyl ammonium modified MMT at 150^{o}C. During the thermal treatment, the cross-linking of the epoxy group took place, yielding an insoluble polymer network. The reinforcement effect by the addition of the clay was confirmed by dynamic viscoelasticity analysis and furthermore, the nanocomposite exhibited flexible properties. Recently, Miyagawa *et al.* (2005) reported the preparation of novel biobased nanocomposites from functionalized vegetable oil and organoclay. They used anhydride-cured epoxidized linseed oil or octyl epoxide linseedate/diglycidyl ether of bisphenol F epoxy matrix for the preparation of nanocomposites. The sonication technique was utilized. Both TEM micrographs and XRD data showed that clay nanoplatelets were completely exfoliated. These homogeneous dispersion and complete exfoliation result in the excellent improvement of the elastic modulus of nanocomposites. In addition, Wool and Sun (2005) gave a very detailed description of preparation and properties of nanoclay (organoclay)-soybean oil composites. In their study, three different functionalized triglyceride monomers: acrylated epoxidized soybean oil, malleinized acrylated epoxidized soybean oil and soybean oil pentaerythritol maleates were used. The results showed that the exfoliated nanocomposites significantly increased the flexural properties.

2.4.8 PLA based nanocomposites

To date, PLA is the biopolymer with the highest potential for a commercial major scale production of renewable packaging materials. Lactic acid, the monomer of PLA, may easily be

produced by fermentation of carbohydrate feedstock. PLA has good mechanical properties, thermal plasticity and biocompatibility and is readily fabricated. It can be formed into films or used to make molded objects. In addition, it is compatible with many foods, such as dairy products, beverage, fresh meat products and ready meals.

However, the large-scale use of PLA packaging material is still hampered by its high cost as well as its relatively low performance compared to synthetic plastics. In this case, the use of nanoclay as a reinforcement agent provides the promise to expand the application of PLA. A lot of publications (Ogata *et al.* 1997; Bandyopadhyay *et al.* 1999; Maiti *et al.* 2002; Pluta *et al.* 2002; Sinha Ray *et al.* 2002a, 2002b, 2002c, 2003a, 2003b; Chang *et al*. 2003; Krikorian *et al*. 2003; Lee *et al*. 2003; Paul *et al*. 2003; Cabedo *et al.* 2006) reported the use of PLA for the preparation of polymer/clay nancomposite materials.

Ogata *et al.* (1997) first prepared PLA/organoclay blends by dissolving the polymer in hot chloroform in the presence of dimethyl distearyl ammonium modified MMT. Their results showed that a strong tendency of tactoid formation was observed by the solvent-cast method.

After that, Bandyopadhyay *et al.* (1999) reported the successful preparation of PLA-organoclay nanocomposites by melt extrusion technique with much improved thermal and mechanical properties. Sinha Ray *et al.* (2002a, 2002b, 2002c) also used melt extrusion techniques for the preparation of PLA/organoclay nanocomposites. XRD patterns and TEM observations clearly established that the silicate layers of the clay were intercalated, and randomly distributed in the PLA matrix. The intercalated nanocomposites exhibited remarkable improvement of material properties in both solid and melt states as compared to that of PLA matrices without clay.

Maiti *et al.* (2002) prepared a series of PLA/layered silicate nanocomposites with three different types of pristine layered silicates, i.e. saponite, MMT, and synthetic mica, and each was modified with alkylphosphonium salts having different chain lengths. Their study showed that miscibility of an organic modifier (phosphonium salt) and PLA is enhanced with a higher chain length of modifier. They also studied the effects of dispersion, intercalation and aspect ratio of the clay on the material properties.

Nanocomposites of the PLA and Polycaprolactone (PCL) blends were obtained by melt-mixing with a properly modified kaolinite (Cabedo *et al.* 2006). Blending of PCL was aimed for decreasing the brittleness of PLA. Also, in this case, all nanocomposites with 4% modified

kaolinite showed better processability, thermal stability and improvement in the mechanical properties with regard to the polymer and blends without clay.

2.4.9 PHB based nanocomposites

PHB is also a naturally occurring polyester produced by numerous bacteria in nature as intracellular reserve of carbon or energy. PHB is a typical highly crystalline thermoplastic with a very low water vapor permeability which is close to that of low density polyethylene (LDPE). However, the stiffness and brittleness of PHB, due to its relatively high melting temperature and high crystallinity, have limited its application (Xing *et al.* 1998). Still, synthesis of PLA nanocomposites could be one of the efficient ways to solve the problems.

Maiti *et al.* (2003) reported the first preparation of PHB/organoclay nanocomposite by melt extrusion method. XRD patterns showed the formation of a well-ordered intercalated nanocomposite structure. However, the nanocomposites based on organically modified MMT showed severe degradation tendency because thermoplastic PHB is very unstable and degrades at elevated temperature near its melting point. Although it seems the formation of nanocomposite materials from PHB is difficult, rather moderate improvements in properties were found.

2.4.10 PCL based nanocomposites

PCL is linear polyester manufactured by ring-opening polymerization of ε-caprolactone. It is a type of synthetic biodegradable polymer from petroleum sources. PCL exhibits high elongation at break and low modulus. Its physical properties and commercial availability make it very attractive as a material for commodity applications. There have been lots of attempts to prepare PCL/organoclay nanocomposites with much improved mechanical and material properties than that of neat PCL (Messersmith and Giannelis 1993 and 1995; Jimenez *et al.* 1997; Gorrasi *et al.* 2002, 2003, 2004; Lepoittevin *et al.* 2002; Pantoustier *et al.* 2002; Utracki *et al.* 2003; Di *et al.* 2003).

An earlier effort to prepare PCL-clay nanocomposites by in situ polymerization of ε-caprolactone in Cr^{3+}-fluorohectorite was not successful (Messersmith and Giannelis 1993). Only a very limited degree of intercalation of the PCL polymer into the hydrophilic clay galleries was observed, meaning the catalytic properties of Cr^{3+}went unutilized. When the inorganic cations were replaced by the protonated 12-aminododecanoic acid, followed by the in situ polymerization of ε-caprolactone at 170 ^{o}C, a higher degree of silicate nanolayer dispersion in

the polymer matrix was achieved (Messersmith and Giannelis, 1995). The PCL-clay nanocomposite film was prepared by a casting technique. It was found that the film showed a five fold reduction in permeability compared to the pure polymer at the addition of 4.8% clay.

Recently, Di *et al.* (2003) reported the preparation of PCL/organoclay nanocomposites in the molten state, using a twin screw extruder. In their study, the exfoliation of the organoclay was achieved via a melt mixing process in an internal mixer and showed a dependence on the type of organic modifier, the organoclay contents, and the processing temperature. The PCL/organoclay nanocomposites exhibited a significant enhancement in their mechanical properties and thermal stability and also showed a much higher complex viscosity than the neat PCL due to the exfoliation of the organoclay.

2.4.11 PBS based nanocomposites

PBS is chemically synthesized by the polycondensation of 1,4-butanediol with succinic acid. PBS has good biodegradability, melt processability, and thermal and chemical resistance. Nanocomposites based on PBS and organoclay often exhibit remarkably improved mechanical and various other properties as compared to those of virgin polymer containing small amount of layered silicate (≤5 wt%).

Sinha Ray *et al.* (2002d, 2003c) reported the first preparation of PBS/organoclay nanocomposites by melt extrusion processing. The intercalated nanocomposites exhibited remarkable improvement of mechanical properties in both solid and melt states as compared with that of PBS matrix without clay. Okada *et al.* (2003) also prepared PBS/organoclay nanocomposite by melt extrusion technique. They used maleic anhydride grafted PBS for the preparation of nanocomposites. XRD patterns and TEM images clearly indicated the formation of intercalated nanostructure.

2.4.12 PVOH based nanocomposites

PVOH is a water soluble polymer extensively used in paper coating, textile sizing, and flexible water-soluble packaging films. PVOH/layered silicate nanocomposite materials may offer a viable alternative for these applications to heat treatments (that may cause polymer degradation) or conventional filled PVOH materials (that are optically opaque) (Strawhecker and Manias 2000).

In 1963, Greenland (1963) reported the first fabrication of PVOH/MMT composites by a

solvent casting method using water as a co-solvent. In 2000, Strawhecker and Manias (2000) used the same solvent casting method in attempts to produce PVOH/MMT nanocomposite films. The inorganic layers promoted a new crystalline phase different to the one of the respective neat PVOH, characterized by higher melting temperature and a different crystal structure. The results showed that for a 5 wt% exfoliated composite, the softening temperature increased by 25 ^{o}C and the Young's modulus tripled with a decrease of only 20% in toughness, whereas there was also a 60% reduction in the water permeability. Furthermore, the nanocomposites retained their optical clarity.

2.5 Future Aspects

For biodegradable packaging materials to compete with non-biodegradable synthetic polymers, the critical mechanical, optical, and barrier properties for the intended application must be matched. The nanocomposite concept represents a stimulating route for creating new and innovative materials, also in the area of biodegradable polymers. Starch, PLA, PCL etc. based biodegradable nanocomposites have been prepared with improved mechanical, barrier and thermal properties. These materials are even able to compete with synthetic polymeric materials in some aspects in the application of food packaging.

On the other hand, nanocomposites can also be designed to be used as a carrier of antimicrobials and additives. Recent studies have demonstrated their ability to stabilize the additives and efficiently control their diffusion into the food system (Sorrentino *et al.* 2007). This control can be especially important for long-term storage of food or for imparting specific desirable characteristics, such as flavor, to a food system.

Despite the great possibilities existing for packaging in bio-based nanocomposite material, the present low level of production, some property limitation and high costs restrict them for a wide range of applications. Therefore, improvements in nanocomposite formulation, production practices, economies of scale, and increasing costs for fossil resources could all be necessary to produce a more favorable economic situation for biodegradable polymers.

2.6 References

Avella, M., De Vlieger, J. J., Errico, M. E., Fischer, S., Vacca, P., and Volpe, M. G. (2005). Biodegradable starch/clay nanocomposite films for food packaging applications. *Food chemistry*. 93: 467-474.

Bandyopadhyay, S., Chen, R., and Giannelis, E. P. (1999). Biodegradable organic inorganic hybrids based on poly(L-lactic acid). *Polym Mater Sci Eng.* 81: 159-160.

Cabedo, L., Feijoo, J. L., Villanueva, M. P., Lagaron, J. M., and Gimenez, E. (2006). Optimization of biodegradable Nanocomposites based on aPLA/PCL blends for food packaging applications. *Macromol. Symp*. 233: 191-197.

Chang, J. H., Uk-An, Y., and Sur, G. S. (2003). Poly(lactic acid) nanocomposites with various organoclays. I. thermomechanical properties, morphology, and gas permeability. *J Polym Sci Part B: Polym Phys.* 41: 94–103.

Chen, B., and Evans, J. R. G. (2005). Thermplastic starch-clay nanocomposites and their characterisitics. *Carbohydrate polymers*. 61: 455-463.

Darder, M., Colilla, M., and Ruiz-Hitzky, E. (2003). Biopolymer-clay nanocomposites based on chitosan intercalated in montmorillonite. *Chem. Mater*. 15: 3774-3780.

De Carvalho, A. J. F., Curvelo, A. A. S., and Agnelli, J. A. M. (2001). A first insight on composites of thermoplastic starch and Kaolin. *Carbohydrate Polymers*. 45: 189-194.

Di, Y., Iannace, S., Maio, E. D., and Nicolais, L. (2003) Nanocomposites by melt intercalation based on polycaprolactone and organoclay. *J Polym Sci Part B: Polym Phys.* 41:670–678.

Fukushima, Y., and Inagaki, S. (1987). Synthesis of an intercalated compound of monmorillonite and 6-polyamide. *Journal of Inclusion Phenomena* 5: 473-482.

Giannelis, E. P. (1996). Polymer layered silicate nanocomposites. *Advanced Materials*. 8(1): 29-35.

Gorrasi, G., Tortora, M., Vittoria, V., Galli, G., and Chiellini, E. (2002). Transport and mechanical properties of blends of poly (ε-caprolactone) and a modified montmorillonite-poly(ε -caprolactone) nanocomposite. *Journal of Polymer Science, Part B: Polymer Physics*. 40: 1118-1124.

Gorrasi, G., Tortora, M., Vittoria, V., Pollet, E., Alexandre, M., and Dubois, P. (2004).

Physical properties of poly (ε-caprolactone) layered silicate nanocomposites prepared by controlled grafting polymerization. *Journal of Polymer Science, Part B: Polymer Physics*, 42: 1466-1475.

Gorrasi, G., Tortora, M., Vittoria, V., Pollet, E., Lepoittenvin, B., and Alexandre, M. (2003). Vapor barrier properties of polycaprolactone montmorillonite nanocomposites: effect of clay dispersion. *Polymer.* 44, 2271-2279.

Greenland, D. J. (1963). Adsorption of poly(vinyl alcohols) by montmorillonite. *J Colloid Sci.* 18: 647–664.

Hiroi, R., Sinha Ray, S., Okamoto, M., and Shiroi T. (2004). Organically modified layered titanate: a new nanofiller to improve the performance biodegradable polylactide. *Macromol Rapid Ommun*. 25: 1359-1363.

Huang, M., Yu, J., and Ma, X. (2005). High mechanical performance MMT-urea and formamide-plasticized thermoplastic cornstarch biodegradable nanocomposites. *Carbohydrate polymers.* 62: 1-7.

Jimenez, G., Ogata, N., Kawai, H., and Ogihara, T. (1997). Structure and thermal/mechanical properties of poly(ecaprolactone)–clay blend. *J Appl Polym Sci.* 64: 2211–2220.

Kalambur, S., and Rizvi, S. S. H. (2004). Rapid report starch-based nanocomposites by reactive extrusion processing. *Polymer International*. 53: 1413-1416.

Kalambur, S., and Rizvi, S. S. H. (2005). Biodegradable and functionally superior starch-polyester nanocomposites from reactive extrusion. *Journal of Applied Polymer Science*. 96: 1072-1082.

Kawasumi, M., Hasegawa, N., Kato, M., Usuki, A., and Okada, A. (1997). Preparation and mechanical properties of polypropylene-clay hybrids. *Macromolecules.* 30: 6333-6338.

Kojima, Y., Usuki, A., Kawasumi, M., Okada, A., Fukushima, Y., Kurauchi, T., and Kamigaito, O. (1993a). Mechanical properties of nylon 6-clay hybrid. *J. mater. Res.* 8: 1185-1189.

Kojima, Y., Usuki, A., Kawasumi, M., Okada, A., Kurauchi, T., and Kamigaito, O. (1993b). Sorption of water in nylon 6-clay hybrid. *J. Appl. Polym. Sci.* 49 : 1259-1264.

Krikorian, V., and Pochan, D. (2003). Poly(L-lactide acid)/layered silicate nanocomposite: fabrication, characterization, and properties. *Chem Mater.* 15: 4317–4324.

Kumar, S. (2004). Polymer/carbon nanotube composites: Challenges and opportunities. *Polymeric Materials Science and Engineering*. 90: 59-60.

Kurokawa, Y., Yasuda, H., and Oya, A. (1996). Preparation of a nanocomposite of polypropylene and smectite. *J. Mater. Sci. Lett.* 15: 1481-1483.

Lee, J. H., Park, T. G., Park, H. S., Lee, D. S., Lee, Y. K., and Yoon, S. C. (2003). Thermal and mechanical characteristics of poly(L-lactic acid) nanocomposite scaffold. *Biomaterials.* 24: 2773–2778.

Lepoittevin, B., Devalckenaere, M., Pantoustier, N., Alexandre, M., Kubies, D., and Calberg, C. (2002). Poly(ecaprolactone)/clay nanocomposites prepared by melt intercalation: mechanical, thermal and rheological properties. *Polymer.* 43: 4017–4023.

Loo, L. S., and Gleason, K. K. (2003). Fourier transforms infrared investigation of the deformation behavior of montmorillonite in nylon6/clay nanocomposite. *Macromolecules.* 36: 2587-2590.

Maiti, P., Yamada, K., Okamoto, M., Ueda, K., and Okamoto, K. (2002). New polylactide/layered silicate nanocomposites: role of organoclay. *Chem Mater*. 14: 4654–4661.

Maiti, P., Batt, C. A., and Giannelis, E. P. (2003). Renewable plastics: synthesis and properties of PHB nanocomposites. *Polym Mater Sci Eng.* 88: 58–59.

Mangiacapra, P., Gorrasi, G., Sorrentino, A., and Vittoria, V. (2006). Biodegradable nanocomposite obtained by ball milling of pectin and montmorillonites. *Carbohdrate Polymer*. 64(4): 516-523.

Mark, J. E. (1996). Ceramic-reinforced polymers and polymer-modified ceramics. *Polym. Eng. Sci.* 36: 2905-2920.

McGlashan, S. A., and Halley, P. J. 2003. Preparaion and characterization of biodegradable starch-based nanocomposite materials. *Polymer international*. 52: 1767-1773.

Messersmith, P. B., and Giannelis, E. P. (1993). Polymer-layered silicate nanocomposites: in situ intercalative polymerization of ε-caprolactone in layered silicates. *Chem Mater*. 5: 1064-1066.

Messersmith, P. B., and Giannelis, E. P. (1995). Synthesis and barrier properties of poly (ε-caprolactone) – layered silicate nanocomposites. *J. Polym. Sci., Part A: Polym Chem*. 33: 1047-1057.

Miyagawa, H., Misra M., Drazal, L. T., and Mohanty, A. K. (2005). Novel biobased

nanocomposites from functionalized vegetable oil and organically-modified layered silicate clay. *Polymer*. 46: 445-453.

Neus Angles, M., and Dufresne, A. (2000). Plasticized starch/tunicin whiskers nanocomposites. 1. Structural analysis. *Macromolecules.* 33: 8344-8353

Neus Angles, M., and Dufresne, A. (2001). Plasticized starch/tunicin whiskers nanocomposite materials. 2. Mechanical behavior. *Macromolecules.* 34: 2921-2931

Ogata, N., Jimenez, G., Kawai, H., and Ogihara, T. (1997). Structure and thermal/mechanical properties of poly(L-lactide)-clay blend. *J. Polym Sci Part B: Polym Phys*. 35: 389-396.

Okada, A., Kawasumi, M., Kurauchi, T., and Kamigaito, O. (1987). Synthesis of. nylon-6-clay hybrid. *Polymer Preparation.* 28: 447–449.

Okada, K., Mitsunaga, T., and Nagase, Y. (2003). Properties and particles dispersion of biodegradable resin/clay nanocomposites. *Korea-Australia Rheology Journal*. 15(1): 43-50.

Olabarrieta, I., Gallstedt, M., Ispizua, I., Sarasua, J. R., and Hedenqvist, M. S. (2006). Properties of aged montmorillonite-wheat gluten composite films. Journal of Agricultural and *Food Chemistry.* 54: 1283-1288.

Pantoustier, N., Lepoittevin, B., Alexandre, M., Kubies, D., Calberg, C., and Jerome, R. (2002). Biodegradable polyester layered silicate nanocomposites based on poly(ε -caprolactone). *Polym Eng Sci.* 42: 1928–1937.

Park, H., Li, X., Jin, C., Park, C., Cho, W., and Ha, C. (2002). Preparation and properties of biodegradable thermoplastic starch/clay hybrids. *Macromol. Mater. Eng.* 287: 553-558.

Park, H., Lee, W., Park, C., Cho, W., and Ha, C. (2003). Enviromentally friendly polymer hybrids. part 1 Mechanical, thermal and barrier properties of thermoplastic starch/clay nanocomposites. *Journal of Materials Science*. 38: 909-915.

Park, H., Misra, M. Drzal, L. T., and Mohanty, A. K. (2004a). “Green” Nanocomposites from cellulose acetate bioplastic and clay: Effect of Eco-friendly Triethyl Citrate Plasticizer. *Biomacromolecules.* 5: 2281-2288.

Park, H., Liang, X., Mohanty, A. K., Misra, M., and Drzal, L. T. (2004b). Effect of Compatibilizer on nanostructure of the biodegradable cellulose acetate/organoclay nanocomposites. *Macromolecules.* 37: 9076-9082.

Paul, M. A., Alexandre, M., Degee, P., Calberg, C., Jerome, R., and Dubois, P. (2003).

Exfoliated polylactide/clay nanocomposites by in situ coordination–insertion polymerization. *Macromol Rapid Commun.* 24: 561–566.

Pinnavaia, T. J., and Beall, G. W. (2001). Polymer-Clay Nanocomposites. John Wiley & Sons, Inc., NewYork.

Pluta, M., Galeski, A., Alexandre, M., Paul, M. A., and Dubois, P. (2002). Polylactide/montmorillonite nanocomposites and microcomposites prepared by melt blending: structure and some physical properties. *Journal of Applied Polymer Science.* 86(6): 1497-1506.

Ray, S., Quek, S. Y., Easteal, A., and Chen, X. D. (2006) The potential use of polymer-clay nanocomposites in food packaging. *International Journal of Food Engineering.* 2 (4): 1-11.

Ruiz-Hitzky, E., and Aranda, P. (1990). Polymer-salt intercalation complexes in layer silicates. *Advanced Materials*. 2(11): 545-547.

Sajilata, M. G., Savitha, K, Singhal, R. S., and Kanetkar, V. R. (2007). Scalping of flavors in packaged foods. *Comprehensive Reviews in Food Science and Safety*. 6: 17-35.

Sinha Ray, S., Okamoto, K., Yamada, K., and Okamoto, M. (2002a). Novel porous ceramic material via burning of polylactide/layered silicate nanocomposite. *Nano Lett.* 2: 423–426.

Sinha Ray, S., Yamada, K., Okamoto, M., and Ueda, K. (2002b). New polylactide/layered silicate nanocomposite: a novel biodegradable material. *Nano Lett.* 2: 1093–1096.

Sinha Ray, S., Maiti, P., Okamoto, M., Yamada, K., and Ueda, K. (2002c). New polylactide/layered silicate nanocomposites. 1. Preparation, characterization and properties. *Macromolecule*. 35: 3104–3110.

Sinha Ray, S., Okamoto, K., Maiti, P., and Okamoto, M. (2002d). New poly(butylenes succinate)/layered silicate nanocomposites.1. Preparation, characterization, and mechanical properties. *J Nanosci Nanotech*. 2: 171–176.

Sinha Ray, S., Yamada, K., Okamoto, M., and Ueda, K. (2003a). New polylactide/layered silicate nanocomposites. 2. Concurrent improvements of material properties, biodegradability and melt rheology. *Polymer*. 44: 857–866.

Sinha Ray, S., Yamada, K., Okamoto, M., Ogami, A., and Ueda, K. (2003b). New polylactide/layered silicate nanocomposites. 3. High performance biodegradable materials. *Chem Mater*. 15: 1456–1465.

Sinha Ray, S., Okamoto, K., and Okamoto, M. (2003c). Structure–property relationship in biodegradable poly(butylene succinate)/layered silicate nanocomposites. *Macromolecules.* 36: 2355–2367.

Sorrentino, A., Gorrasi, G., Tortora, M., vittoria V., Costantino, U., and Marmottini, F. (2005). Incorporation of Mg-Al Hydrotalcite into a biodegradable Poly(ε-caprolactone) by high energy ball milling. *Polymer*. 46, 1601-1608.

Sorrentino, A., Gorrasi, G., and Vittoria, V. (2007). Potential perspectives of bio-nanocomposites for food packaging applications. *Trends in Food Science and Technology*. 18: 84-95.

Strawhecker, K. E., and Manias, E. (2000). Structure and properties of poly(vinyl alcohol)/Na+-montmorillonite nanocomposites. *Chem Mater.* 12: 2943–1949.

Usuki, A., Kato, M., Okada,A., and Kurauchi, T. (1997). Synthesis of polypropylene-clay hybrid. *J. Appl. Polym. Sci.* 63: 137-139.

Utracki, L. A., Simha, R., and Garcia-Rejon, A. (2003). Pressure-volume-temperature dependence of poly-ε-caprolactone/clay nanocomposites. *Macromolecules*. 36: 2114-2121.

Uyama, H., Kuwabara, M., Tsujimoto, T., Nakano, M., Usuki, A., and Kobayashi, S. (2003). Green nanocomposites from renewable resources: plant oil-clay hybrid materials. *Chem. Mater*. 15: 2492-2494.

Vaia, R. A., Ishii, H., and Giannelis, E. P. (1993). Synthesis and properties of two dimensional nanostructures by direct intercalation of polymer melts in layered silicates. *Chem Mater*. 5: 1694-1696.

Vaia, R. A., Jandt, K. D., Kramer, E. J., and Giannelis, E. P. (1995). Kinetics of polymer melt intercalation. *Macromolecules*. 28: 8080-8085.

Vaia, R. A., and Giannelis, E. P. (1997). Polymer melt intercalation in organically-modified layered silicates: model predictions and experiment. *Macromolecules*. 30: 8000-8009.

VanderHart, D. L., Asano, A., and Gilman, J. W. (2001). NMR measurements related to clay dispersion quality and organic-modifier stability in nylon6/clay nanocomposites. *Macromolecules.* 34: 3819-3822.

Wang, Z., and Pinnavaia, T. J. (1998). Nanolayer reinforcement of elastomeric polyurethane. *Chem. Mater.* 10: 3769-3771.

Weiss, J., Takhistov, P., and McClements, D. J. (2006). Functional materials in food

nanotechnology. *Journal of Food Science*. 71(9): R107-R116.

Wilhelm, H. M., Sierakowski, M. R., Souza, G. P., and Wypych, F. (2003). Starch films reinforced with mineral clay. *Carbohydrate Polymers*. 52: 101-110.

Wool, R. P., and Sun, X. Z. (2005). Bio-based polymers and composites. pp. 523-550. Elsevier Inc., UK.

Wu, J. H., and Lerner, M. M. (1993). Structural, thermal, and electrical characterization of layered nanocomposites derived from sodium-montmorillonite and polyethers. *Chem. Mater*. 5: 835-838.

Xing, P., An, Y., Dong, L., and Feng, Z. (1998). Miscibility and crystallization of poly(b-hydroxybutyrate)/poly(vinyl acetate-co-vinyl alcohol) blends. *Macromolecules.* 31: 6898–6907.

Yano, K., Usuki, A., Okada, A., Kurauchi, T., and Kamigaito, O. (1993). Synthesis and properties of polyimide-clay hybrid. *J. polym. Sci., Part A: Polym. Chem.* 31: 2493-2498.

Yano, K., Usuki, A., and Okada, A. (1997). Synthesis and properties of polyimide-clay hybrid films. *J. Polym. Sci., PartA: Polym. Chem.* 35: 2289-2294.

Zheng, J., Li, P., Ma, Y., and Yao, K. (2002). Gelatin/Montmorillonite hybrid nanocomposite. I. preparation and properties. *Journal of Applied Polymer Science*. 86: 1189-1194.

Figures

Figure 2.1 Structure of 2:1 layered silicates (Ray et al. 2006)

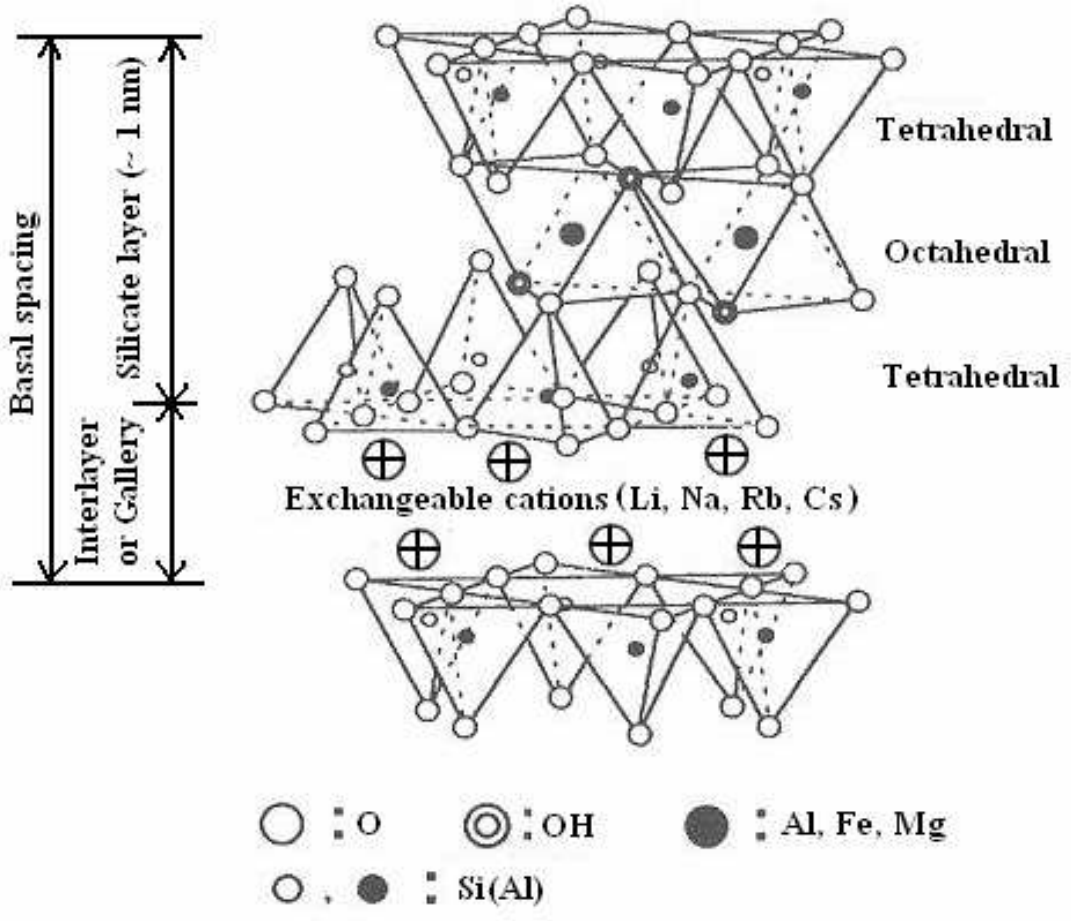

Figure 2.2 Schematic representation of intercalated and exfoliated nanocomposites from layered silicate clay and polymer

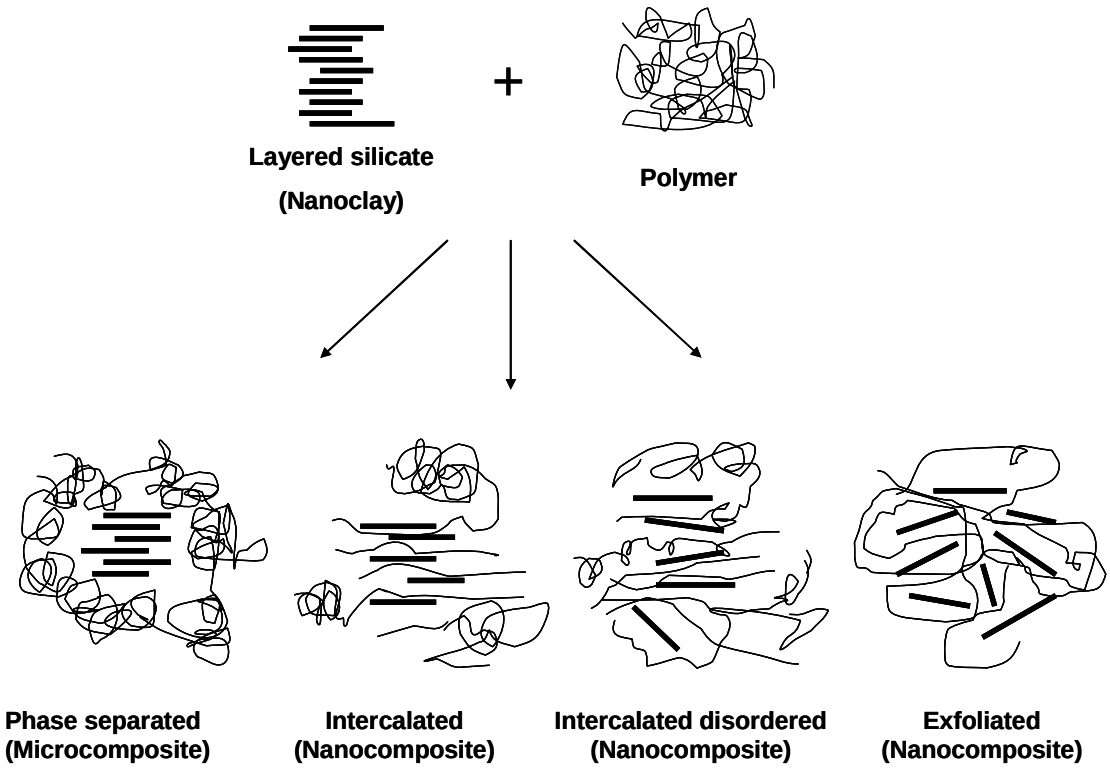

Figure 2.3 Proposed model for the tortuous zigzag diffusion path in a polymer-clay nanocomposite when used as a water vapor/gas barrier

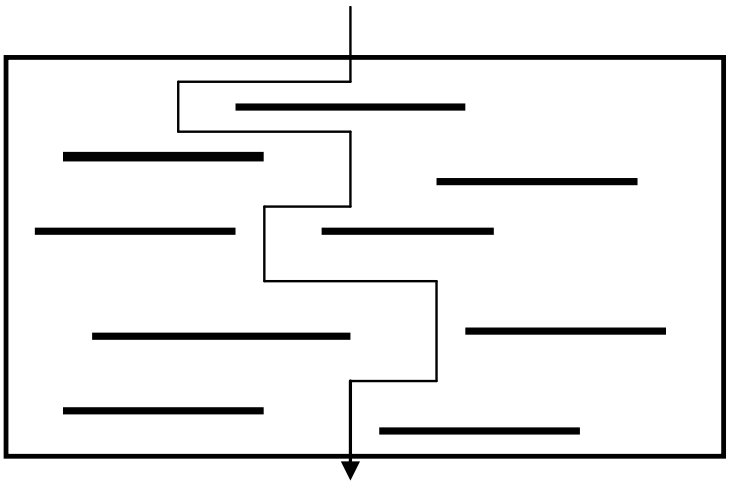

CHAPTER 3 - Use of Extrusion for Synthesis of Starch-Clay Nanocomposites for Biodegradable Packaging Films

In Press, Cereal Chemistry, Dec. 2007

3.1 Abstract

The poor mechanical and barrier properties of biopolymer-based food packaging can potentially be enhanced by the use of layered silicates (nanoclay) to produce nanocomposites. In this study, starch-clay nanocomposites were synthesized by the melt extrusion method. Natural (MMT) and organically modified (I30E) montmorillonite clays were chosen for the nanocomposite preparation. The structures of the hybrids were characterized by X-ray diffraction (XRD) and transmission electron microscopy (TEM). Films were made through casting using granulate produced by a twin-screw extruder. Starch/MMT composite films showed higher tensile strength and better water vapor barrier properties than films from starch/I30E composites, as well as pristine starch, due to formation of intercalated nanostructure. In order to find the best combinations of raw materials, the effects of clay content (0-21 wt% MMT), starch sources (corn, wheat and potato) and amylose content (～0, 28, 55, 70,100%) on barrier and mechanical properties of the nanocomposite films were investigated. With increase in clay content, significantly higher (15-92%) tensile strength (TS) and lower (22-67%) water vapor permeability (WVP) were obtained. The barrier and mechanical properties of nanocomposite films did not vary significantly with different starch source. Nanocomposite films from regular corn starch had better barrier and mechanical properties than either high amylopectin or high amylose-based nanocomposite films. WVP, TS and elongation at break of the films did not change significantly as amylose content increased beyond 50%.

Keywords: extrusion; starch; clay; nanocomposites; biodegradable; packaging

3.2 Introduction

Plastics are widely used packaging materials for food and non-food products due to their desirable material properties and low cost. However, the merits of plastic packaging have been overshadowed by its non-degradable nature, thereby leading to waste disposal problems. The public is also gradually coming around to perceive plastic packaging as something that uses up valuable and scarce non-renewable natural resources like petroleum. Moreover, the production of plastics is relatively energy intensive and results in the release of large quantities of carbon dioxide as a byproduct, which is often believed to cause, or at least contribute to, global warming. Some recent research findings have also linked plastic packaging to some forms of cancer (Kirsch 2005; ElAmin 2005).

Packaging materials based on polymers that are derived from renewable sources may be a solution to the above problems. Such polymers include naturally existing ones such as proteins, cellulose, starches and other polysaccharides, with or without modifications, and those synthesized chemically from naturally derived monomers such as lactic acid. These renewable polymers (or biopolymer) are not only important in the context of petroleum scarcity, but are also generally biodegradable under normal environmental conditions.

Interest and research activity in the area of biopolymer packaging films have been especially intensive over the past ten years (Krochta and De Mulder-Johnston 1997; Tharanathan 2003). For food packaging, important characteristics include mechanical properties such as tensile strength and elongation at break, and barrier properties such as moisture and oxygen permeabilities. In order to compete with synthetic plastics, biopolymer materials should have comparable mechanical and/or barrier properties. This is especially difficult in the case of moisture barrier properties because of the hydrophilic nature of most biopolymers, in comparison with hydrophobic synthetic polymers such as low density polyethylene (LDPE). Moreover, mechanical and oxygen barrier properties of most biopolymer-based packaging materials are moderate to good at low relative humidity (RH), but deteriorate exponentially with RH (Krochta and De Mulder-Johnston 1997).

Among all biopolymers, starch is one of the leading candidates as it is abundant and cheap. The cost of regular and specialty starches ($ 0.20-0.70/lb) compares well with that of synthetic polymers such as LDPE, polystyrene (PS) and polyethylene terephthalate (PET)

($0.50-0.75/lb) (Krochta and De Mulder-Johnston 1997). Moreover, starch is completely and quickly biodegradable and easy to process because of its thermoplastic nature (Doane 1994). Starch consists of two polysaccharides, the linear amylose and the highly branched amylopectin. The relative amounts of amylose and amylopectin depend upon plant sources and affect the material properties and gelatinization behavior of the starch.

Many strategies have been developed to improve the barrier and mechanical properties of starch-based biodegradable packaging films. These include – 1) addition of plasticizers such as glycerol, urea and formamide, which aid in the thermoplastic process and also increase flexibility of the final product by forming hydrogen bonds with starch that replace the strong interactions between its hydroxyl groups (Ma et al 2004); 2) addition of other polymers or biodegradable polymers, like poly (vinyl alcohol) (PVOH), and polylactide (PLA), to produce materials with properties intermediate to the two components (Chen et al 1996; Ke and Sun 2000). The resultant blends can be better processed via extrusion or film blowing, and have mechanical and/ or barrier properties superior to starch alone; and 3) addition of compatilizers to lower the interfacial energy and increase miscibility of two incompatible phases (starch and synthetic biodegradable polymers), leading to a stable blend with improved characteristics (Mani et al 1998).

However, none of the above mentioned methods can adequately meet the requirements of a cost effective biopolymer-based film that has properties close to those of synthetic plastic packaging. High costs of compatilizers and synthetic biodegradable polymers, such as PLA and PVOH, limit the level of their incorporation in starch. The resultant improvement in barrier and mechanical properties is also not very satisfactory. Therefore, there is a significant need for exploring new techniques to meet the challenges of developing high quality starch based packaging films.

The unique properties of nanostructured substances have opened windows of opportunity for the creation of high performance materials with a critical impact on food manufacturing, packaging, and storage (Moraru et al 2003). An example is polymer-layered silicate (PLS) nanocomposites, a promising class of new materials that represent polymers filled with small inorganic silicate clays with a high aspect ratio. These PLS nanocomposites have been the focus of academic and industrial attention in recent years because they often exhibit substantially enhanced physical and/or chemical properties relative to the original polymer matrix (Sinha Ray and Okamoto 2003).

The clays used in PLS nanocomposites include montmorillonite (MMT), hectorite and saponite, and their various modifications. These clays are environmentally friendly, naturally abundant and economical. Like talc and mica, which are better known minerals, these layered silicates belong to the general family of 2:1 layered silicates (or phyllosilicates) (Giannelis 1996). Their crystal structure consists of layers made up of two silica tetrahedral fused to an edge-shared octahedral sheet of either aluminum or magnesium hydroxide. Stacking of the layers leads to a regular van der Waals gap between the layers called the interlayer or gallery. In pristine layered silicates, the interlayer cations are usually hydrated Na+ or K+, showing hydrophilic surface properties.

For real nanocomposites, the clay layers must be uniformly dispersed in the polymer matrix (intercalated or exfoliated), as opposed to being aggregated as tactoids (Figure 3.1).

The nanocomposites can be obtained by several methods, including in-situ polymerization, intercalation from solution or melt intercalation (Sinha Ray and Okamoto 2003). Once clay intercalation or exfoliation has been achieved, improvement in properties can manifest as increase in tensile properties, as well as enhanced barrier properties, decreased solvent uptake, increased thermal stability and flame retardance. A diverse array of polymers have been used in PLS nanocomposite formation, ranging from synthetic non-degradable polymers, such as nylon (Kojima et al 1993a, 1993b), polystyrene (Vaia et al 1995; Vaia and Giannelis 1997), and polypropylene (Kurokawa et al 1996; Usuki et al 1997), to biopolymers, such as polylactide (Sinha Ray et al 2002a, 2002b).

Recently, there have been several attempts to enhance the end-use properties of starch in biodegradable packaging by fabricating starch-clay nanocomposites. De Carvalho et al (2001) provided a first insight in the preparation and characterization of thermoplasticized starch-kaolin composites by melt intercalation techniques. Park et al (2002 and 2003) reported an increase in elongation at break and tensile strength by more than 20 and 25%, respectively, and a decrease in water vapor transmission rate by 35% for potato starch/MMT nanocomposites on addition of 5% clay. Wilhelm et al (2003) observed a 70% increase in tensile strength of Cará root starch/hectorite nanocomposite films at 30% clay level. However, the percentage of elongation decreased by 50%. Very recently, Avella et al (2005) reported the preparation of potato starch/MMT nanocomposite films for food packaging applications. Results showed an increase in mechanical properties. Furthermore, the conformity of the resulting material samples with

actual packaging regulations and European directives on biodegradable materials was verified by migration tests and by putting the films into contact with vegetables and stimulants. Success of the studies above indicates that clays show much promise in improving the mechanical and barrier properties of starch-based packaging materials.

This study describes our attempts to fabricate starch-clay nanocomposites via melt-extrusion processing. The study sets out to investigate the influence of clay type (natural and organically modified clay), clay content, starch source and amylose content on the formation of nanostructure and properties of the starch-clay composite films.

3.3 Materials and methods

3.3.1 Materials

Two types of nanoclay were obtained from Nanocor Inc. (Arlington Heights, IL): natural montmorillonite (MMT) and onium ion modified MMT (Nanomer I30E). Regular corn starch, wheat starch and potato starch, and waxy corn starch were obtained from Cargill Inc. (Cedar Rapids, IA). High amylose corn starches Hylon V (～55% amylose), Hylon VII (～70% amylose) and 100% amylose were obtained from National Starch (Bridgewater, NJ). Glycerol (Sigma, St. Louis, MO) was used as a plasticizer for all studies.

3.3.2 Preparation of the starch-nanoclay composites

A laboratory-scale co-rotating twin screw extruder (Micro-18, American Leistritz, Somerville, NJ) with a six head configuration, and screw diameter and L/D ratio of 18 mm and 30:1, respectively, was used for the preparation of starch-nanoclay composites. The screw configuration and barrel temperature profile (85-90-95-100-110-120 ºC) are shown in Figure 3.2. Dry starch, glycerol (15 wt%), clay (0-21 wt%) and water (19 wt%) mixtures were extruded at screw speed of 200 RPM. The extrudates were ground using a Wiley mill (model 4, Thomas-Wiley Co., Philadelphia, PA) and an Ultra mill (Kitchen Resource LLC., North Salt City, UT) for further use.

3.3.3 Structural characterization of starch-nanoclay composites

X-ray diffraction (XRD) studies of the samples were carried out using a Bruker D8

Advance X-ray diffractometer (40kV, 40mA) (Karlsruhe, Germany). Samples were scanned in the range of diffraction angle 2θ=1-10° at a step of 0.01° and a scan speed of 4 sec/step. The clay basal spacing (d-spacing) can be estimated by Bragg's law:

$$d = \frac{\lambda \cdot \sin\theta}{2} \tag{1}$$

where λ = wavelength of X-ray beam, θ = the angle of incidence.

Transmission electron microscopy (TEM) studies were performed using a Philips CM100 electron microscope (Mahwah, NJ) operating at 100kV. Powder samples were placed onto a carbon-coated copper grid by physically interacting the grid and powders and analyzed to see the dispersion of clay platelets.

3.3.4 Film casting

Powder samples (4%) were dispersed in water and then heated to 95ºC and maintained at that temperature for 10 min, with regular stirring. Subsequently, the suspension was cooled to 65ºC and poured into petri dishes to make the films. The suspension in petri dishes was dried at 23ºC and 50% relative humidity (RH) for 24 hrs, after which the films were peeled off for further testing. The schematic film making methodology is shown in Figure 3.3.

3.3.5 Properties of starch-nanoclay composite films

Water vapor permeability (WVP) was determined gravimetrically according to the standard method E96-00 (ASTM 2000). The films were fixed on top of test cells containing a desiccant (silica gel). Test cells then were placed in a relative humidity chamber at 25ºC and 75% relative humidity (RH). The weight of test cells was measured every 12 hours over three days and the changes in the weight were plotted as a function of time. The slope of each line was calculated by linear regression (R^2>0.99), and the water vapor transmission rate (WVTR) was calculated from the slope of the straight line (G/t) divided by the transfer area (A):

$$WVTR = \frac{\left(\frac{G}{t}\right)}{A} \quad \text{g/h•m}^2 \tag{2}$$

where G = weight change (g), t = time (h) and A = test area (m^2),

WVP was then calculated using equation (3):

$$WVP = \frac{WVTR \times d}{\Delta p} \qquad \text{g•mm/kPa•h•m}^2 \tag{3}$$

where d = film thickness (mm) and Δp = partial pressure difference across the films (kPa).

Tensile properties of the films were measured using a texture analyzer (TA-XT2, Stable Micro Systems Ltd., UK), based on standard method ASTM D882-02 (ASTM 2002). Films were cut into 1.5 cm wide and 8 cm long strips and conditioned at 23ºC and 50% RH for three days before testing. The crosshead speed was 1 mm/min. Tensile strength (TS) and elongation at break (%E) were calculated using equations (4) and (5):

$$TS = \frac{Lp}{a} \times 10^{-6} \qquad \text{MPa} \tag{4}$$

where L_p = peak load (N), and a = cross-sectional area of samples (m^2).

$$\%E = \frac{\Delta l}{l} \times 100 \tag{5}$$

where Δl = increase in length at breaking point (mm), and l = original length (mm).

3.3.6 Experimental design and statistical analysis

WVP tests were replicated three times, while tensile tests were replicated five times. All the data were analyzed using OriginLab (OriginLab Corporation, Northampton, MA) scientific graphing and statistical analysis software. Statistical significance of differences in means were calculated using the Bonferroni LSD multiple-comparison method at $P<0.05$.

3.4 Results and discussion

3.4.1 Structure of starch-nanoclay composites

The XRD studies provided information on the intercalation and exfoliation processes and the short-range order of the molecular constituents in the clay-polymer composites. It is generally thought that during the intercalation process the polymer enters the clay galleries and forces apart the platelets, thus increasing the gallery spacing (d-spacing) (McGlashan and Halley 2003). According to Bragg's law, this would cause a shift of the diffraction peak towards a lower angle. As more polymers enter the gallery, the platelets become disordered and some platelets are even pushed apart from the stacks of clay particles (partial exfoliated). This will cause XRD

peaks with a wider distribution or even further shift to the left side. TEM images provide further evidence for the occurrence of intercalation and exfoliation processes. TEM allows a qualitative understanding of the internal structure, spatial distribution and dispersion of nanoparticles within the polymer matrix through direct visualization.

Figures 3.4 and 3.5 show the XRD patterns of composites with different nanoclay type and content. It should be noted that Lin (Counts) refers to intensity of diffracted X-rays. It is clear that the dispersion states of nanoclays in the starch matrix depended on the type of clay used. The natural MMT exhibited a single peak at $2\theta = 7.21^{\circ}$, whereas the starch/MMT hybrids showed prominent peaks at $2\theta = 4.98^{\circ}$ (Figure 3.4). It also can be seen from Figure 3.4 that starch blank exhibited a featureless curve in the range of 1-10˚ due to the amorphous character of gelatinized starch. The appearance of the new peak at 4.98˚ (d-spacing = 1.77 nm) with disappearance of the original peak of the nanoclay at $2\theta = 7.21^{\circ}$ (d-spacing = 1.23 nm) and increase of d-spacing indicated the formation of nanocomposite structure with intercalation of starch in the gallery of the silicate layers of MMT. From Figure 3.5, it can be seen that the organically modified nanoclay I30E alone exhibited an intensive peak in the range of $2\theta = 3.930$-4.16° (d-spacing ~2.25 nm), whereas starch-I30E hybrids showed weak peaks just under the original peak of the I30E. This implied that little or no intercalation/exfoliation was achieved in the starch matrix.

The above results clearly showed that compatibility and optimum interactions between starch matrix, organic modifiers (if any) and the silicate layer surface were crucial to the formation of intercalated or exfoliated starch-layered silicate nanocomposites. Original MMT is usually hydrated sodium cations and Nanomer I30E is the modified clay which alkylammonium cations replaced the sodium cations in the clay galleries and thus render the normally hydrophilic silicate surface organophilic. The added functional groups lower the surface energy of the silicate surface and increase the gallery spacing (from 1.77 to 2.25nm) of the modified clay. Therefore, compared with natural MMT, I30E doesn't show appreciable miscibility in the hydrophilic starch matrix. It migh have a good compatibility with polycaprolactone (PCL) (Kalambur and Rizvi 2004). On the other hand, in the case of natural MMT, due to the strong interactions between small amounts of polar hydroxyl groups of starch and glycerol, and the silicate layers of the nanoclay (inorganic MMT), the starch chains combined with glycerol molecules can intercalate into the interlayers of the nanoclay.

TEM micrographs of typical starch-MMT and starch-I30E composites are presented in Figure 3.6. The TEM results corresponded well with the XRD patterns. Starch-MMT composites exhibited a multilayered nanostructure (Figure 3.6-a), whereas starch-I30E composites showed almost no intercalated multilayered morphology, but instead had particle agglomerates or tactoids (appearing as dark spots in Figure 3.6-b).

Figure 3.7 shows the effects of clay content (up to 21 wt% MMT) on the structure of the nanocomposites. It can be seen that the only change was the intensity of peak, which increased with higher clay content. There was no shift in any of the peaks with varying clay contents, indicating that the clay content did not have any significant effect on the occurrence of intercalation or exfoliation. Figures 3.8 and 3.9 show the XRD patterns of 6 wt% MMT-based nanocomposites made from different starches. The data indicated that irrespective of the starch source (corn, wheat and potato) and amylose content (~0, 28, 55, 70, and 100%), complete disruption of the original nanolayer spacing of MMT was achieved, accompanied by starch-MMT intercalation at a higher d-spacing. Starch source or type did not have any effect on further changes of d-spacing of the nanocomposites. Although the MMT level was constant (6%) for all nanocomposites, interestingly the intensity of the XRD peaks appeared to increase with amylose content, with a maximum at 70% amylose. This may suggest the occurrence of partial exfoliation of clay platelets with the penetration of starch biopolymers into the silicate layers leading to their dispersal. It was hypothesized that as amylose content increased beyond 50%, the degree of exfoliation decreased with more of the starch-MMT nanocomposite present in the intercalated state leading to greater intensity of XRD peaks.

Figure 3.10 shows XRD patterns of corn starch-clay composites before and after film formation. The data indicated that film making procedure didn’t have a significant effect on XRD results.

XRD curve is related to the distribution of clay interlayer spacing. We saw a constant structure at $2\theta=5°$ (d-spacing=1.77nm), indicating that most clay interlayer spacing is in the range of 1.77nm. This interlayer spacing can be related to the thickness of starch molecular chain (about 0.5nm) and, thus, to its intercalation as a monolayer covering the interlayer surface of the clay. There do exist some other structures containing two starch molecular chains or half of starch chain inside the clay galleries, leading to the wider XRD distribution.

3.4.2 Water vapor permeability (WVP)

Tables 3.1-3.2 and Figures 3.11 – 3.12 show the moisture barrier properties of the starch-nanoclay composite films. Water vapor permeability (WVP) of the films was examined at a RH difference of 0/75% across the films. Table 3.1 shows the effects of clay type on WVP of corn starch based composite films. First, it can be clearly seen that, at the same clay level, WVP of the starch-MMT composite films was significantly lower than that of films made from starch-I30E composites. Second, there was no significant difference in WVP when the I30E content increased from 0 to 9%, while WVP decreased significantly with the addition of 3 to 9% MMT. It was obvious that the addition of I30E did not help in improving the barrier properties of the films, which indicated that improvement in film properties depended on the occurrence of the intercalation or exfoliation (formation of nanocomposites).

Generally, water vapor transmission through a hydrophilic film depends on both diffusivity and solubility of water molecules in the film matrix. When the nanocomposite structure is formed, the impermeable clay layers mandate a tortuous pathway for water molecules to traverse the film matrix, thereby increasing the effective path length for diffusion. The decreased diffusivity due to formation of intercalated nanostructure, in the case of starch-MMT composites, reduced the WVP. On the other hand, addition of I30E did not lead to intercalated structure thus there were no improvements in WVP of films made from starch-I30E composites.

Figure 3.11 shows the effect of 0-21% MMT on WVP of wheat starch-nanoclay composite films. WVP decreased sharply as clay content increased from 0 to 6%. With further increase in MMT content to 21%, the WVP continued to decrease, although more gradually. WVP of wheat starch with 21% clay was 0.57 g•mm/kPa•h•m^2, which was almost 70% lower than WVP of the wheat starch blank. The observed dramatic decrease in WVP is of great significance for use of starch-based films in food packaging and other applications where good barrier properties are needed.

Table 3.2 and Figure 3.12 show the effects of starch source and amylose content on WVP. Literature suggests that films made from different types of starches have different properties. These differences are generally related to the content of amylose and amylopectin (Lourdin et al 1995; Phan et al 2005). Rindlav-Westling et al (1998) reported better barrier properties of high amylose films as compared to high-amylopectin films. Phan et al (2005) even reported that the WVP of films was directly proportional to the amylopectin content. Higher

amylopectin led to higher WVP. They suggested that the effect of amylose content on the WVP of the starch could be attributed to the crystallization of amylose chains in the dried films. Amylose films showed B-type crystalline structure, whereas amylopectin films were completely amorphous. In general, diffusion of moisture is easier in amorphous systems than in crystalline ones. However, from Table 3.2, it can be seen that no significant difference in WVP was found between corn, wheat and potato starch-based nanocomposite films using MMT, although there are some slight differences in amylose content between corn, wheat and potato starches. It should be noted that irrespective of starch sources, the WVP decreased with increase in clay content from 0 to 9%. In Figure 3.12, normal corn starch based films presented better barrier properties than either amylopectin or high amylose based nanocomposite films. When amylose content reached 50%, the WVP almost remained constant. This may be related to XRD patterns and be possibly explained for the following reasons. First, the highest temperature used for extrusion processing was 120 ºC, which probably was not high enough for complete gelatinization of high amylose starch. Lower gelatinization means a lower amount of starch chains available for interlayer penetration, thus affects the degree of clay exfoliation. Second, the presence of plasticizer (glycerol) may affect the properties of the high amylose films. Amylopectin was more sensitive than amylose to glycerol plasticization as reported by Lourdin et al (1995). They reported the properties of plasticized films were not improved by the presence of glycerol and remained constant when amylose content was higher than 40%. Third, the presence of mineral clay might affect the starch network structure and crystallization of amylose films.

3.4.3 Tensile properties

Tables 3.3 to 3.4 and Figures 3.13 to 3.14 show the tensile properties of the starch-nanoclay composite films. Tensile properties such as tensile strength (TS) and elongation at break (%E) have been evaluated from the experimental stress-strain curves obtained for all prepared nanocomposite films. Variability of TS and %E data exist due to several reasons: mixing procedure, the dispersion of nanoparticles, film casting, and also testing instrument.

Tables 3.3 and 3.4 show the effects of clay type and clay content on tensile properties. When comparing Tensile strength of the starch/MMT and starch/I30E films (Table 3.3), it was obvious that addition of natural MMT helped improve the tensile strength of the films. TS increased with the increasing of clay content. Similar to WVP, I30E still did not give any help to

the tensile strength of the films. For Elongation at break (Table 3.4), no trends and no significant difference could be found here for starch/MMT and starch/I30E films.

With increasing MMT content (Figure 3.13), the TS increased rapidly from 14.05 to 27.02 MPa. However, %E did not exhibit much improvement. It even decreased with the increasing of MMT content. This was coincident with the report by Lee et al (2005), which suggested that good dispersion of clay platelets in the polymer reduced tensile ductility and impact strength compared to neat polymer.

Theoretically, the complete dispersion of clay layers in a polymer optimizes the number of available reinforcing elements for carrying an applied load and deflecting cracks. The coupling between the tremendous surface area of the clay and the polymer matrix facilitates stress transfer to the reinforcement phase, allowing for such tensile and toughening improvements.

Tables 3.5 to 3.6 show the tensile strength and elongation at break of different starch source based nanocomposite films. No significant differences of TS and %E were seen between corn, wheat and potato based nanocomposite films. Figure 3.14 shows the effects of amylose content on tensile properties. As is known, amylose helps improve the mechanical properties of the films (Wolff et al 1951; Lourdin et al 1995). Lourdin et al (1995) reported that for unplasticized films, a continuous increase in tensile strength was observed as amylose increased from 0 to 100%. However, the results presented here were quite similar to WVP discussed above; regular corn starch-based nanocomposite films presented the highest tensile strength (TS); Elongation at break (%E) decreased with the increased amylose content; when amylose content reached above 50%, both TS and %E did not change significantly.

3.5 Conclusions

Biodegradable starch-clay nanocomposites were prepared by dispersing clay particles into the starch matrix via melt extrusion processing. Two types of clay, MMT and I30E, were chosen for the hybrid preparation. Starch/MMT showed better clay dispersion in the starch matrix. The dispersion of nanoclays in the starch matrix depended on the compatibility and the polar interactions among the starch, glycerol, and the silicate layers. The starch/MMT composite films

showed higher tensile strength and better barrier properties to water vapor than the starch/I30E hybrids, as well as starch blank, due to the formation of intercalated or exfoliated nanostructure. The clay content had great effects on the properties of the nanocomposite films. With the increasing of clay content, higher tensile strength and better barrier properties were obtained. Normal corn starch-based films presented better barrier and mechanical properties than either amylopectin or high amylose-based nanocomposite films. WVP, TS and elongation at break of the films did not change significantly as amylose content increased beyond 50%.

The results presented here for starch-MMT nanocomposites proved that the concept of nanocomposite technology can be applied to improve the properties of starch based packaging materials. However, better performance is still needed for extending its application. Further studies including influence of plasticizers and extrusion processing conditions on starch-MMT nanocomposites are under investigation.

3.6 Acknowledgements

The authors would like to thank Mr. Eric Maichel, Operations Manager, KSU Extrusion Center, for conducting all extrusion runs. We also would like to thank KSU milling lab for providing milling facilities. This is Contribution Number 07-214-J from the Kansas Agricultural Experiment Station, Manhattan, Kansas 66506.

3.7 References

ASTM. 2000. Standard test method for water vapor transmission of materials, E96-00. In Annual Book of ASTM Standards, Philadelphia, PA. American Society for Testing and Material.

ASTM. 2002. Standard test method for tensile properties of thin plastic sheeting, D882-02. In Annual Book of ASTM Standards, Philadelphia, PA. American Society for Testing and Material.

Avella, M., De Vlieger, J. J., Errico, M. E., Fischer, S., Vacca, P., and Volpe, M. G. 2005. Biodegradable starch/clay nanocomposite films for food packaging applications. Food Chemistry. 93: 467-474.

Chen, L., Iman, S. H., Stein, T. M., Gordon, S. H., Hou, C. T., and Greene, R. V. 1996. Starch-polyvinyl alcohol cast film-performance and biodegradation. Polym. Prepr. 37: 461-462.

De Carvalho, A. J. F., Curvelo, A. A. S., and Agnelli, J. A. M. 2001. A first insight on composites of thermoplastic starch and Kaolin. Carbohydrate Polymers. 45: 189-194.

Doane, W. M. 1994. Opportunities and challenges for new industrial uses of starch. Cereal Foods Worlds. 39(8): 556-563.

ElAmin, A. 2005. Common plastics packaging chemical linked to cancer. FoodProductionDaily e-newsletter (May 31, 2005). Retrieved from http://www.foodproductiondaily.com/news/ng.asp?id=60333-common-plastics packaging

Giannelis, E. P. 1996. Polymer layered silicate nanocomposites. Advanced Materials. 8(1): 29-35.

Kalambur S. B. and Rizvi, S. S. 2004. Starch-based nanocomposites by reactive extrusion processing. Polym. Int. 53: 1413-1416.

Ke, T., and Sun, X., 2000. Physical properties of poly(lactic acid) and starch composites with various blending Ratios. Cereal Chem. 77(6): 761-768.

Kirsch, C. 2005. Compounds in plastic packaging act as environmental estrogens altering breast genes. EurekAlert e-newsletter (April 18, 2005). Retrieved from http://www.eurekalert.org/pub_releases/2005-04/fccc-cip041405.php.

Kojima, Y., Usuki, A., Kawasumi, M., Okada, A., Fukushima, Y., Kurauchi, T., and Kamigaito, O.. 1993a. Mechanical properties of nylon 6-clay hybrid. J. Mater. Res. 8: 1185-1189.

Kojima, Y., Usuki, A., Kawasumi, M., Okada, A., Kurauchi, T., and Kamigaito, O. 1993b. Sorption of water in nylon 6-clay hybrid. J. Appl. Polym. Sci. 49 : 1259-1264.

Krochta, J.M., and De Mulder-Johnston, C., 1997. Edible and biodegradable polymer films: challenges and opportunities. Food Technology. 51(2): 61-74.

Kurokawa, Y., Yasuda, H., and Oya, A., 1996. Preparation of a nanocomposite of polypropylene and smectite. J. Mater. Sci. Lett. 15: 1481-1483.

Lee, J. H., Jung, D., Hong, C.E., Rhee, K. Y., and Advani, S. G. 2005. Properties of polyethylene-layered silicate nanocomposites prepared by melt intercalation with a PP-g-MA compatibilizer. Composites Science and Technology. 65: 1996-2002.

Lourdin, D., Della Valle, G., and Colonna, P. 1995. Influence of amylose content on starch films and foams. Carbohydrate Polymer. 27: 261-270.

Ma, X., Yu, J., and Feng, J., 2004. Urea and formamide as a mixed plasticizer for thermoplastic starch. Polymer International. 53: 1780-1785.

Mani, R., Tang, J., and Bhattacharya, M. 1998. Synthesis and characterization of starch-graft-polycaprolactone as compatibilizer for starch/polycaprolactone blends. Macromolecular Rapid Communications. 19(6): 283-286.

McGlashan, S. A., and Halley, P. J. 2003. Preparation and characterization of biodegradable starch-based nanocomposite materials. Polymer International. 52: 1767-1773

Moraru, C. I., Panchapakesan, C. P., Huang, Q., Takhistov, P., Liu, S., and Kokini, J. L. 2003, Nanotechnology: A new fronitier in food science. Food Technology. 57(12): 24-29.

Park, H., Li, X., Jin, C., Park, C., Cho, W., and Ha, C. 2002. Preparation and properties of biodegradable thermoplastic starch/clay hybrids, Macromol. Mater. Eng. 287: 553-558.

Park, H., Lee, W., Park, C., Cho, W., and Ha, C. 2003. Enviromentally friendly polymer hybrids part 1 Mechanical, thermal and barrier properties of thermoplastic starch/clay nanocomposites, Journal of Materials Science. 38: 909-915.

Phan, D., Debeaufort, F., LUU, D., and Voilley, A. 2005. Functional properties of edible agar-based and starch-based films for food quality preservation. J. Agric. Food Chem. 53: 973-981.

Rindlav-Westling, A., Stading, M., Hermansson, A. M., and Gatenholm, P. 1998. Structure, mechanical and barrier properties of amylose and amylopectin films. Carbohydrate Polymers. 36: 217-224.

Sinha Ray, S., Yamada, K., Okamoto, M., and Ueda, K. 2002a. New polylactide/layered silicate nanocomposite: a novel biodegradable material. Nano Lett. 2: 1093–1096.

Sinha Ray, S., Maiti, P., Okamoto, M., Yamada, K., and Ueda, K. 2002b. New polylactide/layered silicate nanocomposites. 1. Preparation, characterization and properties. Macromolecule. 35: 3104–3110.

Sinha Ray, S., and Okamoto, M. 2003. Polymer/layered silicate nanocomposites: a review from preparation to processing. Prog. Polym. Sci. 28: 1539-1641.

Tharanathan, R. N. 2003. Biodegradable films and composite coatings: past, present and future. Trends in Food Science & Technology. 14: 71-78.

Usuki, A., Kato, M., Okada, A., and Kurauchi, T., 1997. Synthesis of polypropylene-clay hybrid. J. Appl. Polym. Sci. 63 : 137-139.

Vaia, R. A., Jandt, K. D., Kramer, E. J., and Giannelis, E. P. 1995. Kinetics of polymer melt intercalation. Macromolecules. 28: 8080-8085.

Vaia, R. A., and Giannelis, E. P., 1997. Polymer melt intercalation in organically-modified layered silicates: model predictions and experiment. Macromolecules. 30: 8000-8009.

Wilhelm, H. M., Sierakowski, M. R., Souza, G. P., and Wypych, F. 2003. Starch films reinforced with mineral clay. Carbohydrate Polymers. 52: 101-110.

Wolff, I. A., Davis, H. A., Cluskey, J. E., Gundrum, L. J., and Rist, C. E. 1951. Preparation of films from amylose. Industrial and Engineering Chemistry. 43 (4): 915-919.

Figures and Tables

Figure 3.1 Schematic representation of intercalated and exfoliated nanocomposites from layered silicate clay and polymer

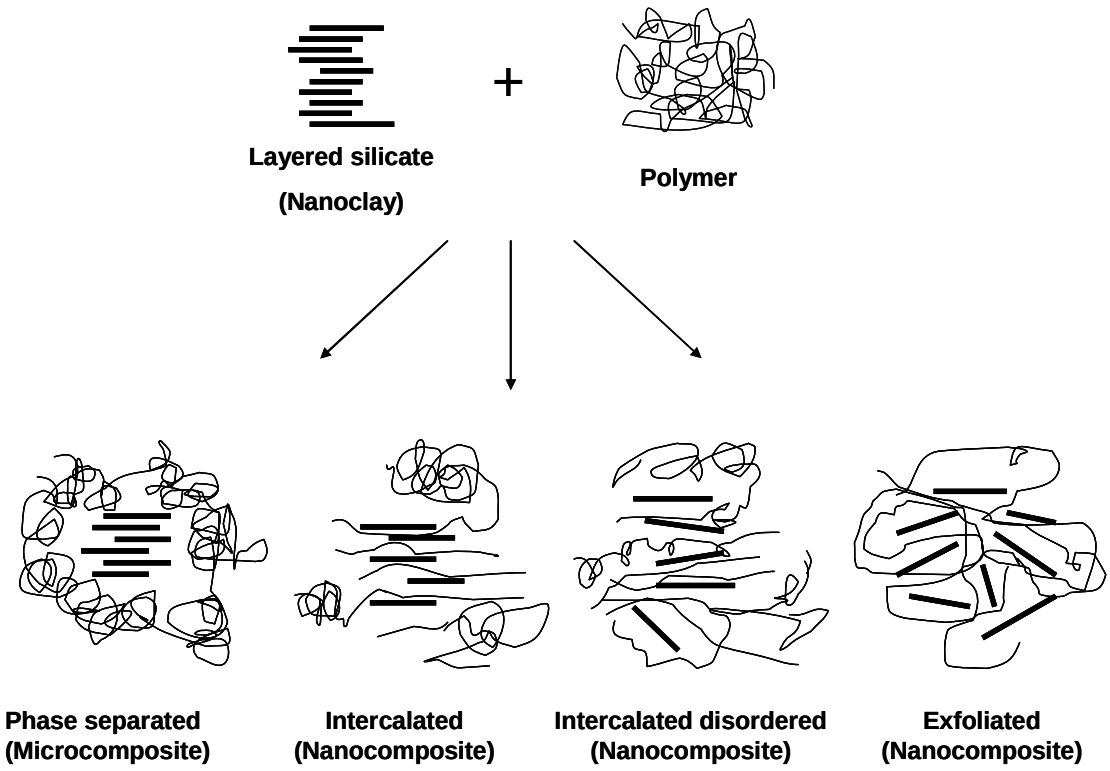

Figure 3.2 Screw configuration and temperature profile for lab-scale extruder used in the study.

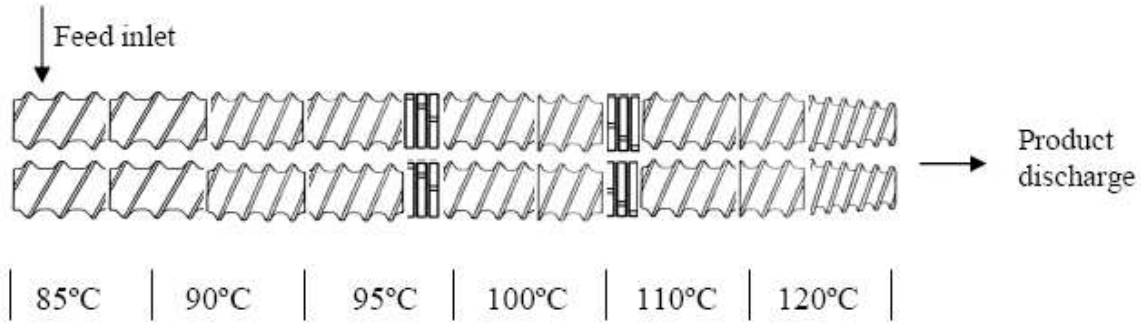

SE [a,b]				KB[c]	SE		KB	SE		
2-30-60	2-30-60	2-20-60	2-15-60	4-4-20-30F	2-15-60	2-15-30	5-2-20-45R	2-15-60	2-10-30	2-10-60

[a] SE-Screw elements: double flighted-pitch length-total element length (2-30-60).

[b] All screws are forward and intermeshing.

[c] KB-Kneading blocks: number of discs-length of disc-total element length-staggering angle of disc-forward (F) or reverse (R) (4-4-20-45 F).

Figure 3.3 Schematic representation of film making process.

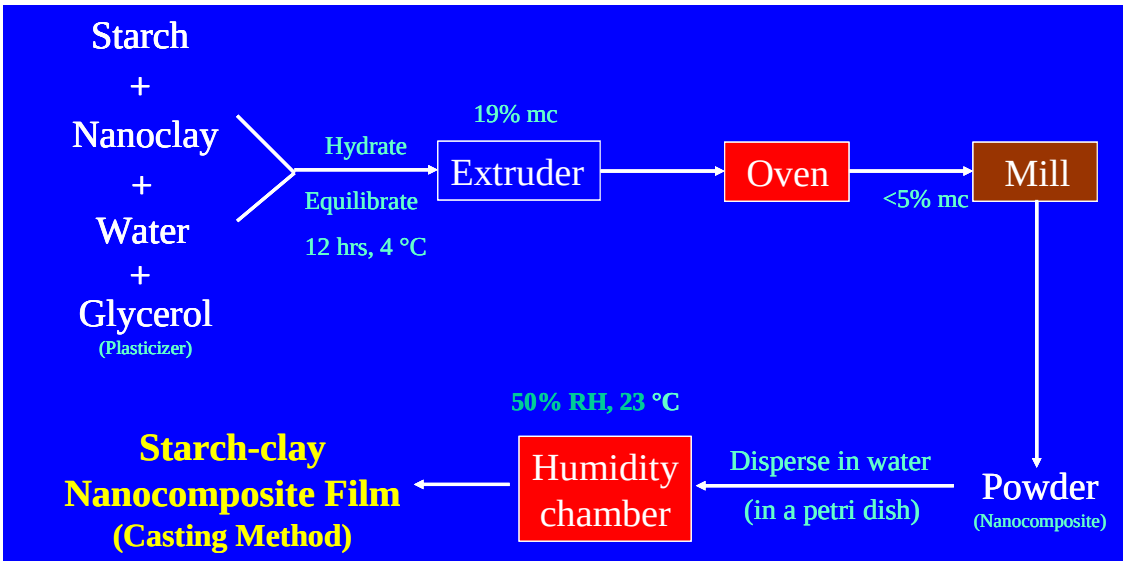

Figure 3.4 XRD patterns of (1) natural montmorillonite (MMT), (2) corn starch blank (0% MMT), and (3 and 4) corn starch/nanoclay hybrids with 3 and 6% MMT, respectively.

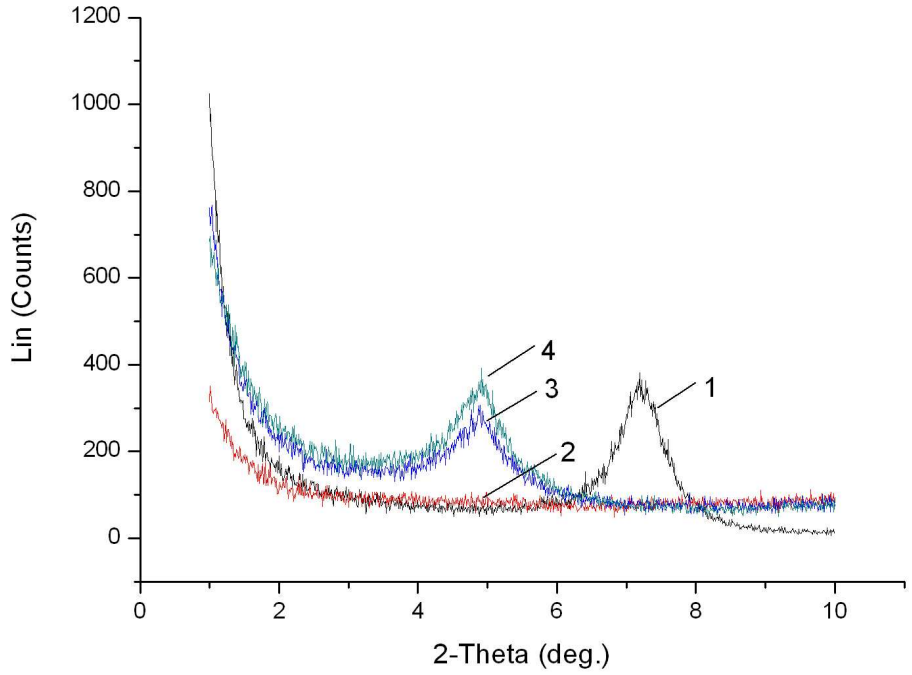

Figure 3.5 XRD patterns of (1) original nanomer I30E, (2) corn starch blank (0% I30E), and (3 and 4) corn starch/nanoclay hybrids with 3 and 6% I30E, respectively.

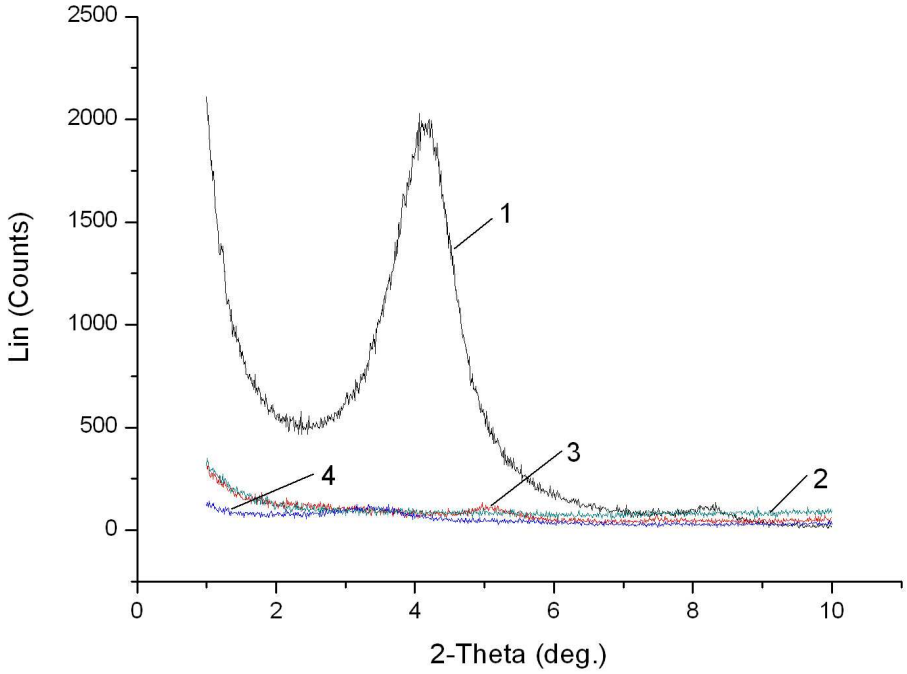

Figure 3.6 TEM images of (a) starch-6% MMT and (b) starch-6% I30E composites.

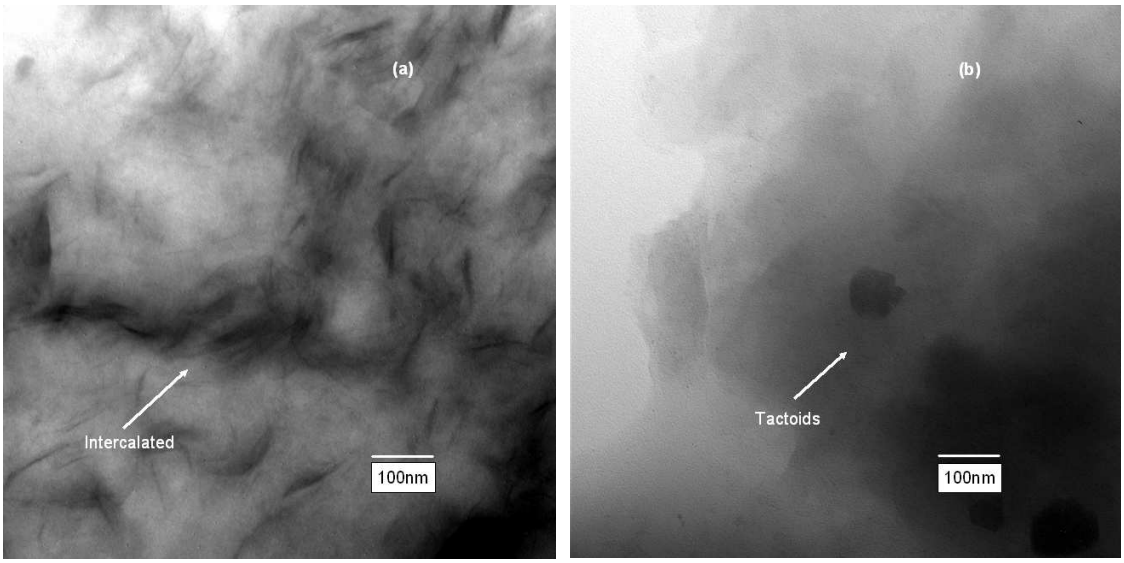

Figure 3.7 XRD patterns of (1) wheat starch blank (0% MMT), and (2, 3, 4, 5, and 6) wheat starch-clay nanocomposites with 3, 6, 9, 15, 21% MMT, respectively.

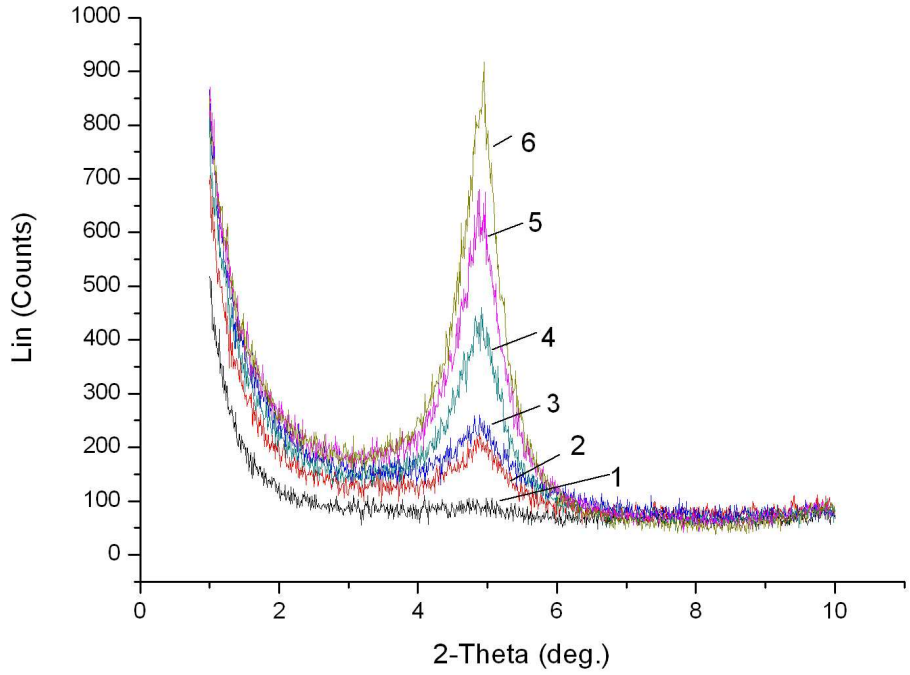

Figure 3.8 XRD patterns of 6% MMT nanocomposites with (1) corn (2) wheat and (3) potato Starches.

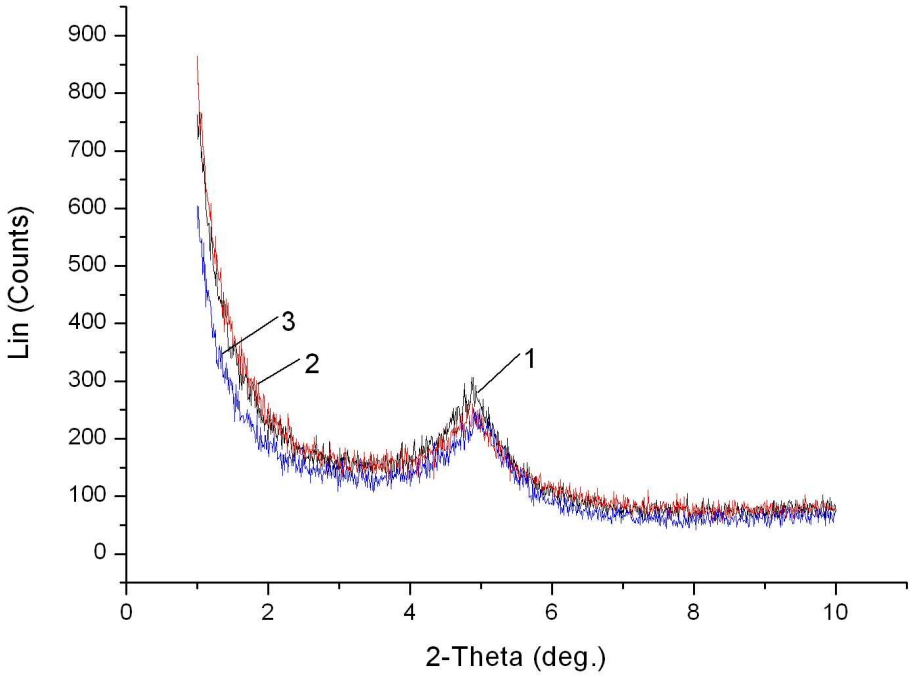

Figure 3.9 XRD patterns of 6% MMT nanocomposites with (1) waxy corn starch, (2) regular corn starch, (3) Hylon V, (4) Hylon VII, and (5) 100% amylose.

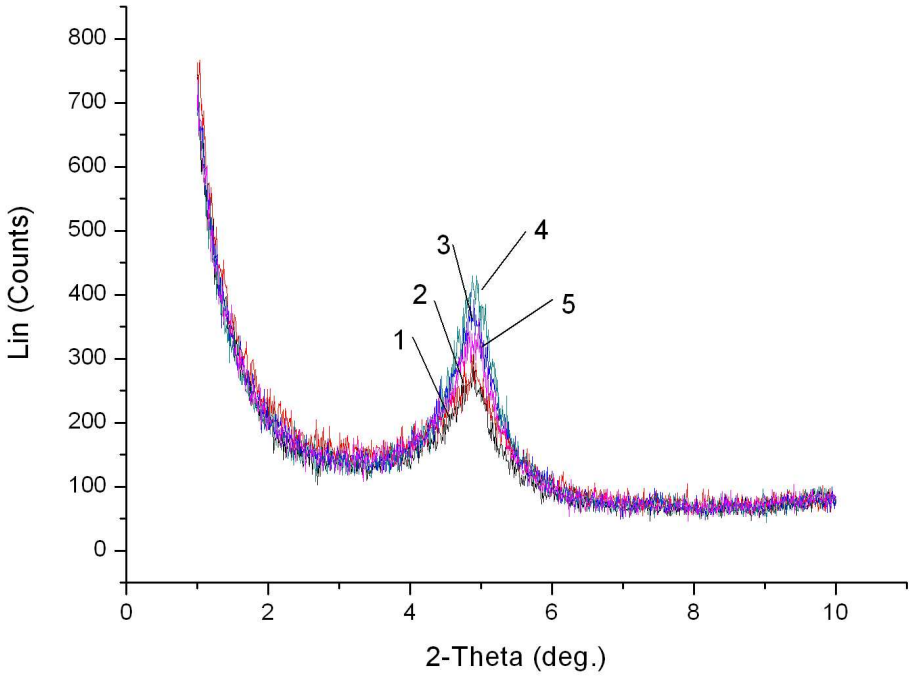

Figure 3.10 XRD patterns of corn starch-clay nanocomposites 1) before, and 2) after film formation.

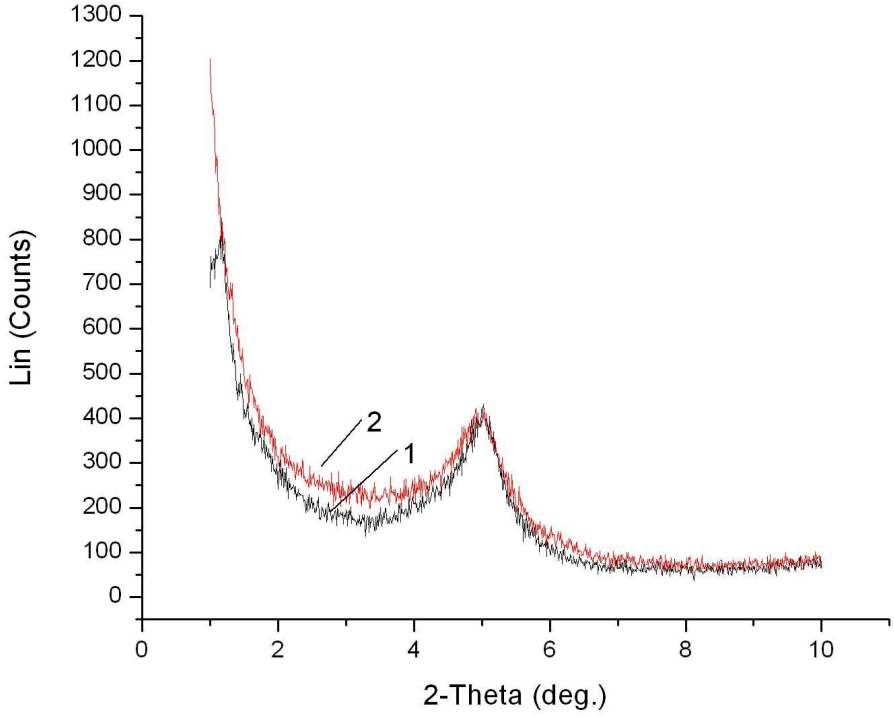

Figure 3.11 Effect of clay (MMT) content on water vapor permeability (WVP) of wheat starch-based nanocomposite films. Error bars indicate the standard deviation. Data points with different letters imply significant difference (P<0.05).

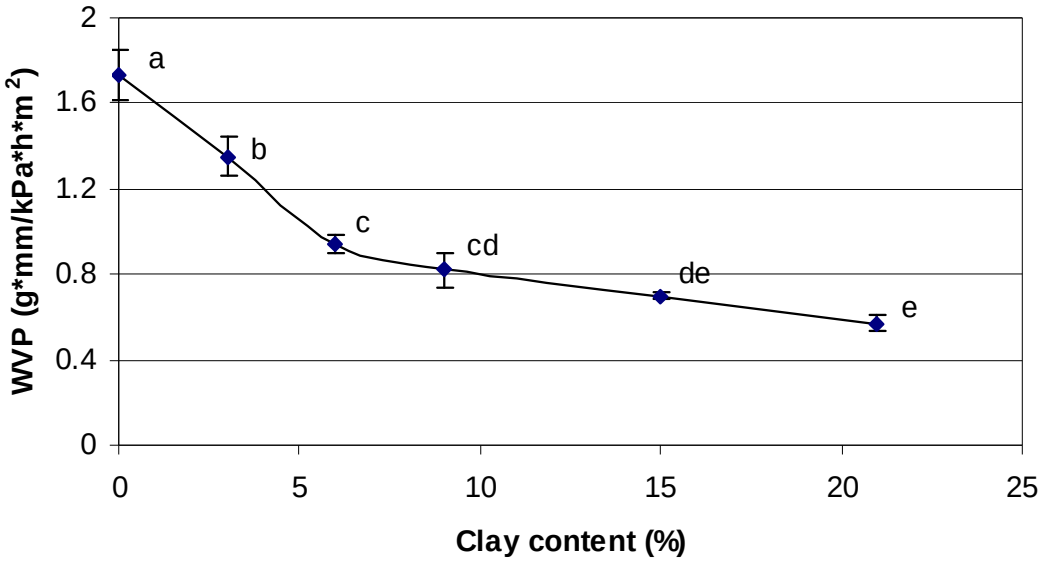

Figure 3.12 Effect of amylose content on water vapor permeability (WVP) of corn starch-based nanocomposite films with 6% clay (MMT). Error bars indicate the standard deviation. Data points with different letters imply significant difference (P<0.05).

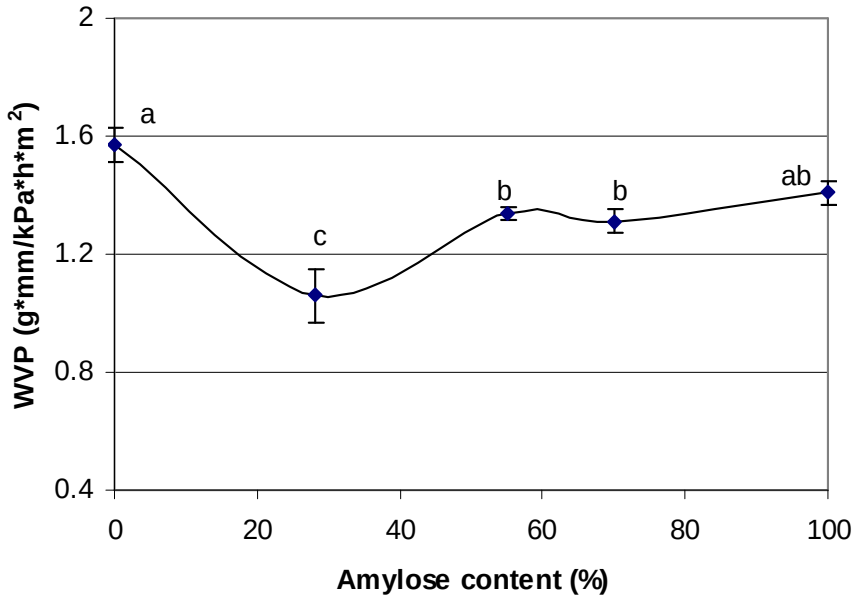

Figure 3.13 Effect of clay content (MMT) on tensile properties of wheat starch-based nanocomposite films. Error bars indicate the standard deviation. Data points with different letters imply significant difference (P<0.05).

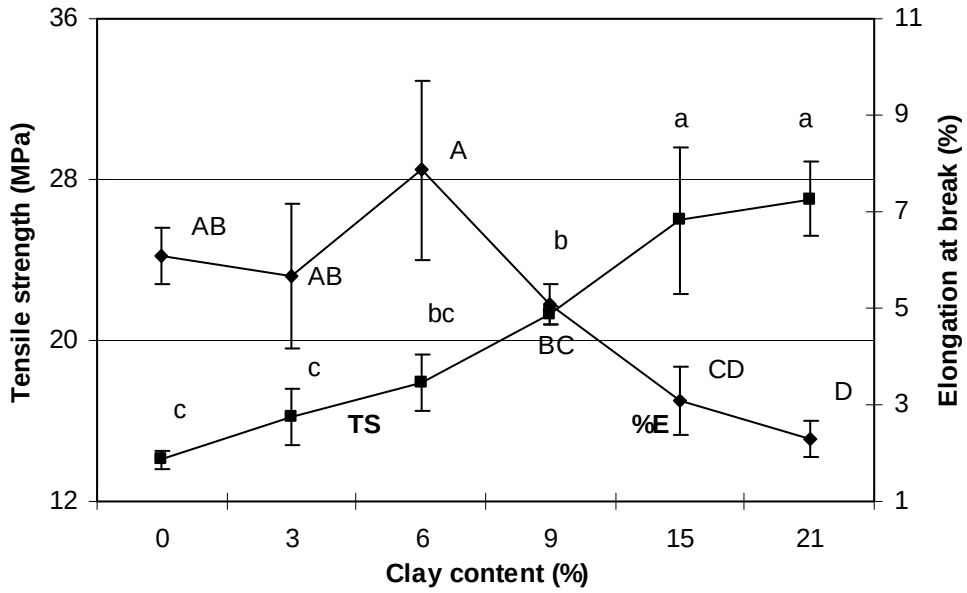

Figure 3.14 Effect of amylose content on tensile properties of corn starch-based nanocomposite films with 6% MMT. Error bars indicate the standard deviation. Data points with different letters imply significant difference (P<0.05).

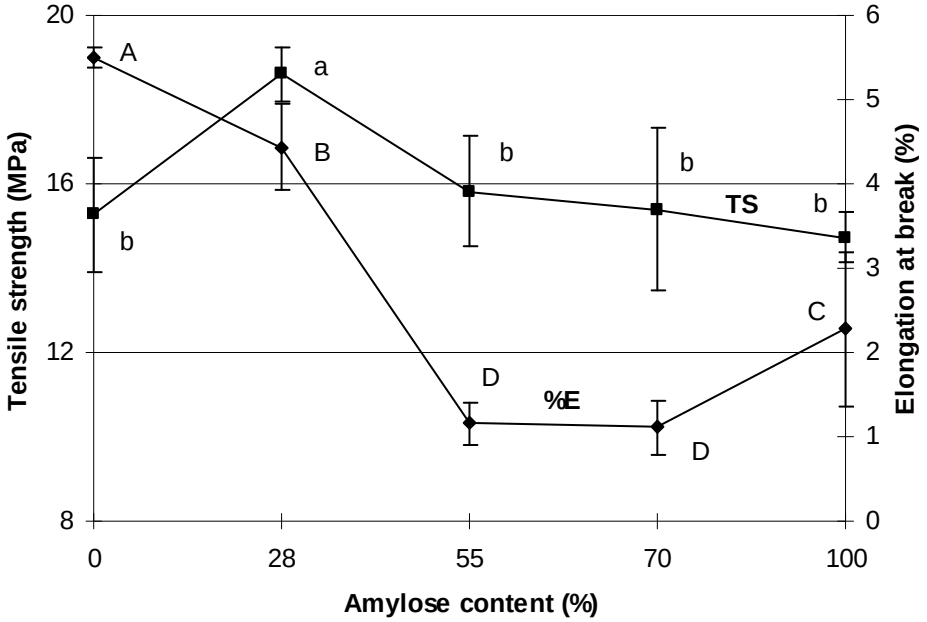

Table 3.1 Effect of clay type on WVP of corn starch-based films

	WVP ($g \cdot mm/kPa \cdot h \cdot m^2$)	
Clay content	Starch-MMT	Starch-I30E
0% clay	1.61 ± 0.08^{a}	1.61 ± 0.08^{ae}
3% clay	1.42 ± 0.04^{b}	1.63 ± 0.12^{e}
6% clay	1.06 ± 0.09^{c}	1.58 ± 0.08^{e}
9% clay	0.77 ± 0.04^{d}	1.56 ± 0.14^{e}

Mean ± standard deviation of each analysis

Means with the same letters are not significantly different ($P<0.05$).

Comparisons are made within the same row and column; n=3 for all treatments

Table 3.2 Effect of starch type on WVP of starch-MMT nanocomposite films

	WVP ($g \cdot mm/kPa \cdot h \cdot m^2$)		
MMT content	Corn starch	Wheat starch	Potato starch
0%	1.61 ± 0.08^{a}	1.73 ± 0.12^{ae}	1.81 ± 0.15^{ah}
3%	1.42 ± 0.04^{b}	1.35 ± 0.09^{bf}	1.22 ± 0.10^{bi}
6%	1.06 ± 0.09^{c}	0.94 ± 0.04^{cg}	0.98 ± 0.06^{cij}
9%	0.77 ± 0.04^{d}	0.82 ± 0.08^{dg}	0.84 ± 0.05^{dj}

Mean ± standard deviation of each analysis

Means with the same letters are not significantly different ($P<0.05$).

Comparisons are made within the same row and column; n=3 for all treatments

Table 3.3 Effect of clay type on tensile strength of corn starch based films

	Tensile strength (MPa)	
Clay content	Starch-MMT	Starch-I30E
0% clay	14.22±0.98^{cd}	14.22±0.98^{d}
3% clay	16.68±2.32^{bc}	12.41±4.19^{cd}
6% clay	18.60±0.63^{b}	13.37±3.01^{d}
9% clay	23.58±0.58^{a}	13.22±1.35^{d}

Mean ± standard deviation of each analysis

Means with the same letters are not significantly different ($P<0.05$).

Comparisons are made within the same row and column; n=5 for all treatments

Table 3.4 Effect of clay type on %Elongation of corn starch based films

	Elongation at break (%)	
Clay content	Starch-MMT	Starch-I30E
0% clay	5.26±0.83^{abc}	5.26±0.83^{c}
3% clay	6.27±1.20^{a}	3.20±0.81^{d}
6% clay	4.44±0.52^{b}	4.51±0.91^{bcd}
9% clay	4.82±0.35^{ab}	4.99±0.85^{ac}

Mean ± standard deviation of each analysis

Means with the same letters are not significantly different ($P<0.05$).

Comparisons are made within the same row and column; n=5 for all treatments

Table 3.5 Effect of starch type on tensile strength

	Tensile Strength (MPa)		
Clay content	Corn starch	Wheat starch	Potato starch
0% clay	14.22 ± 0.98^{cd}	14.05 ± 0.42^{dg}	14.57 ± 0.41^{dk}
3% clay	16.68 ± 2.32^{bc}	16.21 ± 1.4^{cf}	16.39 ± 0.30^{cj}
6% clay	18.60 ± 0.63^{b}	17.87 ± 1.4^{bf}	18.66 ± 0.50^{bi}
9% clay	23.58 ± 0.58^{a}	21.27 ± 0.44^{e}	22.25 ± 1.07^{eh}

Mean ± standard deviation of each analysis

Means with the same letters are not significantly different ($P<0.05$).

Comparisons are made within the same row and column; n=5 for all treatments

Table 3.6 Effect of starch type on elongation at break

	Elongation at Break (%)		
Clay content	Corn starch	Wheat starch	Potato starch
0% clay	5.26 ± 0.83^{abe}	6.08 ± 0.6^{cde}	5.47 ± 0.67^{e}
3% clay	6.27 ± 1.20^{af}	5.66 ± 1.49^{cdf}	5.91 ± 0.73^{ef}
6% clay	4.44 ± 0.52^{bh}	7.86 ± 1.86^{cg}	6.49 ± 0.61^{egh}
9% clay	4.82 ± 0.35^{abj}	5.09 ± 0.42^{dj}	6.06 ± 0.58^{ei}

Mean ± standard deviation of each analysis

Means with the same letters are not significantly different ($P<0.05$).

Comparisons are made within the same row and column; n=5 for all treatments

CHAPTER 4 - Effects of Plasticizers on the Structure and Properties of Starch-Clay Nanocomposite Films

Submitted to Carbohydrate Polymers, Oct. 2007

4.1 Abstract

Global concerns due to the overuse of petroleum-based packaging material are being actively addressed using nanotechnology. In this study, biodegradable starch-clay nanocomposites were prepared through melt extrusion method. The morphology and film properties of the nanocomposites were monitored as different plasticizers were manipulated. It was found that the decreasing of glycerol content led to a tendency of complete clay exfoliation. The films with 5% glycerol exhibited the lowest water vapor permeability (0.41g·mm/kPa·h·m^2), highest tensile strength (35MPa), and glass transition temperature (53.78ºC), however, the elongation at break was low (2.15%). As compared to conventional plasticizer – glycerol, urea and formamide were tested as substituted plasticizers for starch-clay nanocomposites. The use of urea and formamide improved the dispersion of clay platelets. Compared to glycerol and urea, formamide has an intermediate hydrogen bond forming ability with starch. However, formamide plasticized nanocomposite films exhibited the lowest water vapor permeability (0.58 g·mm/kPa·h·m^2), highest tensile strength (26.64MPa) and glass transition temperature (54.74ºC), when used at the same level (15 %). The results suggested that the balance of the interactions between starch, clay surface, and plasticizers might control the formation of nanocomposite structure and further affect the performance of the nanocomposite films.

Keywords: Plasticizer; Starch; Clay; Nanocomposite; Film

4.2 Introduction

Polymer layered silicate (PLS) nancomposites have been the focus of academic and industrial attention in recent years because the final composites often exhibit a desired enhancement of physical (mechanical, barrier) and/or chemical properties relative to the neat polymer matrix, even at very low silicate clay contents (Sinha Ray & Okamoto, 2003). In addition, these silicate clays are environmentally friendly, naturally abundant, and economical. Normally, natural or organically modified clay, which in the pure state has a stacked structure of parallel silicate layers, is put in direct contact with the polymer matrix and then nanocomposites can be obtained by several methods, including in situ polymerization, intercalation from solution, or melt intercalation (Sinha Ray & Okamoto, 2003). For real nanocomposites, the clay platelets must be uniformly dispersed in the polymer matrix (intercalated or exfoliated), as opposed to being aggregated as tactoids (Figure 4.1). A diverse array of matrix polymers have been used in PLS nanocomposite formation, ranging from synthetic non-degradable polymers such as nylon (Kojima et al., 1993a, 1993b; Dennis et al., 2001), polystyrene (Vaia, Jandt, Kramer & Giannelis, 1995; Vaia & Giannelis, 1997), and polypropylene (Kurokawa, Yasuda & Oya, 1996; Usuki, Kato, Okada & Kurauchi, 1997) to biopolymers such as polylactide (Sinha Ray, Yamada, Okamoto & Ueda, 2002; Sinha Ray, Maiti, Okamoto, Yamada & Ueda, 2002) and starch (De Carvalho, Curvelo & Agnelli, 2001; Park, Li, Jin, Park, Cho & Ha, 2002; Park, Lee, Park, Cho, & Ha, 2003; Wilhelm, Sierakowski, Souza & Wypych, 2003; Avella, De Vlieger, Errico, Fischer, Vacca & Volpe, 2005).

Starch is attractive because it is a cheap material and has fast biodegradability. Under high temperature and shear, starch can be processed into a moldable thermoplastic, known as thermoplastic starch (TPS). During the thermoplastic process, water contained in starch and the added plasticizers play an indispensable role because the plasticizers can form hydrogen bonds with the starch, replacing the strong interactions between the hydroxyl groups of the starch molecules, and thus making starch thermoplastic. (Hulleman, Janssen & Feil, 1998; Ma & Yu, 2004; Ma, Yu & Feng, 2004).

In a previous study (Chapter 3), we fabricated starch-clay nanocomposites by extrusion processing using glycerol as the plasticizer. The results indicated that the interactions between the starch matrix and clay surface were crucial to the formation of nanostructure. Because the

plasticizers play an indispensable role in the starch thermoplastic process, it was hypothesized that plasticizers might also participate in the interactions between starch and clay surface and therefore could greatly affect the formation of nanostructure and further influence the mechanical and water vapor barrier properties of starch-clay nanocomposite films.

In the present study, we tested the influence of glycerol content and different plasticizers (glycerol, urea, and formamide) on the formation of nanostructure and properties of the starch-clay nanocomposite films.

4.3 Materials and methods

4.3.1 Materials

Native cornstarch was obtained from Cargill Inc. (Cedar Rapids, IA). Montmorillonite (MMT) nanoclay was obtained from Nanocor Inc. (Arlington Heights, IL). Glycerol, urea, and formamide were obtained from Sigma (St. Louis, MO).

4.3.2 Preparation of plasticized starch-clay nanocomposites

Glycerol (0-20 wt%), urea (15 wt%), and formamide (15 wt%) were used to plasticize the starch/clay nanocomposite system. The nanocomposite preparation was performed using a lab-scale co-rotating twin-screw extruder (Micro-18, American Leistritz, Somerville, NJ) with a six-head configuration and screw diameter of 18 mm and L/D ratio of 30:1. The screw configuration and barrel temperature profile (85-90-95-100-110-120 ºC from feed zone to die) are shown in Figure 4.2. Dry starch, plasticizers, clay (6 wt%), and water (19 wt%) mixtures were extruded at a screw speed of 200 RPM. The extrudates were ground using a Wiley mill (model 4, Thomas-Wiley Co., Philadelphia, PA) and an Ultra mill (Kitchen Resource LLC., North Salt City, UT) for further use.

4.3.3 Structural characterization of starch-nanoclay composites

X-ray diffraction (XRD) studies of the samples were carried out using a Bruker D8 ADVANCE x-ray diffractometer (40kV, 40mA) (Karlsruhe, Germany). Samples were scanned in the range of diffraction angle 2θ=1-10° at a step of 0.01° and a scan speed of 4 sec/step. The clay basal spacing (d-spacing) can be estimated by Bragg's law:

$$d = \frac{\lambda \cdot \sin\theta}{2} \quad (1)$$

where λ = wavelength of X-ray beam, θ = scattering angle.

Transmission electron microscopy (TEM) studies were performed using a Philips CM100 electron microscope (Mahwah, NJ) operating at 100kV. Powder samples were placed onto a carbon-coated copper grid by physically interacting the grid and powders and analyzed to see the dispersion of clay platelets.

4.3.4 Film casting

Powder samples (4%) were dispersed in water, heated to 95ºC and maintained at that temperature for 10 min, with regular stirring. Subsequently, the suspension was cooled to 65ºC and poured into petri dishes to make the films. The suspension in petri dishes was dried at 23ºC and 50% relative humidity (RH) for 24 hrs, after which the films were peeled off for further testing.

4.3.5 Properties of starch-nanoclay composite films

Water vapor permeability (WVP) was determined gravimetrically according to the standard method E96-00 (ASTM, 2000). All measurements were replicated three times. The films were fixed on top of test cells containing a desiccant (silica gel). Test cells then were placed in a relative humidity chamber at 25ºC and 75% relative humidity (RH). The weight of test cells was measured every 12 hours over three days and the changes in the weight were plotted as a function of time. The slope of each line was calculated by linear regression (R2>0.99), and the water vapor transmission rate (WVTR) was calculated from the slope of the straight line (G/t) divided by the transfer area (A):

$$WVTR = \frac{\left(\frac{G}{t}\right)}{A} \quad \text{g/h•m2} \quad (2)$$

where G = weight change (g), t = time (h) and A = test area (m2)

WVP was then calculated using equation (3):

$$WVP = \frac{WVTR \times d}{\Delta p} \quad \text{g•mm/kPa•h•m2} \quad (3)$$

where d = film thickness (mm) and Δp = partial pressure difference across the films (kPa).

Tensile properties of the films were measured using a texture analyzer (TA-XT2, Stable Micro Systems Ltd., UK), based on standard method ASTM D882-02 (ASTM, 2002). All measurements were replicated five times. Films were cut into 1.5 cm wide and 8 cm long strips and conditioned at 23ºC and 50% RH for three days before testing. The crosshead speed was 1 mm/min. Tensile strength (TS) and elongation at break (%E) were calculated using equations (4) and (5):

$$TS = \frac{L_p}{a} \times 10^{-6} \quad \text{MPa} \tag{4}$$

where Lp = peak load (N), and a = cross-sectional area of samples (m2).

$$\%E = \frac{\Delta l}{l} \times 100 \tag{5}$$

where Δl = increase in length at breaking point (mm), and l = original length (mm)

4.3.6 Differential scanning calorimetry

Differential scanning calorimetry (DSC) was used to measure Glass transition temperature (T_g) of starch-clay nanocomposite films. The test was performed with a Q100 DSC (TA Instruments, New Castle, DE) equipment, fitted with a cooler system using liquid nitrogen. Samples of the formulated films were first equilibrated at 23ºC and 50% RH for over three days. Then 8 -10mg samples were weighed in aluminium pans and hermetically sealed; an empty pan was used as reference. Each sample was heated from -20 to 120ºC at a heating rate of 10ºC/min. The Glass transition temperature (T_g) was defined as the midpoint of the transition inflection observed in thermograms. All measurements were performed in triplicates.

4.3.7 Water content

Samples of the formulated films were equilibrated at 23ºC and 50% RH for over three days. Then 2g sample films were dried in the oven at 105ºC until constant weight was obtained. Water content can be calculated using equation (6):

$$\%\text{water content} = \frac{Wo - Wf}{Wo} \times 100 \tag{6}$$

where Wo was the weight of sample before drying, Wf was the weight of sample after drying. All measurements were performed in triplicates.

4.3.8 Statistical analysis

All the data were analyzed using OriginLab (OriginLab Corporation, Northampton, MA) scientific graphing and statistical analysis software. Statistical significance of differences in means were calculated using the Bonferroni LSD multiple-comparison method at $P<0.05$.

4.4 Results and discussion

4.4.1 Effect of glycerol content

Figure 4.3 shows the effects of glycerol content on XRD patterns of starch-clay nanocomposites. The treatments with 15 and 20% glycerol showed new intensive peaks at lower angles than native MMT. It is generally thought that during the intercalation process the polymer enters the clay galleries and forces apart the platelets, thus increasing the gallery spacing (McGlashan & Halley, 2003). According to Bragg's law, this would cause a shift of the diffraction peak towards a lower angle. The appearance of the new peak at $2\theta = 4.976^{\circ}$ (d-spacing = 1.77 nm) with disappearance of the original peak of the nanoclay at $2\theta = 7.210^{\circ}$ (d-spacing = 1.23 nm) and increase of d-spacing indicated the formation of nanocomposite structure with intercalation of starch chains (plasticizers) in the gallery of the silicate layers of MMT. Compared to the two treatments mentioned above, a much wider peak distribution was found for the treatment with 10% glycerol. As for the treatments with 0 and 5% glycerol, further shift of the peaks to smaller angles and even broader peaks were observed. The changes seen in the XRD patterns might be explained by more polymers entering the clay galleries and pushing the platelets further apart (Dennis et al., 2001). At the first step, the platelets can loose their ordered, crystalline structure and become disordered with the platelets no longer parallel. Some clay platelets may even be pushed apart and exfoliated from the stacks of clay particles. The result is that the XRD peak doesn't shift to the left side, but has a broader and wider distribution (intercalated disordered structure). At the second step, as more and more polymers enter the galleries, the clay gallery spacing further increases, leading the XRD peak to continue shifting to the left side. At the same time, more clay platelets are pushed apart by polymers and exfoliated from the stacks of clay particles. As a result, the XRD peak (at the lower angle) becomes wider and wider and finally broadens into the baseline (complete exfoliated nanocomposite structure). For the treatments with 15 and 20% glycerol, most clay platelets are still in ordered, parallel

state. For 10% glycerol, platelets began to lose their ordered structure and were no longer parallel. For 0 and 5% glycerol, large amounts of the clay platelets were exfoliated and randomly distributed in the starch matrix.

The intercalated and exfoliated nanostructure can be confirmed by TEM images. Figure 4.4 was representative of TEM images of the starch-clay nanocomposites with 5 and 10% glycerol. In Figure 4.4-a, more single, disordered clay platelets can be seen, indicating that more exfoliated structures were obtained. Whereas in Figure 4.4-b, we can see an ordered, multilayered nanostructure and also a small amount of single clay platelets distributing around the corner meaning lower delamination and dispersion of platelets for the treatments with 10% glycerol.

The nanostructure of the polymer/clay hybrids depends on the compatibility and interactions among the polymer, the silicate layers, and plasticizers. Due to the strong polar interactions between a small amount of polar hydroxyl group of starch and glycerol in the starch chains and the silicate layers of the inorganic MMT, the starch chains combined with glycerol molecules can intercalate into the interlayers of the clay. With the increasing content of glycerol, it might be possible that some glycerol molecules escape from the starch matrix and interact with the silicate layers first. This will lead to the inhibition of more starch chains from entering the clay galleries, resulting in the incomplete dispersion of clay platelets in the starch matrix.

Figure 4.5 shows the effects of glycerol content on WVP. Nanocomposite films with 5% glycerol exhibit the lowest water vapor permeability (0.41g·mm/kPa·h·m^2), indicating that the occurrence of exfoliation was helpful for improving the barrier properties of the films. At the same time, small amounts of glycerol may help direct interactions between starch chains and silicate layers of the clay. That's why the samples with 0% glycerol didn't show very appreciable WVP performance compared to 5% glycerol samples, although it also exhibited partially exfoliated structure. With the increased glycerol content (5-20%), WVP increased too, probably because the large amount of glycerol inhibited the full dispersion of clay platelets in the starch matrix, leading to intercalated nanostructure rather than exfoliated structure. Furthermore, higher glycerol content also increased the hydrophilicity of the starch films (Mali, Grossmann, Garcia, Martino & Zaritzky, 2006). The higher levels of glycerol provided more active sites by exposing hydrophilic hydroxyl groups in which the water molecules could be absorbed.

Figure 4.6 shows the effect of glycerol content on tensile properties. Similar to the WVP

results, the film with 5% glycerol had the highest tensile strength (35MPa) due to the formation of exfoliated structure. At the same time, with the increase of glycerol content, the elongation increased. That's because, as a plasticizer, the presence of glycerol facilitates the movement of starch chains, imparting increased film flexibility (Mali et al., 2006).

Table 4.1 shows the effect of glycerol content on the glass transition temperature (T_g) and water content of starch based nanocomposite films. In Table 4.1, the T_g of the films with different glycerol content displayed almost the same trends as WVP and tensile strength. The films with 5% and 10% glycerol exhibited the highest T_g, indicating the formation of intercalated or exfoliated nanocomposite structure also affected the thermal properties of the films. Normally, increasing glycerol content decreased T_g because the polymer matrix became less dense and movements of polymer chains were facilitated with the addition of plasticizer (Mali et al., 2006). When intercalated or exfoliated nanostructure was formed, the dispersion of clay platelets restricted the free movements of the starch chains and the effect of plasticizer on T_g becomes not so significant. The T_g results can also be related to water content of the starch based films (Table 4.1). Lower water content was found for films with 5 and 10% glycerol. Water exerted a plasticizing effect, acting as a mobility enhancer; its low molecular weight leads to an increase in molecular mobility of polymers (Mali et al., 2006). The formation of exfoliated structure inhibited the absorbance of water molecules into the starch matrix, thus increasing glass transition temperature.

4.4.2 Effect of different plasticizers

For conventional starch based films, glycerol was the most commonly used plasticizer. In order to further investigate the role of plasticizers on the formation of nanocomposite structure, two different plasticizers (urea and formamide) with amino groups were selected for the preparation of starch-clay nanocomposites. Glycerol was used as a contrast.

Figure 4.7 shows the chemical structures of glycerol, urea, and formamide. Ma et al. (2004) reported that the amino groups in urea and formamide are more advantageous to the formation of hydrogen bonds with starch during the starch thermoplastic process, compared with the hydroxyl groups in glycerol. The researchers pointed out that each urea molecule has two amino groups, and thus can form more stable hydrogen bonds with starch than formamide. Therefore, the order of the hydrogen bond-forming abilities with starch was

urea>formamide>glycerol. However, it should be noted here that it might be possible that the presence of amino groups also made it easier for urea and formamide to interact with the clay surface first, which will lead to the plasticizers intercalating into the clay galleries and inhibiting more polymers from entering the clay galleries.

Figure 4.8 shows the XRD patterns of starch-clay nanocomposites based on three different plasticizers. The treatment with glycerol as a plasticizer exhibited a peak at $2\theta = 4.976^{\circ}$, whereas treatments with both urea and formamide exhibited peaks at $2\theta = 3.860^{\circ}$. The left shift of the XRD curve indicated that more polymers (and/or plasticizers) entered the clay gallery and the clay platelets were forced further apart (clay gallery spacing increased).

Figure 4.9 shows the effect of three plasticizers on WVP of starch-clay nanocomposite films. The use of urea and formamide as the plasticizers significantly decreased the WVP of the films as compared to glycerol plasticized films. This may indicate that the use of urea and formamide assisted in directing the interactions between the starch matrix and clay surface. More starch chains entered the clay galleries, leading to the decrease of WVP. When comparing WVP of starch-clay nanocomposite films based on glycerol, urea, and formamide, WVP of formamide was the lowest (0.58 g·mm/kPa·h·m^2), indicating that the balance of the interactions between starch, clay, and plasticizers might control the properties of nanocomposite films. A urea molecule has two amino groups, and it can form more stable hydrogen bonds with starch than can glycerol and formamide, but at the same time it was also the easiest for urea to react with the clay surface. Therefore, more urea molecules may escape from the starch matrix and react with the clay surface first, resulting in intercalation of the plasticizers, other than starch polymers. Formamide has an intermediate hydrogen bond forming ability, and it may function as a bridge between the starch and clay surface, leading to more polymers entering the clay galleries and stronger connections between them.

Table 4.2 shows the tensile properties of starch-clay nanocomposite films based on three plasticizers. The films based on formamide exhibited the highest tensile strength (26.64MPa). However, the films based on glycerol exhibited the highest elongation. Urea is a high melting solid with little internal flexibility, hence urea plasticized nanocomposite films showed the lowest elongation.

Table 4.3 shows the T_g and water content of starch-clay nanocomposite films plasticized by different plasticizers. Similar to the results of WVP and tensile properties, the films

plasticized with formamide exhibited the highest T_g (54.74ºC) and lowest water content (9.75%).

4.5 Conclusions

It was demonstrated in the study that the presence of plasticizers greatly affected the formation of nanostructure and barrier, mechanical, and thermal properties of the nanocomposite films. When the glycerol content decreased from 20 to 5%, the degree of clay exfoliation increased. Films with 5% glycerol exhibited the lowest water vapor permeability (0.41g•mm/kPa•h•m^2), highest T_g (53.78ºC), and highest tensile strength (35MPa), but low elongation at break (2.15%). Urea and formamide were tested as substituted plasticizers for the starch-clay nanocomposites. The XRD results indicated that the use of urea and formamide increased the degree of clay exfoliation. Compared to glycerol and urea, formamide has an intermediate hydrogen bond forming ability with starch. However, formamide plasticized nanocomposite films exhibited the lowest water vapor permeability (0.58 g·mm/kPa·h·m^2), highest tensile strength (26.64MPa) and glass transition temperature (54.74ºC), when used at the same level (15 %). It was concluded that the balance of the interactions between starch, clay surface, and plasticizers might control the formation of nanocomposite structure and further affect the performance of the nanocomposite films.

4.6 Acknowledgements

The authors would like to thank Mr. Eric Maichel, Operations Manager, KSU Extrusion Center, for conducting all extrusion runs. We also would like to thank the KSU milling lab for providing milling facilities. This is Contribution Number 08-126-J from the Kansas Agricultural Experiment Station, Manhattan, Kansas 66506.

4.7 References

ASTM. (2000). Standard test methods for water vapor transmission of materials, E96-00. In Annual Book of ASTM Standards, Philadelphia, PA. American Society for Testing and Material.

ASTM. (2002). Standard test method for tensile properties of thin plastic sheeting, D882-02. In Annual Book of ASTM Standards, Philadelphia, PA. American Society for Testing and Material.

Avella, M., De Vlieger, J. J., Errico, M. E., Fischer, S., Vacca, P. & Volpe, M. G. (2005). Biodegradable starch/clay nanocomposite films for food packaging applications. Food Chemistry, 93: 467-474.

De Carvalho, A. J. F., Curvelo, A. A. S. & Agnelli, J. A. M. (2001). A first insight on composites of thermoplastic starch and Kaolin. Carbohydrate Polymers, 45, 189-194.

Dennis, H. R., Hunter, D. L., Chang, D., Kim, S., White, J. L., Cho, J. W. & Paul, D. R. (2001). Effect of melt processing conditions on the extent of exfoliation in organoclay- based nanocomposites. Polymer, 42, 9513-9522.

Hulleman, S. H., Janssen, F. H. P., & Feil, H. (1998). The role of water during plasticization of native starches. Polymer, 39, 2043-2048.

Kojima, Y., Usuki, A., Kawasumi, M., Okada, A., Fukushima, Y., Kurauchi, T. & Kamigaito, O. (1993a). Mechanical properties of nylon 6-clay hybrid. Journal of Materials Research, 8, 1185-1189.

Kojima, Y., Usuki, A., Kawasumi, M., Okada, A., Kurauchi, T. & Kamigaito, O. (1993b). Sorption of water in nylon 6-clay hybrid. Journal of Applied Polymer Science, 49, 1259-1264.

Kurokawa, Y., Yasuda, H. & Oya, A. (1996). Preparation of a nanocomposite of polypropylene and smectite. Journal of Materials Science Letters, 15, 1481-1483.

Ma, X., & Yu, J. G. (2004). The plasticizers containing amide groups for thermoplastic starch. Carbohydrate Polymers, 57, 197-203.

Ma, X., Yu, J. & Feng, J. (2004). Urea and formamide as a mixed plasticizer for thermoplastic starch. Polymer international, 53, 1780-1785.

Mali, S., Grossmann, M. V. E., Garcia, M. A., Martino, M. N. & Zaritzky, N. E. (2006).

Effects of controlled storage on thermal, mechanical and barrier properties of plasticized films from different starch sources. Journal of Food Engineering, 75, 453-460.

McGlashan, S. A. & Halley, P. J. (2003). Preparation and characterization of biodegradable starch-based nanocomposite materials. Polymer International 52: 1767-1773.

Park, H., Li, X., Jin, C., Park, C., Cho, W. & Ha, C. (2002). Preparation and properties of biodegradable thermoplastic starch/clay hybrids. Macromolecular Materials and Engineering, 287, 553-558.

Park, H., Lee, W., Park, C., Cho, W. & Ha, C. (2003). Enviromentally friendly polymer hybrids. Part 1. Mechanical, thermal and barrier properties of thermoplastic starch/clay nanocomposites. Journal of Materials Science, 38, 909-915.

Sinha Ray, S., Yamada, K., Okamoto, M., & Ueda, K. (2002). New polylactide/layered silicate nanocomposite: a novel biodegradable material. Nano Letters, 2, 1093–1096.

Sinha Ray, S., Maiti, P., Okamoto, M., Yamada, K., & Ueda, K. (2002). New polylactide/layered silicate nanocomposites. 1. Preparation, characterization and properties. Macromolecules, 35, 3104–3110.

Sinha Ray, S. & Okamoto, M. (2003). Polymer/layered silicate nanocomposites: a review from preparation to processing. Progress in Polymer Science, 28, 1539-1641.

Usuki, A., Kato, M., Okada, A. & Kurauchi, T. (1997). Synthesis of polypropylene-clay hybrid. Journal of Applied Polymer Science, 63, 137-139.

Vaia, R. A., Jandt, K. D., Kramer, E. J. & Giannelis, E. P. (1995). Kinetics of polymer melt intercalation. Macromolecules, 28, 8080-8085.

Vaia, R. A. & Giannelis, E. P. (1997). Polymer melt intercalation in organically-modified layered silicates: Model predictions and experiment. Macromolecules, 30, 8000-8009.

Wilhelm, H. M., Sierakowski, M. R., Souza, G. P. & Wypych, F. (2003). Starch films reinforced with mineral clay. Carbohydrate Polymers, 52, 101-110.

Figures and Tables

Figure 4.1 Schematic representation of intercalated and exfoliated nanocomposites from layered silicate clay and polymer

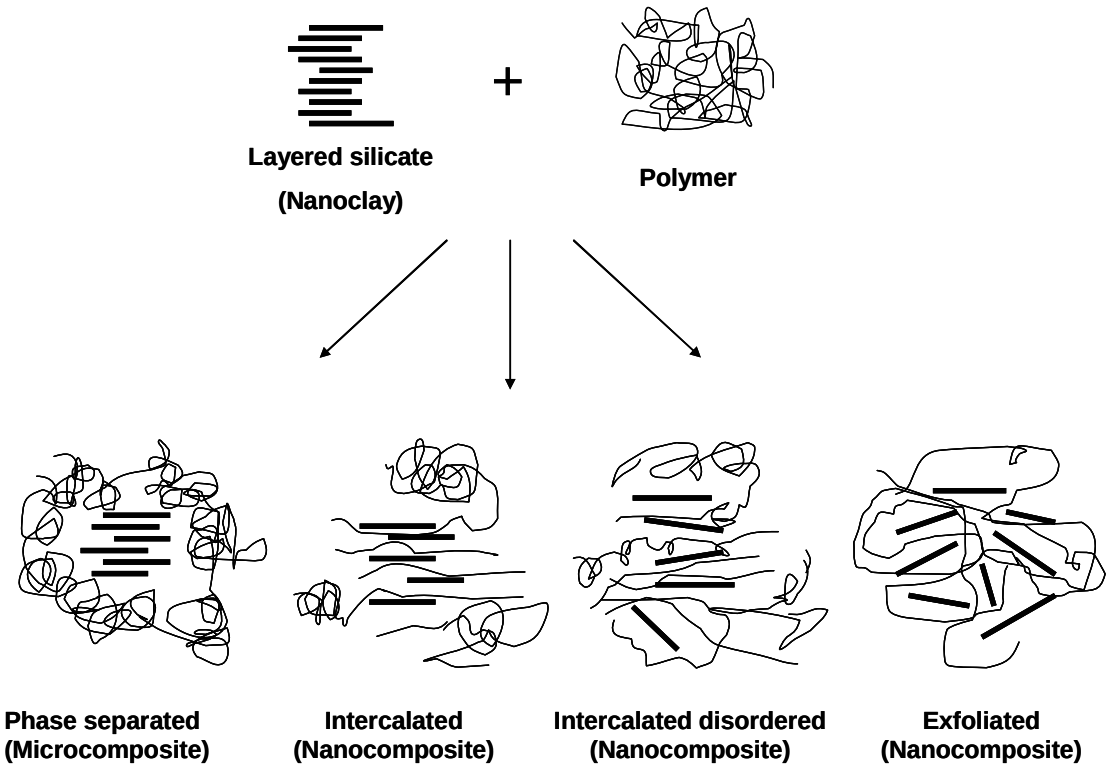

Figure 4.2 Screw configuration and temperature profile for lab-scale extruder used in the study.

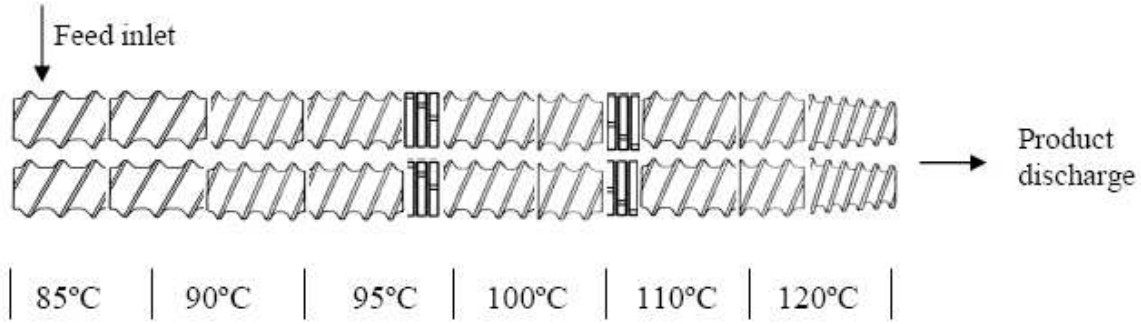

SE [a,b]				KB[c]	SE		KB	SE		
2-30-60	2-30-60	2-20-60	2-15-60	4-4-20-30F	2-15-60	2-15-30	5-2-20-45R	2-15-60	2-10-30	2-10-60

[a] SE-Screw elements: double flighted-pitch length-total element length (2-30-60).

[b] All screws are forward and intermeshing.

[c] KB-Kneading blocks: number of discs-length of disc-total element length-staggering angle of disc-forward (F) or reverse (R) (4-4-20-45 F).

Figure 4.3 Effect of glycerol content on XRD patterns (1 to 5: 0 to 20 wt% glycerol; 6: natural montmorillonite-MMT).

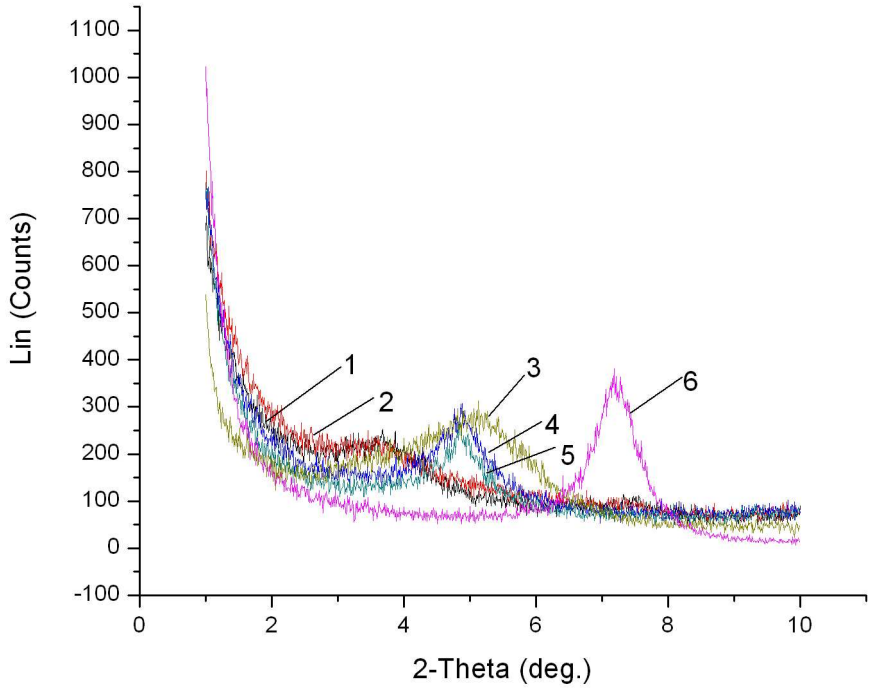

Figure 4.4 TEM images of starch/clay (6%MMT) nanocomposites with (a) 5% glycerol, and (b) 10% glycerol.

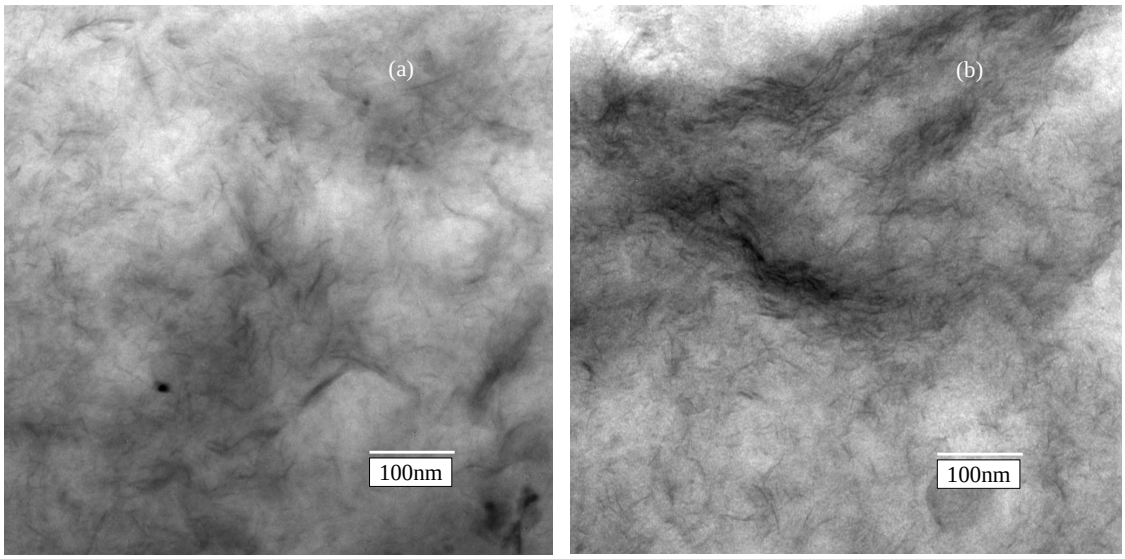

Figure 4.5 Effect of glycerol content on WVP of corn starch based nanocomposite films with 6% MMT. Error bars indicate the standard deviation. Data points with different letters imply significant difference (P<0.05).

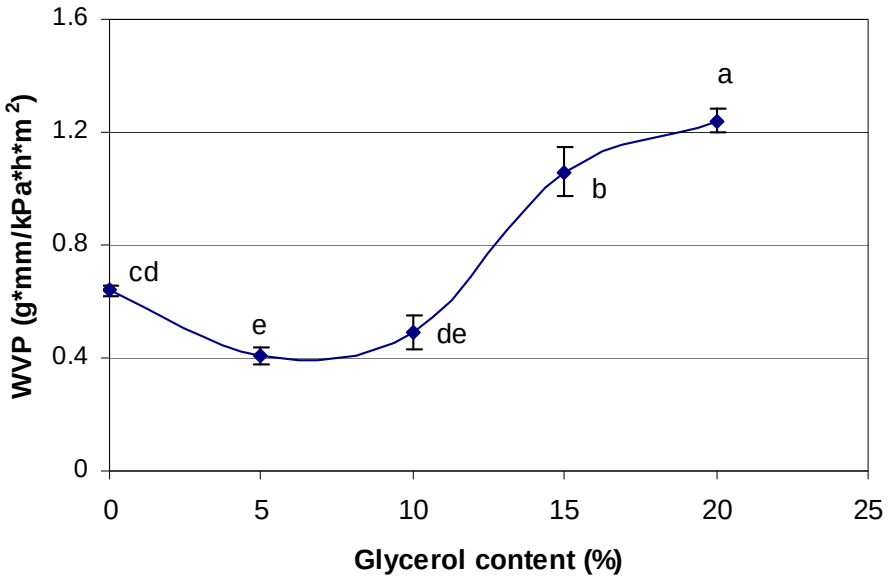

Figure 4.6 Effect of glycerol content on tensile properties of corn starch based nanocomposite films with 6% MMT. Error bars indicate the standard deviation. Data points with different letters imply significant difference (P<0.05).

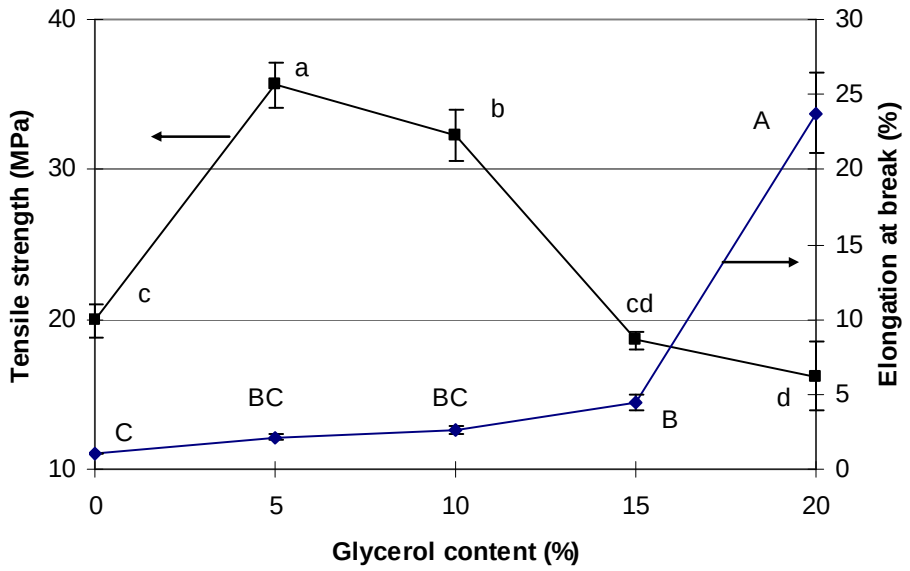

Figure 4.7 Chemical structures of (a) glycerol , (b) urea, and (c) formamide.

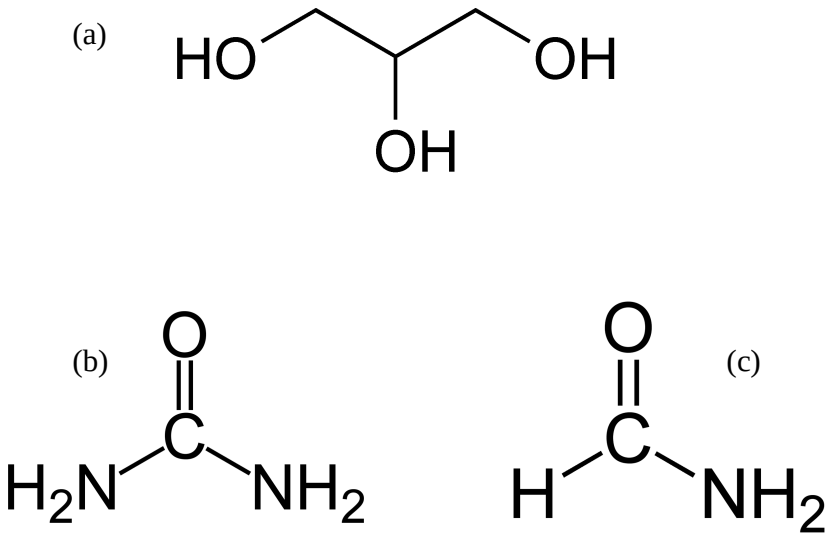

Figure 4.8 XRD patterns of corn starch-clay nanocomposites plasticized with 15% (1) glycerol, (2) urea, and (3) formamide with 6% MMT.

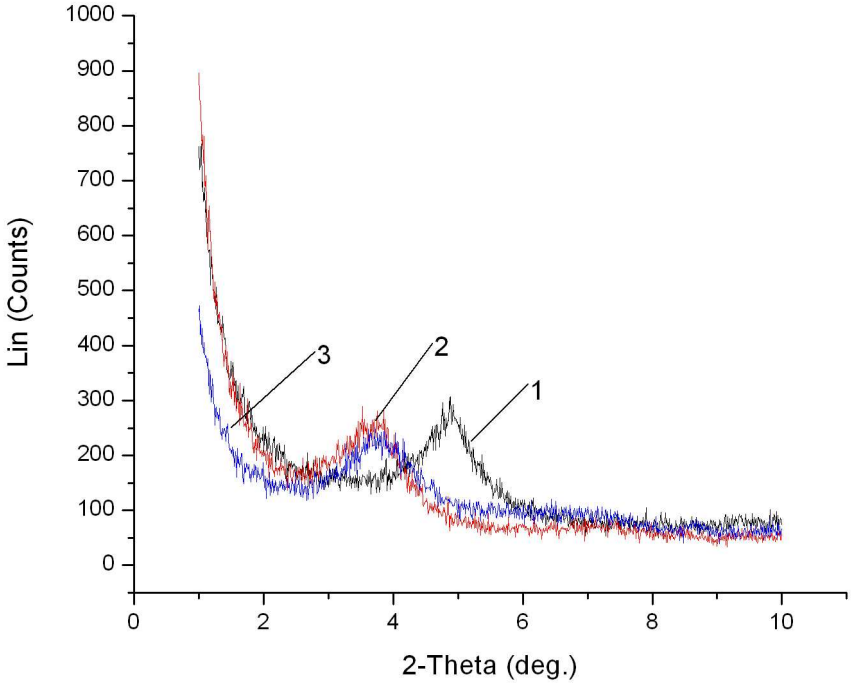

Figure 4.9 Water vapor permeability (WVP) of corn starch-based nanocomposite films with different plasticizers. Error bars indicate the standard deviation. Columns with different letters imply significant difference (P<0.05).

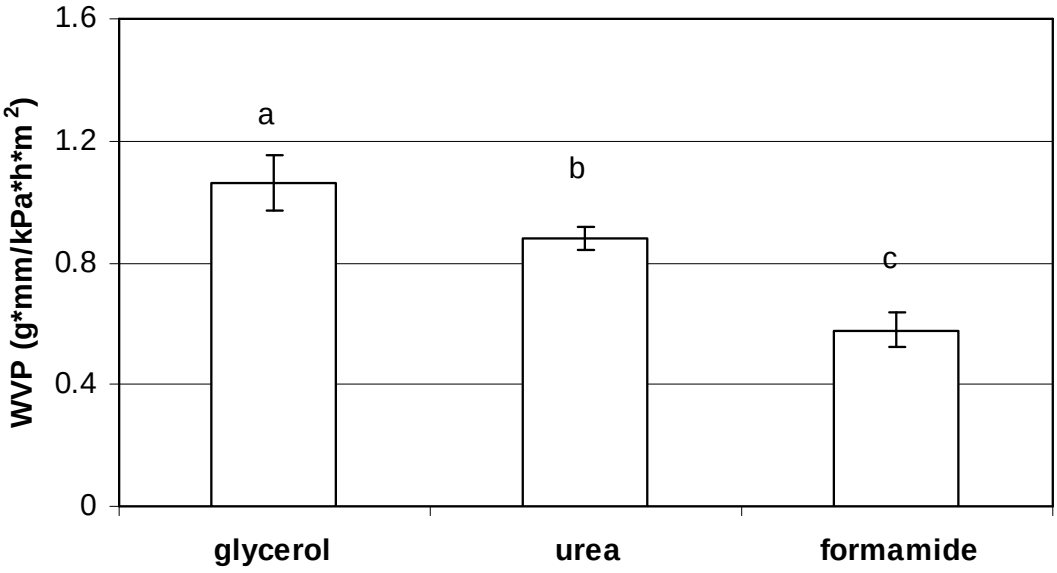

Table 4.1 Glass transition temperature (T_g) and water content of starch-clay nanocomposite films with different glycerol content.

Glycerol Content (%)	Glass Transition-T_g (ºC)	Water Content (%)
0	52.36±1.90[a]	11.81±0.12[ab]
5	53.78±4.10[a]	10.47±0.15[b]
10	53.42±2.25[a]	10.10±0.52[b]
15	50.71±2.76[a]	13.06±1.73[ab]
20	48.97±2.12[a]	15.03±2.67[a]

Mean ± standard deviation of each analysis

Means with the same letters are not significantly different (P<0.05).

Comparisons are made within the same column; n=3 for all treatments

Table 4.2 Tensile properties of corn starch-based nanocomposite films with different plasticizers.

	Tensile strength (MPa)	Elongation at break (%)
Glycerol	18.60±0.63[b]	4.44±0.52[a]
Urea	21.19±2.69[b]	2.49±0.55[b]
Formamide	26.64±3.02[a]	3.25±0.59[b]

Mean ± standard deviation of each analysis

Means with the same letters are not significantly different ($P<0.05$).

Comparisons are made within the same column; n=5 for all treatments

Table 4.3 Glass transition temperature (T_g) and water content of starch-clay nanocomposite films with different plasticizers

Plasticizer	Glass Transition-T_g (ºC)	Water Content (%)
Glycerol	50.71±2.76[a]	13.06±1.73[a]
Urea	53.37±0.79[a]	11.63±0.18[ab]
Formamide	54.74±1.21[a]	9.75±0.21[b]

Mean ± standard deviation of each analysis

Means with the same letters are not significantly different (P<0.05).

Comparisons are made within the same column; n=3 for all treatments

CHAPTER 5 - Effects of Melt Extrusion Conditions on the Structure and Properties of Starch-Clay Nanocomposite Films

To be submitted to Journal of Food Engineering, Nov. 2007

5.1 Abstract

Corn starch-clay nanocomposites were prepared from a co-rotating twin screw extruder. Screw configuration, barrel temperature profile, screw speed, and moisture content were varied to determine their effects on the structure and properties of nanocomposite films. All melt-intercalated samples were characterized by X-ray diffraction, water vapor barrier, and mechanical property tests. It was demonstrated that the degree of exfoliation and dispersion of nanoclay in the starch matrix was significantly affected by melt extrusion conditions. Increasing the shear stress (low to high shear intensity screw configuration, screw speed from 200 to 250 RPM, barrel moisture content from 40 to 20%) improved the exfoliation and dispersion of nanoclay, leading to improved barrier properties and tensile strength. The treatment with 20% moisture content exhibited almost complete clay exfoliation and the lowest water vapor permeability (0.27 g•mm/kPa•h•m^2) and highest tensile strength (39.30 MPa) of all treatments., Increasing temperature also improved the dispersion of clay platelets in the starch matrix in this study. However, this result might be applicable to the system only under a certain circumstance. In addition, this paper also demonstrated the importance of both chemistry and processing effects on clay exfoliation and dispersion. When polymer and clay are chemically compatible, good process conditions (shear intensity, temperature etc.) will enable significant improvement in clay exfoliation and dispersion.

Keywords: Extrusion condition; Starch; Clay; Nanocomposite

5.2 Introduction

In the last few years, great attention has been devoted to hybrid organic-inorganic systems, and in particular, to those in which layered silicates are dispersed at a nanometric level in a polymeric matrix (Sinha Ray and Okamoto, 2003). Such nanocomposites possess unusual properties, which are very different from their microscale counterparts. Nanocomposites often show improved mechanical, thermal, and barrier properties. The enhanced properties are presumably due to the synergistic effects of the nanoscale structure and the interaction of the fillers and the polymer.

To obtain nanocomposites, polymer chains must diffuse into the galleries between silicate layers to produce structures ranging from intercalated to exfoliated (Figure 5.1). It is generally thought that intercalation occurs when a small amount of polymer penetrates into the galleries, resulting in finite expansion of the silicate layers. This leads to a well-ordered, multilayered structure with a repeat distance of a few nanometers and is observed in systems with limited miscibility. Extensive polymer penetration leads to exfoliation or delamination of silicate layers. An exfoliated nanocomposite consists of nanometer thick platelets distributed homogeneously throughout the polymer matrix. In contrast, when the polymer and silicate are immiscible, the layers do not separate and exist as agglomerates or tactoids. As a summary, the achievement of exfoliation (delamination) of these layered silicates in a polymer matrix is essential for preparing objective nanocomposites.

During the early stages of development, synthesis of polymer layered silicate (PLS) nanocomposites involved either intercalation of a suitable monomer followed by polymerization (i.e., in-situ polymerization) (Okada et al., 1987; Messersmith and Giannelis, 1993) or polymer intercalation from solution (i.e., intercalation of dissolved polymer from a solution) (Aranda and Ruiz-Hitzky, 1992; Wu and Lerner, 1993). However, for most important polymers, both in-situ polymerization and intercalation from solution are limited because neither a suitable monomer nor a compatible polymer-silicate solvent system is always available. Vaia et al. (1993) discovered a more versatile and environmentally benign approach based on direct polymer melt intercalation. The process involves mixing the layered silicate with the polymer and heating the mixture above the softening point of the polymer. Accordingly, some very easy, accessible processing techniques such as melt-extrusion can be directly used for nanocomposite synthesis.

Extruders are thermo-mechanical mixers that consist of one or more screws in a barrel. Transport of material within the extruder takes place by the rotational, and sometimes also oscillating, movement of the screw(s). During transportation, the materials may encounter different levels of restrictions, leading to different levels of mixing. The extruder barrel may be heated, or sometimes cooled. These variables significantly affect the properties of the products inside and outside the extruder. Therefore, it might be anticipated that melt extrusion processing conditions also would be one of the important factors influencing the nature of the nanocomposites formed (i.e., the achievement of exfoliation).

The nanocomposites of interest in this study are made from native corn starch and layered silicate clay (MMT). There are several studies describing the fabrication of starch-clay nanocomposites by melt extrusion processing (Avella et al., 2005; Huang et al., 2005; Xu et al., 2005). However, most of these studies are focused on the chemistry or compatibility of starch and silicate clay. To the knowledge of the authors, there are no studies that have examined how the resulting starch-nanoclay structure is affected by the design of extrusion conditions.

This paper describes a collaboration aimed at examining the effects of melt extrusion processing conditions on the formation of nanocomposites from starch and silicate clay. An extensive study on how different extruder screw configurations, barrel temperature profiles, screw speeds, and barrel moisture content affect the formation of the nanostructure, the degree of dispersion of MMT platelets in the starch matrix, and the properties of nanocomposite films was conducted.

5.3 Materials and methods

5.3.1 Materials

Native corn starch was obtained from Cargill Inc. (Cedar Rapids, IA). Montmorillonite (MMT) was obtained from Nanocor Inc. (Arlington Heights, IL). Glycerol (Sigma, St. Louis, MO) was used as a plasticizer for all studies.

5.3.2 Preparation of starch-clay nanocomposites

Experimental studies of blending the MMT (10% based on dry starch) and glycerol (15% based on dry starch) into corn starch were carried out in a co-rotating twin-screw extruder

(Micro-18, American Leistritz, Somerville, NJ) with a six-head configuration, screw diameter of 18 mm, and L/D ratio of 30. To study the effects of processing parameters, different screw configurations, temperature profiles, screw speeds, and barrel moisture content were evaluated. The feed rate was kept constant.

Screw configurations: Three different screw configurations were evaluated with the temperature profile 65ºC, 70ºC, 80ºC, 90ºC, 105ºC, and 120ºC (from feed zone to die), screw speed 200RPM, and moisture content 40% (based on dry starch). The shear intensity of mixing was changed by changing the screw configuration. The descriptors low, medium, and high shear intensity screw configuration used in this paper are a qualitative indication of the intensity of mixing and are meaningful only in this study. Table 5.1 shows the screw configurations used in the study. The co-rotating screw configurations used in the study differed in the number of kneading disc blocks in the screw. The low shear intensity screw had one kneading block. The medium shear intensity configuration had two kneading blocks, and the high shear intensity configuration incorporated three kneading blocks. The discs in the kneading block can be fabricated at different staggering angles to facilitate movement of the starch forward, reverse, or not at all. Within a kneading block section, the inclusion of a reverse or neutral kneading element in the kneading block section causes an element of polymer to spend more time in the kneading block and increases the shear intensity of the screw configuration.

Temperature profiles: Three different temperature profiles were evaluated under the medium shear intensity screw configuration, screw speed 200 RPM, and moisture content 40% (based on dry starch). The complete temperature profiles from feed zone to die are shown in Table 5.2. The descriptors low, medium, high temperature profile used in this paper are meaningful only in this study.

Screw speeds: Two screw speeds (200RPM and 250RPM) were evaluated under the low shear intensity screw configuration, medium temperature profile, and moisture content 40% (based on dry starch).

Barrel moisture content: Three levels of moisture content (20%, 30%, and 40% based on dry starch) were evaluated under the high shear intensity screw configuration, medium temperature profile, and screw speed of 200RPM.

The specific mechanical energy (SME) is a key process parameter in extrusion. It relates to the specific work input from the motor to the material being extruded. SME can be computed

as

$$SME = \frac{(L_r - L_e)\left(N_a / N_b\right)(P)(3600)}{\dot{m}} \qquad \text{kJ/kg} \qquad (1)$$

where Lr, motor load while running with product (%); Le, motor load while running empty (%); Na, actual screw speed, RPM; Nb, base screw speed, 500 RPM; P, rated power of extruder, 2.2 kW; $\dot{m}$, mass flow rate, kg/h

After the extrusion processing, the extrudates were ground using a Wiley mill (model 4, Thomas-Wiley Co., Philadelphia, PA) and an Ultra mill (Kitchen Resource LLC., North Salt City, UT) for further use.

5.3.3 Film casting

Powder samples (4%) were dispersed in water, heated to 95ºC and maintained at that temperature for 10 min, with regular stirring. Subsequently, the suspension was cooled to 65ºC and poured into petri dishes to make the films. The suspension in petri dishes was dried at 23ºC and 50% relative humidity (RH) for 24 hrs, after which the films were peeled off for further testing.

5.3.4 Structural characterization

X-ray diffraction (XRD) studies of nanocomposites were carried out using a Bruker D8 Advance X-ray diffractometer (40kV, 40mA) (Karlsruhe, Germany). Samples were scanned in the range of diffraction angle 2θ=1-10° at a step of 0.01° and a scan speed of 4 sec/step.

5.3.5 Properties of starch-clay nanocomposite films

Water vapor permeability (WVP) was determined gravimetrically according to the standard method E96-00 (ASTM, 2000). The films were fixed on top of test cells containing a desiccant (silica gel). Test cells then were placed in a relative humidity chamber at 25ºC and 75% relative humidity (RH). The weight of test cells was measured every 12 hours over three days and the changes in the weight were plotted as a function of time. The slope of each line was calculated by linear regression (R^2>0.99), and the water vapor transmission rate (WVTR) was calculated from the slope of the straight line (G/t) divided by the transfer area (A):

$$WVTR = \frac{\left(\frac{G}{t}\right)}{A} \quad \text{g/h•m2} \tag{2}$$

where G = weight change (g), t = time (h) and A = transfer area (m2)

WVP was then calculated using equation (3):

$$WVP = \frac{WVTR \times d}{\Delta p} \quad \text{g•mm/kPa•h•m2} \tag{3}$$

where d = film thickness (mm) and Δp = partial pressure difference across the films (kPa).

Tensile properties of the films were measured using a texture analyzer (TA-XT2, Stable Micro Systems Ltd., UK), based on standard method ASTM D882-02 (ASTM, 2002). Films were cut into 1.5 cm wide and 8 cm long strips and conditioned at 23ºC and 50% relative humidity for three days before testing. The crosshead speed was 1 mm/min. Tensile strength (TS) and elongation at break (%E) were calculated using equations (4) and (5):

$$TS = \frac{L_p}{a} \times 10^{-6} \qquad \text{MPa} \tag{4}$$

where Lp = peak load (N), and a = cross-sectional area of samples (m2).

$$\%E = \frac{\Delta l}{l} \times 100 \tag{5}$$

where Δl = increase in length at breaking point (mm), and l = original length (mm)

5.3.6 Statistical analysis

WVP tests were replicated three times, while tensile tests were replicated five times. All the data were analyzed using OriginLab (OriginLab Corporation, Northampton, MA) scientific graphing and statistical analysis software. Statistical significance of differences in means was calculated using the Bonferroni LSD multiple-comparison method at $P < 0.05$.

5.4 Results and discussion

5.4.1 Effect of screw configuration

Figure 5.2 shows the XRD scans of starch-clay nanocomposite samples produced from low to high shear intensity screw configurations. As seen in Figure 5.2, the position of XRD

peak (2θ value) almost did not change, however, the peak height decreased, and a wider peak distribution was found with the increase of shear intensity. Usually, the changes seen in the XRD patterns can be interpreted by polymer entering the clay galleries pushing the platelet apart (i.e., intercalation) (Dennis et al., 2001). As more polymers enter the galleries, two possible changes can occur. First, the platelets can loose their ordered, crystalline structure and become disordered with the platelets no longer parallel. The result is that the XRD peak becomes broader (intercalated disordered). Second, the polymers that enter the galleries push the platelets far enough apart that the platelet separation exceeds the sensitivity of XRD (exfoliation). From intercalation to exfoliation, the XRD peak decreases and gradually broadens into the baseline. Therefore, the results obtained from XRD patterns (Figure 5.2) demonstrated that changes of screw configuration have a strong effect on the delamination and dispersion of the clay platelets in the starch matrix. With the increase of shear intensity, better delamination and dispersion of clay platelets were achieved.

Figure 5.3 shows the WVP of starch-clay nanocomposite films under different screw configurations. As a result of better delamination and dispersion of clay platelets, high shear intensity screw configuration led to the lowest WVP (0.48 g•mm/kPa•h•m^2) of the films, whereas low shear intensity led to the highest WVP (0.85 g•mm/kPa•h•m^2). Similar results can be found for the tensile properties (Table 5.3). With the increase of the shear intensity, tensile strength increased and elongation decreased due to the better dispersion of clay platelets in the starch matrix.

5.4.2 Effect of temperature profiles

The different temperature profiles employed during extrusion processing also influenced the intercalation and exfoliation of clay platelets. Temperature might have two important effects counter to each other on the starch-clay processing system. First, the starch-clay mixtures in the extruder may be subjected to a higher shear stress at a low processing temperature than at a high processing temperature. Accordingly, higher shear stress may lead to better fracturing and delamination of clay platelets. Second, increasing temperature may help improve the complete gelatinization of starch and lead to a better flow of starch chains. Greater gelatinization means more disruption of starch granules and more leaching of amylose and amylopectin from the granule and thus facilitates the starch chains entering the clay galleries.

In Figure 5.4, XRD patterns of starch-clay nanocomposites based on different temperature profiles were compared. With increased temperature, a lower peak height and wider peak distribution was observed. This indicates that, to some extent, increasing temperature may also improve the dispersion of clay platelets in the starch matrix. However, due to the two opposite effects mentioned above, this result might just occur in the system under a certain condition. Another study involving temperature effects had different conclusions. Di et al. (2003) used a Haake Rheomix 600 internal mixer for the preparation of polycaprolacone/organoclay nanocomposites. They compared two different mixing temperatures: 100 and 180ºC and concluded that better clay dispersion was observed at a low temperature (100ºC) because the organoclay was subjected to a higher shear stress at a low processing temperature than at a high processing temperature.

It should be noted that for the low temperature XRD curve, there was a small peak at $2\theta=1.47°$ (Figure 5.4), likely because a partial of clay particles are totally fractured by the shear force at low temperature.

Figure 5.5 shows the WVP of starch-clay nanocomposite films based on different temperature profiles. Higher temperature profile led to a lower WVP than did medium and low temperature profile. As seen in Table 5.4, although the results are not statistically significant, the trend shows that higher temperature led to a slightly higher tensile strength.

5.4.3 Effect of screw speeds

Screw speed is another factor that can affect the shear intensity and mechanical energy input. As seen in Figure 5.6, the XRD curve under the higher screw speed (250 RPM) tends to a wider distribution indicating a better delamination and dispersion of the clay platelets. Results of WVP (Figure 5.7) and tensile properties (Table 5.5) reflected the same trends.

Previous studies (Krook et al., 2002; Incarnato et al., 2003) also had examined the effect of screw speed on nanoclay dispersion and come to similar conclusions. Krook et al. (2002) found a decrease in XRD peak intensity of polyesteramide-clay samples with increasing screw rotation speed from 30 to 60 RPM in a twin-screw extruder. They attributed these results to higher shear rates at higher screw speeds, which promoted delamination of clay platelets, especially in composites with higher clay content. Incarnato et al. (2003) used a twin-screw extruder to produce polyamide-layered silicate nanocomposites. They used three different screw

speeds - 50, 80, and 100 RPM and determined that the hybrids from 50 RPM exhibited bigger stack size and a less homogeneous silicate layer distribution. The results pointed out that a high level of shear stress aided in the breakup of clay particles and improved clay platelet exfoliation and alignment with the flow.

5.4.4 Effect of moisture content

Figure 5.8 shows the XRD patterns of starch-clay nanocomposites affected by different barrel moisture content. With the decrease of moisture content, XRD diffraction curves gradually broaden into the baseline indicating better delamination and dispersion of clay platelets were achieved. For the treatment with 20% moisture, clay platelets were almost fully exfoliated and homogeneously distributed in the starch matrix. Better dispersion of clay platelets also brought better moisture barrier properties and tensile properties (Figure 5.9 and Table 5.6). As seen in Figure 5.9 and Table 5.6, the treatment with 20% moisture had significantly lower WVP (0.27 g•mm/kPa•h•m^2) and higher tensile strength (39.30 MPa) than those treatments with 30 and 40% moisture. However, the elongation at break was still very low.

In extrusion processing, moisture content is a critical parameter that can significantly affect specific mechanical energy (SME) input and the performance of the extrudate (Ilo et al., 1996; Riaz, 2000). Other parameters like screw configuration, barrel temperature, and screw speed also affected SME, which was well examined by researchers (Erdemir et al., 1992; Lo et al., 1998; Guha and Ali 2006; Lei et al. 2007). Results of these researches also followed some well-known relationships between extrusion process and system variables. Decreasing moisture content and increasing screw speed resulted in increased SME. Increasing barrel temperature decreased SME. Screw configurations with more kneading blocks, which increased shearing, also increased SME. Therefore, SME is a good indicator of the changes of extrusion process variables.

We calculated the specific mechanical energy input of the treatments with different screw configuration and moisture content (Figure 5.10). We can see SME increased rapidly with decreasing moisture content. During extrusion runs, the SME is coupled to the shear stress along the barrel. Typically, higher shear stress in the extruder leads to a higher torque on the engine and thus to a higher SME (van den Einde et al., 2004). Higher SME promoted the energy transfer to the silicate surface and intensive shear stress directly peeled the clay platelets apart from each

other. Therefore, it makes sense that the treatment with 20% moisture content achieved almost complete clay exfoliation.

However, Dennis et al. (2001) presented different trends with a polyamide 6-organoclay system. They used four different types of extruders and for each of the twin-screw extruder types, the best delamination and dispersion were obtained using the medium shear intensity screw configuration. The results indicated that increasing shear intensity was not the complete solution to clay exfoliation.

We recognized there were limited numbers of experimental conditions explored in this study, and no optimal extrusion conditions were identified that would result in the desired nanostructure and properties. Based on the conditions used for the starch-nanoclay system in this study, higher levels of shear intensity will help the break-up of the clay particles into single clay platelets, thus facilitating the homogeneous distribution of clay platelets in the starch matrix.

5.4.5 Mechanisms for clay exfoliation and dispersion in starch matrix

In previous studies (Chapter 3 and 4), we focused on the compatibility and chemistry effect among the starch, nanoclay, and plasticizers and demonstrated their importance to the formation of intercalated and exfoliated structure. In this study, processing effect was proved to be another important factor influencing the structure of nanocomposites. Increasing the shear intensity (screw configuration, screw speed, barrel moisture content) and barrel temperature improved the exfoliation and dispersion of nanoclay in the starch matrix.

We can summarize the mechanisms for clay exfoliation and dispersion in starch matrix from this study and our previous studies (Chapter 3 and 4), depending on chemistry and processing effects. First, as mentioned by Dennis et al. (2001), clay and polymer systems must be chemically compatible with each other. If there is no apparent compatibility of the clay and the polymer, even if processing can be optimized to produce intercalants or tactoids that are minimized in stack size, clay exfoliation does not occur. An example is that starch/MMT showed intercalated structure, whereas starch/I30 didn't (Chapter 3). Second, regarding the chemistry effect, the increase of chemical compatibility will lead to more polymer chains entering the clay galleries (driven by either physical or chemical affinity of the polymer for the clay surface). As an example, when we decreased glycerol content or changed the plasticizer from glycerol to formamide (Chapter 4), more starch chains entered the clay galleries. The excessive penetration

of polymer chains pushed the clay platelets apart from each other and resulted in the delamination of the clay platelets. As seen from XRD patterns, the XRD diffraction peaks shifted to the lower angle, indicating higher gallery spacing was obtained. Third, regarding the processing effect (specifically for shear intensity effects), when we increased the shear intensity in this study, the XRD diffraction peak did not move to the lower angle, but instead, lower peak heights and wider peak distributions were obtained. This indicated that in this study clay dispersion was not due to excessive polymer chains entering the clay galleries and pushing clay platelets apart. It was the shear force that directly peeled the clay platelets apart from each other. At the same time, the rotational movements of screws in the extruder improved the distribution of those single platelets in the starch matrix. With increasing of shear intensity, almost all the clay platelets were peeled apart and homogeneously distributed in the starch matrix, leading to the formation of exfoliated structure.

5.5 Conclusions

It has been demonstrated that the degree of exfoliation and dispersion of nanoclay in the starch matrix is significantly affected by melt extrusion conditions. Increasing the shear intensity (screw configuration, screw speed, barrel moisture content) improved the exfoliation and dispersion of nanoclay. The better exfoliation and dispersion of clay improved barrier properties and tensile strength. The treatment with 20% moisture content exhibited almost complete clay exfoliation, and the lowest WVP (0.27 g•mm/kPa•h•m^2) and highest tensile strength (39.30 MPa) of all treatments. Increasing temperature also improved the dispersion of clay platelets in the starch matrix in this study. However, the result might be applicable to the system only under a certain circumstance. Mechanisms for clay exfoliation and dispersion in the starch matrix were summarized and should be considered when designing a polymer-clay nanocomposite system. Compatibility is a must for polymer-clay nanocomposite preparation and the processing conditions are important variables that should be optimized to effect a high degree of clay delamination and dispersion.

5.6 Acknowledgements

The authors would like to thank Mr. Eric Maichel, Operations Manager, KSU Extrusion Center, for conducting all extrusion runs. We would also like to thank the KSU milling lab for providing milling facilities. This is Contribution Number 08-136-J from the Kansas Agricultural Experiment Station, Manhattan, Kansas 66506.

5.7 References

Aranda, P., & Ruiz-Hitzky, E. (1992). Poly(ethylene oxide)-silicate intercalation materials. Chemistry of Materials, 4, 1395-1403.

ASTM. (2000). Standard test methods for water vapor transmission of materials, E96-00. In Annual Book of ASTM Standards, American Society for Testing and Material: Philadelphia, PA.

ASTM. (2002). Standard test method for tensile properties of thin plastic sheeting, D882-02. In Annual Book of ASTM Standards, American Society for Testing and Material: Philadelphia, PA.

Avella, M., De Vlieger, J. J., Errico, M. E., Fischer, S., Vacca, P., & Volpe, M. G. (2005). Biodegradable starch/clay nanocomposite films for food packaging applications. Food Chemistry, 93, 467-474.

Dennis, H. R., Hunter, D. L., Chang, D., Kim, S., White, J. L., Cho, J. W., & Paul, D. R. (2001). Effect of melt processing conditions on the extent of exfoliation in organoclay- based nanocomposites. Polymer, 42, 9513-9522.

Di, Y. W., Iannace, S., Di Maio, E., & Nicolais, L. (2003). Nanocomposites by melt intercalation based on polycaprolactone and organoclay. Journal of Polymer Science: Part B: Polymer Physics, 41, 670-678.

Erdemir, M. M., Edwards, R. H., & McCarthy, K. L. (1992). Effect of screw configuration on mechanical energy transfer in twin-screw extrusion of rice flour. LWT, 25, 502-508.

Guha, M., & Ali, S. Z. (2006). Extrusion cooking of rice: effect of amylose content and barrel temperature on product profile. Journal of Food Processing and Preservation, 30, 706-716.

Huang, M., Yu, J., & Ma, X. (2005). High mechanical performance MMT-urea and formamide-plasticized thermoplastic cornstarch biodegradable nanocomposites. Carbohydrate polymers, 62, 1-7.

Ilo, S., Tomschik, U., Berghofer, E., & Mundigler, N. (1996). The effect of extrusion operating conditions on the apparent viscosity and properties of extrudates in twin-screw extrusion cooking of maize grits. Lebensm Wiss. Technol., 29(7), 593-598.

Incarnato, L., Scarfato, P., Russo, G. M., Di Maio, L., Iannelli, P., & Acierno, D. (2003).

Preparation and characterization of new melt compounded copolyamide nanocomposites. Polymer, 44, 4625-4634.

Krook, M., Albertsson, A. C., Gedde, U. W., & Hedenqvist, M. S. (2002). Barrier and mechanical properties of montmorillonite/polyesteramide nanocomposites. Polymer Engineering and Science, 42(6), 1238-1246.

Lei, H., Fulcher, R. G., Ruan, R., & van Lengerich, B. (2007). Assessment of color development due to twin-screw extrusion of rice-glucose-lysine blend using image analysis. LWT, 40, 1224-1231.

Lo, T. E., Moreira, R. G., & Castell-Perez, M. E. (1998). Effect of operating conditions on melt rheological characteristics during twin-screw food extrusion. Transactions of ASAE. 41(6), 1721-1728.

Messersmith, P. B., & Giannelis, E. P. (1993). Polymer-layered silicate nanocomposites: in situ intercalative polymerization of ε-caprolactone in layered silicates. Chemistry of Materials, 5, 1064-1066.

Okada, A., Kawasumi, M., Kurauchi, T., & Kamigaito, O. (1987). Synthesis and characterization of a nylon-6 clay hybrid. Polymer Preparation, 28, 447-448.

Riaz, M. N. (2000). Extruders in Food Applications. Technomic Publishing Company, Inc., Lancaster, PA.

Sinha Ray, S., & Okamoto, M. (2003). Polymer/layered silicate nanocomposites: a review from preparation to processing. Progress in Polymer Science, 28, 1539-1641.

Vaia, R. A., Ishii, H., & Giannelis, E. P. (1993). Synthesis and properties of two-dimensional nanostructures by direct intercalation of polymer melts in layered silicates. Chemistry of Materials, 5, 1694-1696.

Van den Einde, R. M., Bolsius, A., van Soest J. J. G., Janssen, L. P. B. M., van der Goot, A. J., & Boom, R. M. (2004). The effect of thermomechanical treatment on starch breakdown and the consequences for process design. Carbohydrate Polymer, 55, 57-63.

Wu, J., & Lerner, M. M. (1993). Structural, thermal, and electrical characterization of layered nanocomposites derived from sodium-montmorillonite and polyethers. Chemistry of Materials, 5, 835-838.

Xu, Y., Zhou, J., & Hanna, M. A. (2005). Melt-intercalated starch acetate nanocomposite foams as affected by type of organoclay. Cereal Chemistry, 82(1), 105-110.

Figures and Tables

Figure 5.1 Schematic representation of intercalated and exfoliated nanocomposites from layered silicate clay and polymer.

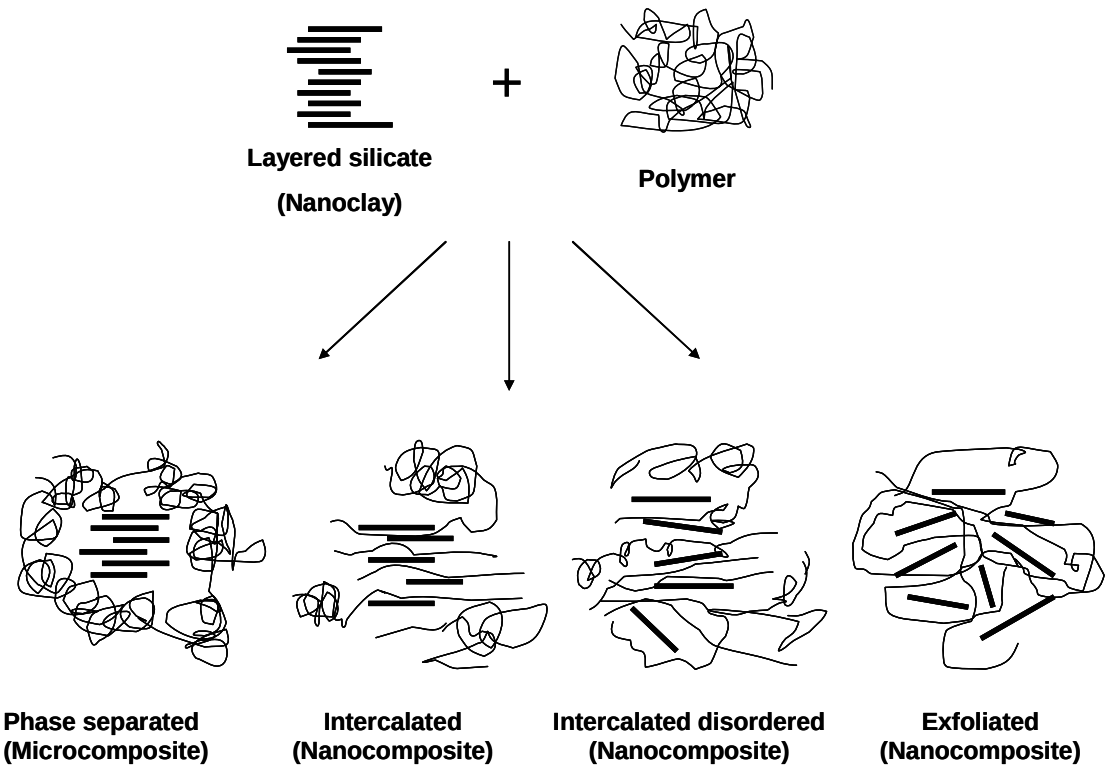

Figure 5.2 XRD patterns of starch-clay nanocomposites produced from (1) low, (2) medium, and (3) high shear intensity screw configurations.

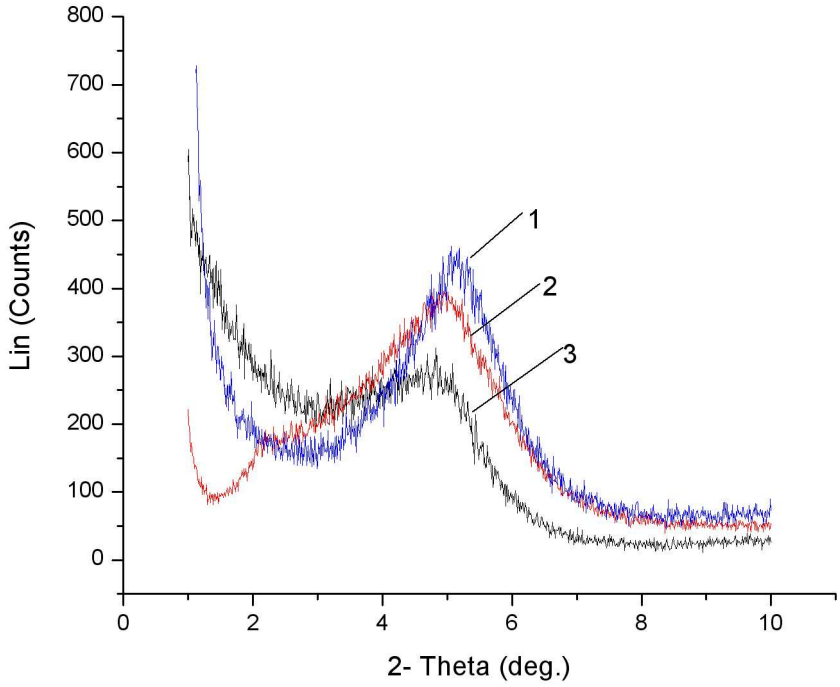

Figure 5.3 WVP of starch-clay nanocomposite films based on different shear intensity screw configurations. Error bars indicate the standard deviation. Columns with different letters imply significant difference (P<0.05).

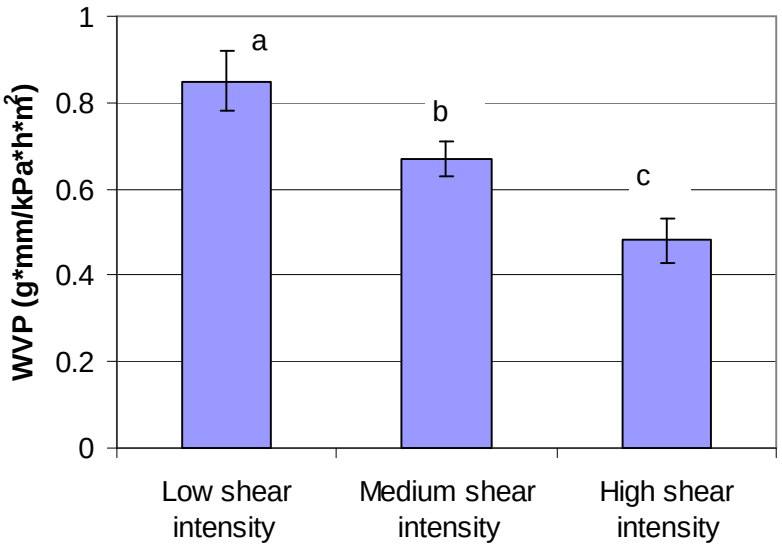

Figure 5.4 XRD patterns of starch-clay nanocomposites based on (1) low, (2) medium, and (3) high temperature profiles.

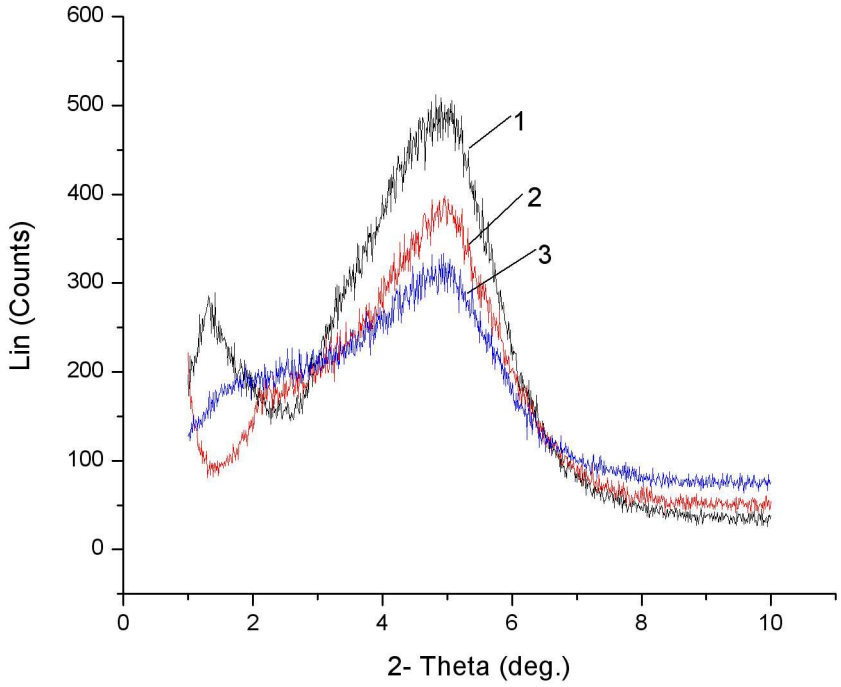

Figure 5.5 WVP of starch-clay nanocomposite films based on different temperature profiles. Error bars indicate the standard deviation. Columns with different letters imply significant difference (P<0.05).

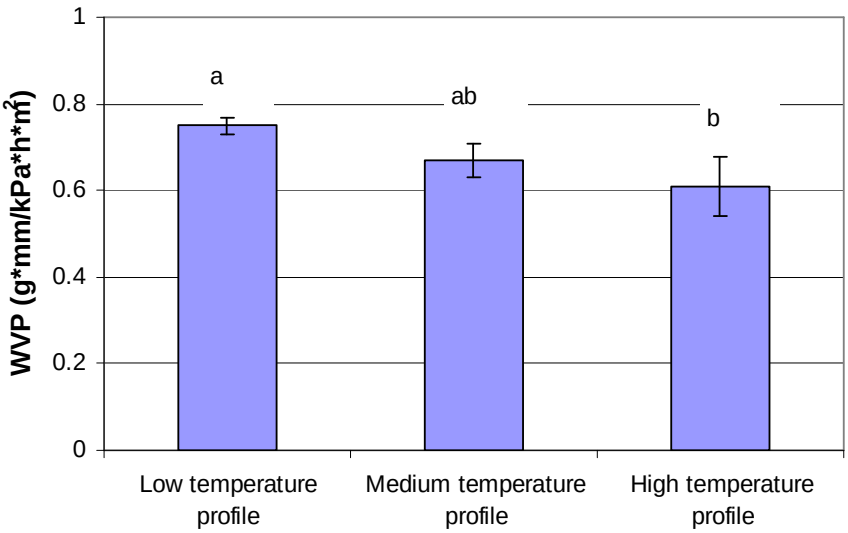

Figure 5.6 XRD patterns of starch-clay nanocomposites based on screw speeds of (1) 200, and (2) 250 RPM.

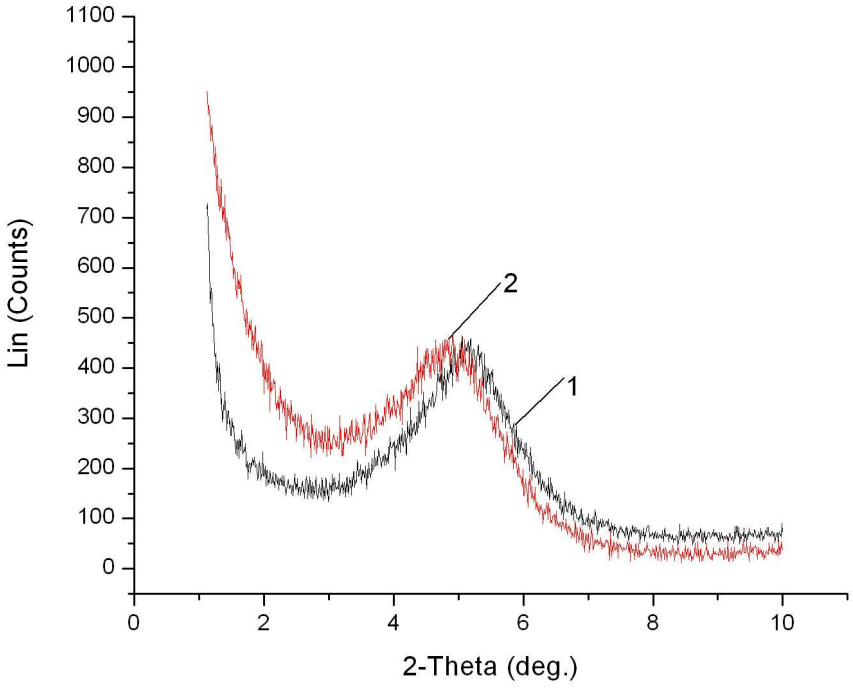

Figure 5.7 WVP of starch-clay nanocomposite films based on different screw speeds. Error bars indicate the standard deviation. Columns with different letters imply significant difference (P<0.05).

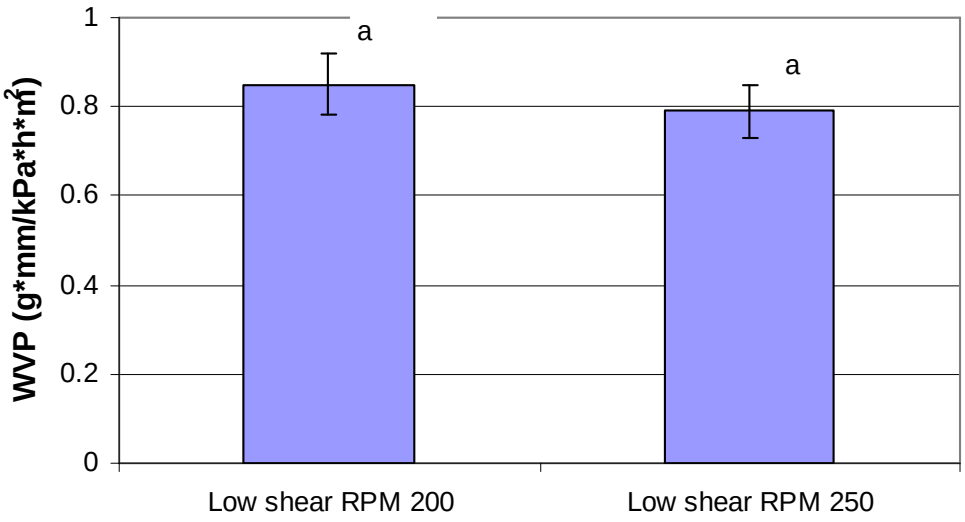

Figure 5.8 XRD patterns of starch-clay nanocomposites based on different barrel moisture content: (1) 20%, (2) 30%, and (3) 40% based on dry starch.

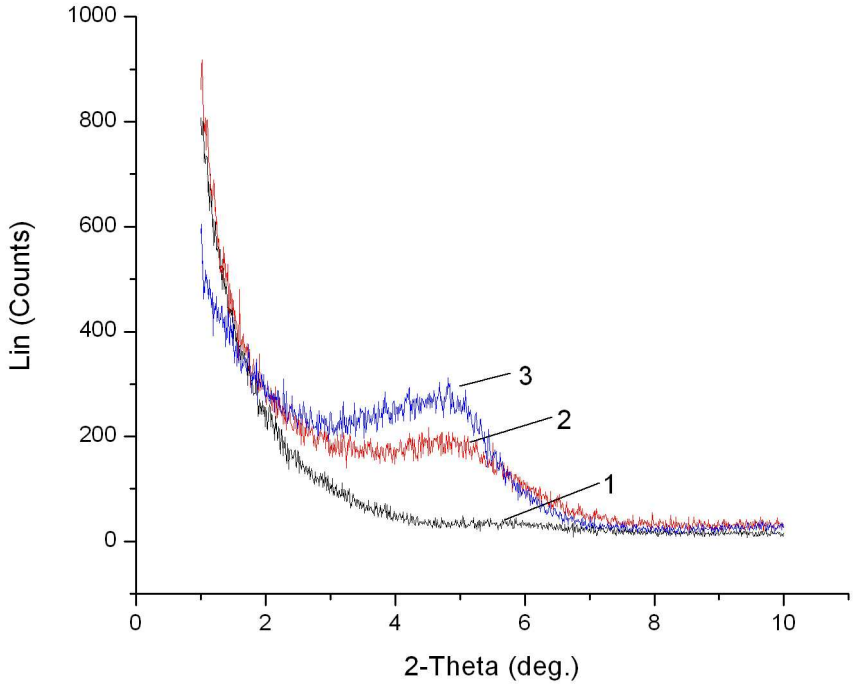

Figure 5.9 WVP of starch-clay nanocomposite films based on different barrel moisture content. Error bars indicate the standard deviation. Columns with different letters imply significant difference (P<0.05).

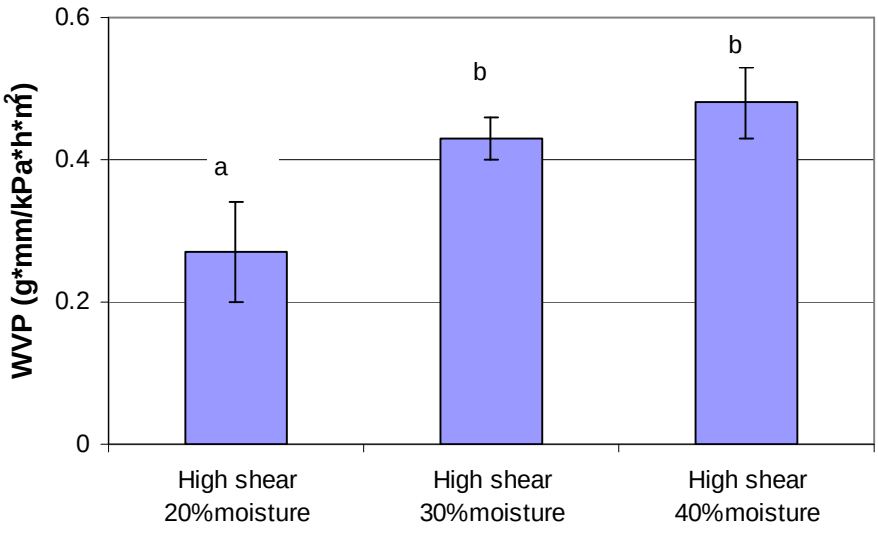

Figure 5.10 Specific mechanical energy (SME) input of the treatments with different screw configuration (under 40% moisture content) and barrel moisture content (under high shear screw configuration).

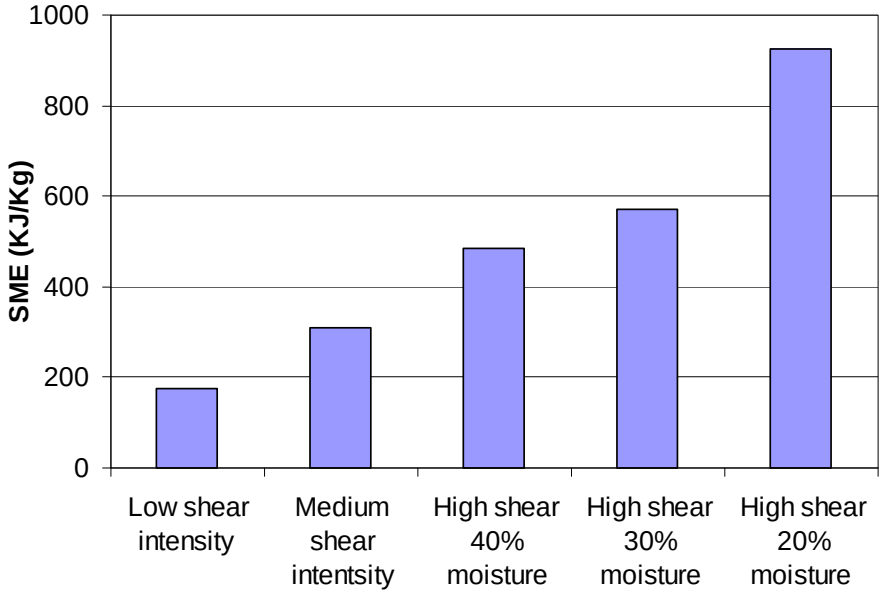

Table 5.1 Screw configuration

Types of Elements	Low shear screw configuration	Medium shear screw configuration	High shear screw configuration
Conveying elements[a]	2-30-60	2-30-60	2-30-60
	2-30-60	2-30-60	2-30-60
	2-20-60	2-20-60	2-20-60
	2-15-60	2-15-60	2-15-60
Kneading block[b]	4-4-20-45-F	4-4-20-30-F	4-4-20-30-F
Conveying elements	2-15-60	2-15-60	2-15-60
	2-15-30	2-15-30	2-15-30
Kneading block		5-2-20-45-R	5-2-20-45-R
Conveying elements	2-15-60	2-15-60	2-15-60
Kneading block			4-4-20-30-R
Conveying elements	2-10-30	2-10-30	2-10-30
	2-10-90	2-10-60	2-10-60

[a] Conveying elements: double flighted-pitch length-total element length (2-30-60).

[b] Kneading block: number of discs-length of disc-total element length-staggering angle of disc-forward (F) or reverse (R) (4-4-20-45 F)

Table 5.2 Temperature Profiles in Extruder

Temperature Profiles	Zones					
	1	2	3	4	5	6
Low temperature Profile	65[a]	70	75	80	90	100
Medium Temperature Profile	65	70	80	90	105	120
High Temperature Profile	65	70	85	100	120	140

[a] All data are presented as ºC.

Table 5.3 Tensile properties of starch-clay nanocomposite films based on different shear intensity screw configurations

	Tensile strength (MPa)	Elongation at break (%)
Low shear intensity	21.45±2.45[b]	4.09±0.51[a]
Medium shear intensity	25.43±0.69[b]	3.61±0.56[ab]
High shear intensity	30.52±3.74[a]	2.85±0.85[b]

Mean ± standard deviation of each analysis

Means with the same letters are not significantly different ($P<0.05$).

Comparisons are made within the same column; n=5 for all treatments

Table 5.4 Tensile properties of starch-clay nanocomposite films based on different temperature profiles

	Tensile strength (MPa)	Elongation at break (%)
Low temperature profile	24.01±2.42[a]	3.76±1.10[a]
Medium temperature profile	25.43±0.69[a]	3.61±0.56[a]
High temperature profile	25.22±2.07[a]	3.48±0.86[a]

Mean ± standard deviation of each analysis

Means with the same letters are not significantly different ($P<0.05$).

Comparisons are made within the same column; n=5 for all treatments

Table 5.5 Tensile properties of starch-clay nanocomposite films based on different screw speeds

	Tensile strength (MPa)	Elongation at break (%)
200 RPM	21.45±2.45[a]	4.09±0.51[a]
250 RPM	23.70±1.70[a]	3.42±0.51[a]

Mean ± standard deviation of each analysis

Means with the same letters are not significantly different ($P<0.05$).

Comparisons are made within the same column; n=5 for all treatments

Table 5.6 Tensile properties of starch-clay nanocomposite films based on different barrel moisture content

	Tensile strength (MPa)	Elongation at break (%)
20% moisture	39.30±2.07[a]	2.83±0.50[a]
30% moisture	33.87±2.89[b]	2.14±0.81[a]
40% moisture	30.52±3.74[b]	2.85±0.85[a]

Mean ± standard deviation of each analysis

Means with the same letters are not significantly different ($P<0.05$).

Comparisons are made within the same column; n=5 for all treatments

CHAPTER 6 - Summary and Future Research

Starch-clay nanocomposites with exfoliated structure were successfully prepared through Extrusion processing. Both chemistry among starch, clay, and plasticizers and extrusion processing conditions have great effects on clay exfoliation and dispersion. With the formation of intercalated and exfoliated structure, WVP and TS showed significant improvements. However, the incorporation of clays sacrificed the elongation of starch based films. Figure 6.1, 6.2 and 6.3 summarize the WVP and tensile data of commercial LDPE films and films in this study. It can be seen the elongation at break caused the major differences. Starches alone form brittle films because of the forming of starch network by means of hydrogen bonds. The addition of plasticizers increases the flexibility of starch based films because the plasticizers can form hydrogen bonds with the starch, replacing the strong interactions between the hydroxyl groups of the starch molecules. However, the high modulus of clay platelets decreases the flexibility of the films.

There are several researches that can be done to further improve properties of starch-clay nanocomposite films. Influence of aspect ratio and clay orientation on barrier and mechanical properties of nanocomposites should be investigated. Lu and Mai (2005) reported that the aspect ratio of exfoliated silicate platelets has a critical role in controlling the microstructure of polymer-clay nanocomposites and their barrier properties. Weon and Sue (2005) utilized a large-scale simple shear process to alter the clay aspect ratio and orientation within the reference nanocomposite. They found that the modulus, strength, and heat distortion temperature of nanocomposites decreased as the clay aspect ratio and degree of orientation were reduced. Furthermore, the reduction of clay aspect ratio and orientation led to an increase in fracture toughness and ductility. Average platelet orientation increases modestly with increasing shear rate, while the average platelet orientation moves somewhat closer to the flow direction. In an ideal case, clay particles are completely exfoliated and uniformly dispersed along the preferred oreientation ($\theta=0°$) in the polymer matrix (Figure 6.4). PVOH-starch-clay nanocompoiste film could be another research topic. PVOH is a biodegradable polymer and has excellent mechanical properties and superior oxygen permeabilities. Furthermore, PVOH are chemically compatible with starch and nanoclay.

References

Lu, C. S., and Mai, Y, W. 2005 Influence of aspect ration on barrier properties of polymer-clay nanocomposites. Physical Review Letters. 95(8): 088303-1.

Weon J. I., and Sue, H. J. 2005 Effects of clay orientation and aspect ration on mechanical behavior of nylon-6 nanocomposite. Polymer, 46: 6325-6334.

Figures

Figure 6.1 WVP summary

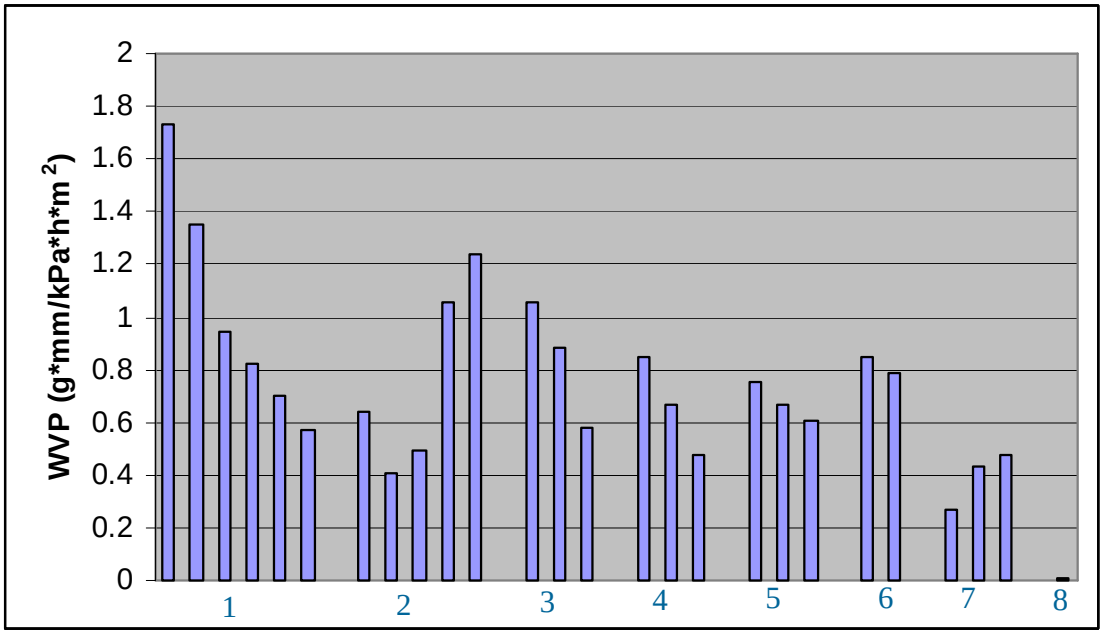

1. clay content 2. glycerol content 3. different plasticizer 4. screw configuration
5. temperature profile 6. screw speed 7. moisture content 8. LDPE films

Figure 6.2 Tensile strength summary

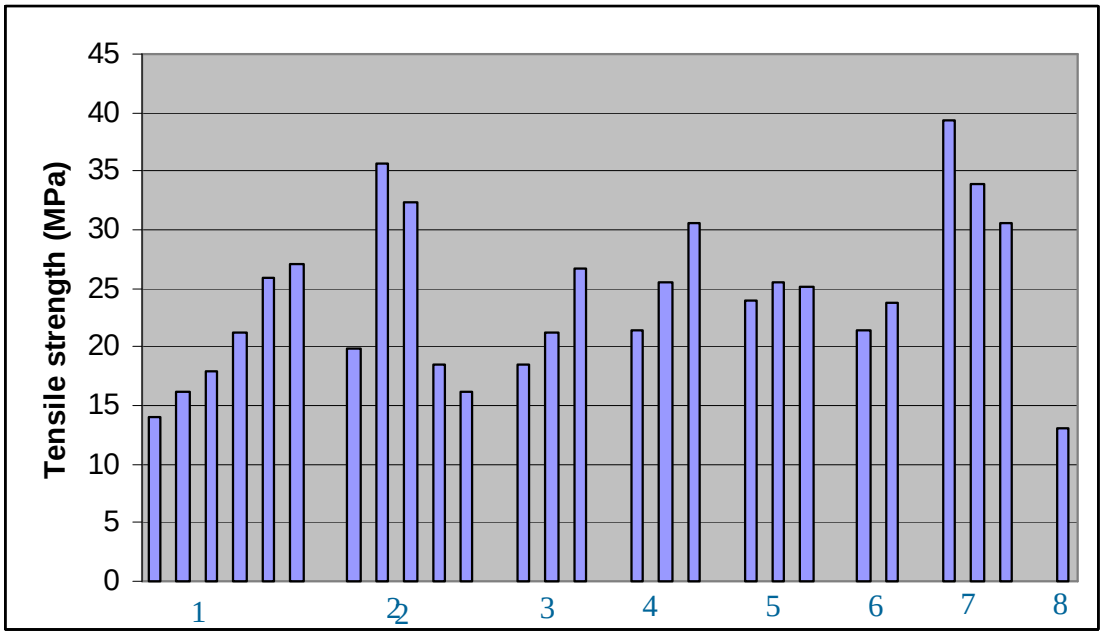

1. clay content 2. glycerol content 3. different plasticizer 4. screw configuration
5. temperature profile 6. screw speed 7. moisture content 8. LDPE films

Figure 6.3 Elongation at break summary

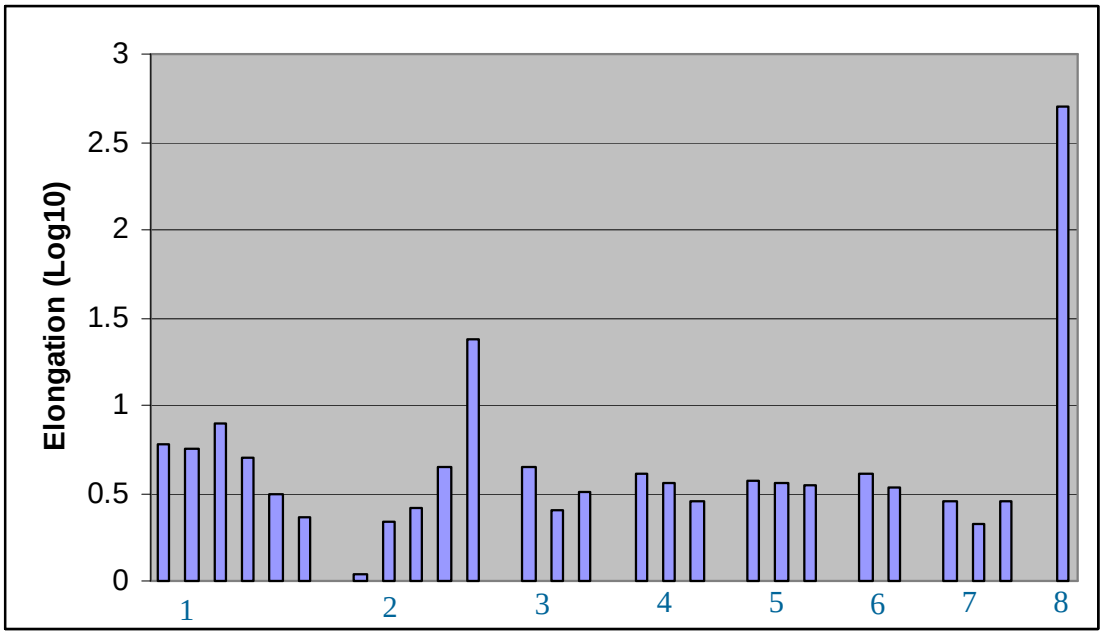

1. clay content 2. glycerol content 3. different plasticizer 4. screw configuration 5. temperature profile 6. screw speed 7. moisture content 8. LDPE films

Figure 6.4 Schematic of exfoliated clay morphologies, where inset (a) shows the state of intercalation and inset (b) ideal exfoliated and dispersed clay platelets along the preferred orientation in the polymer matrix (Lu and Mai 2005).